UNCONVECTIONAL AND CONVENTIONAL RESERVOIR CHARACTERIZATION OF LOWER GORU FORMATION IN GAMBAT-LATIF BLOCK LOWER INDUS BASIN PAKISTAN

BY

Syed Abbas Raza

M.Phil. Geophysics

2020-2022

DEPARTMENT OF EARTH SCIENCES

Quaid-e-Azam University Islamabad

IN THE NAME OF ALLAH

the Most Gracious & the Most Merciful

And look at the mountain how they are set!
And at the earth how it is spread out

(AL-QURAN)

CERTIFICATE

This thesis submitted by **Syed Abbas Raza** son of **Syed Ali Mirza Hussain** is acknowledged in its present form by the Department of Earth Sciences, Quaid-i-Azam University Islamabad as sufficient for the requirement of the award of M.Phil. degree in Geophysics.

Recommended By

Associate Prof Dr. Shazia Naseem _____

(Supervisor)

Prof. Dr. Aamir Ali _____

(Chairperson Department of Earth Sciences)

External Examiner _____

Department of Earth Sciences Quaid-i-Azam University Islamabad, Pakistan

ACKNOWLEDGEMENT

I would first like to thank my thesis supervisor Asst. Professor **Dr. Shazia Naseem,** of the Earth Sciences at QAU. She consistently allowed this research to be my own work, but steered me in the right the direction whenever he thought I needed it.

I would also like to thank the experts who were involved in this research project: Mr. Syed M. Naqi Naqvi, and Mr. Babar Ali. Without their passionate participation and input, this research could not have been successfully completed. I am gratefully indebted to them for their very valuable comments on this thesis.

Finally, I must express my very profound gratitude to my brothers and to my friends for providing me with unfailing support and continuous encouragement throughout my years of study and through the process of researching and writing this thesis. This accomplishment would not have been possible without them. Thank you.

SYED ABBAS RAZA

DEDICATION

Dedicated to my lovely parents

Contents

List Of Figures

Chapter-01

Chapter-02

Chapter-03

Chapter-04

Chapter-05

Chapter-06

Chapter-07

ABSTRACT

The demands in the energy production over the globe is increasing day by day. Subsequently demands in exploration and production of conventional and unconventional hydrocarbon reservoir have increased over the past decades. For hydrocarbon exploration, seismic surveys are the most apposite method because it provides precise and detailed spatial coverage of the subsurface. This study pertains to explore the hydrocarbon within the both conventional and unconventional domains. The methodology to carry out this research work includes 3D seismic data interpretation, petrophysical analysis, seismic inversion analysis, 3D static modeling and TOC estimation.

The 3D seismic data interpretation is done by marking major and minor faults, and marking horizons. This information is then used to map the contour. The structural analysis from assigned 3D seismic cube show that normal faulting is present within the study area and the horizons are marked on the basis of the well tops after correlation with seismic data.

The petrophysical analysis is done by using the well log data to estimate the effective porosity, lithofacies identification, saturation of water and this information will lead to mark the promising hydrocarbon zone within the reservoir. The petrophysical analysis is performed on all Tajjal wells available. This analysis is used to delineate the lithology, effective porosity and hydrocarbon saturation. The average effective porosity ranges are from 6 to 14%, 9.1% and average hydrocarbon ranges is from 50-74 %, 74% within zone of interest of B Interval and C Interval sands for Tajjal-01.. For Tajjal-02 (water wet), the average effective porosity is 8.30-9.30% and 7% and average hydrocarbon ranges from 47% and 55% within both the B and C intervals of the Lower Goru Formation, respectively.

In inversion analysis, various algorithms and techniques were opted to analyses for better understanding of lower Goru sands and shales. The acoustic impedance (AI) sections are the end results of seismic inversion. The acoustic impedance (Al) is the property of the layer, and this property of the layer is used to make quantitative interpretations of seismic data. Model-based Inversion uses a forward model to figure out how to make the synthetic seismic data that is used in the inversion process. Sparse spike inversion gives best result as compare to all other inversion types.

3D static reservoir modelling is used to define reservoir properties in a more realistic 3D geological model in the subsurface. The primary goal of the static type modelling is to determine the accurate amount of hydrocarbons that are contained in the subsurface. These hydrocarbon volume calculations can be performed for the entire reservoir or separately for a fault segment or any layer that was designated as a zone of interest during the model's building. Another important outcome is to

accurately locate the hydrocarbon bearing zones in the subsurface for further developments of study area. Modelling was carried at B and C-intervals both for conventional reservoir parameters and unconventional reservoir parameters like porosity, permeability, water saturation, and TOC content along with facies distribution on whole reservoir intervals. Some promising zones were also identified based on static reservoir modelling study. TOC (total organic content) is calculated using the Passey et al (1990) equation. The ΔLogR technique is used to determine total organic content of the shale portions in the lower part of Goru formation. The results show that in B interval (Talhar shale) has a greater organic content than the C interval shale part. Total organic carbon content all show that the B interval shale (Talhaar shale) has potential for shale gas based on high values of total organic carbon content.

Chapter-01

INTRODUCTION:

Seismic method is the tool that is mostly used in the exploration in 1915s and this method gives information about the geological structure and help us in getting information about change in behavior of subsurface (Chopra and Marfurt, 2005). For the identification of the anomalous zone, the seismic refraction method is failed that is the case, seismic reflection method is used. Because of this reason the seismic reflection becomes the most important method regarding to identification of the anomalous zone.

In the 3D seismic survey, several of the seismic environments such as pores pressure, fluid saturation is interpreted (Yilmaz, 2001). While the faults are helpful in describe the geological structure and finding the zone of interest (Badely, 1985).

The borehole data describes about the reservoir properties. The Petrophysical analysis gives information about the reservoir properties such a volume of shale, porosities, saturation of water. Through petrophysical information the reservoir zonation can be performed (Fischetti et al., 2002).Forward modeling has been performed, is improving the subsurface image (Fagin, 1991). The structure interpretation is the most common application of the forward modeling (Mellman and Kunzinger, 1992).

In acquisition process, wave pass through the earth and the change in shape of the wave occurred. Due to absorption and attenuation, the distortion in the wave occurred (Veeken and Silva, 2004).It concludes of the amplitude and phase of the wave but do not characterize the true properties of the reflector. The recorded seismic wave is Bandlimited nature and the low frequency is missing and maximum recording is 80Hz. Through inversion, the low and high frequency using well data is added. This will enhance the resolution of seismic data and remove non-uniqueness in impedance inversion (Vazquez et al., 2004).

Shale oil/gas having tight nature consists of low permeability but having 8 to 10 times more reservoir that will fulfill the world's energy needs. The horizontal drilling combined with hydraulic fracturing is performed. But for this purpose, the potential and maturity of the shale is determined (Zou et al., 2010).

In the study area, the Lower Goru formation shale and the Sembar formation within the study area are the main perspective of gas shale information.

1.1 Introduction to Gambat-Latif Area:

The study area is located in the Khairpur district, province of Sindh, Pakistan. The Gambat-Latif area is located within Lower Indus Basin. It is situated at 68° 31' E and 27° 21' N with the 47m high from the sea level. The three Dimensional project of the study area is 675 square Km coverage and the 10 square Km 3D seismic data is accepted for the dissertation aims. The location of project area within Figure 1.1.

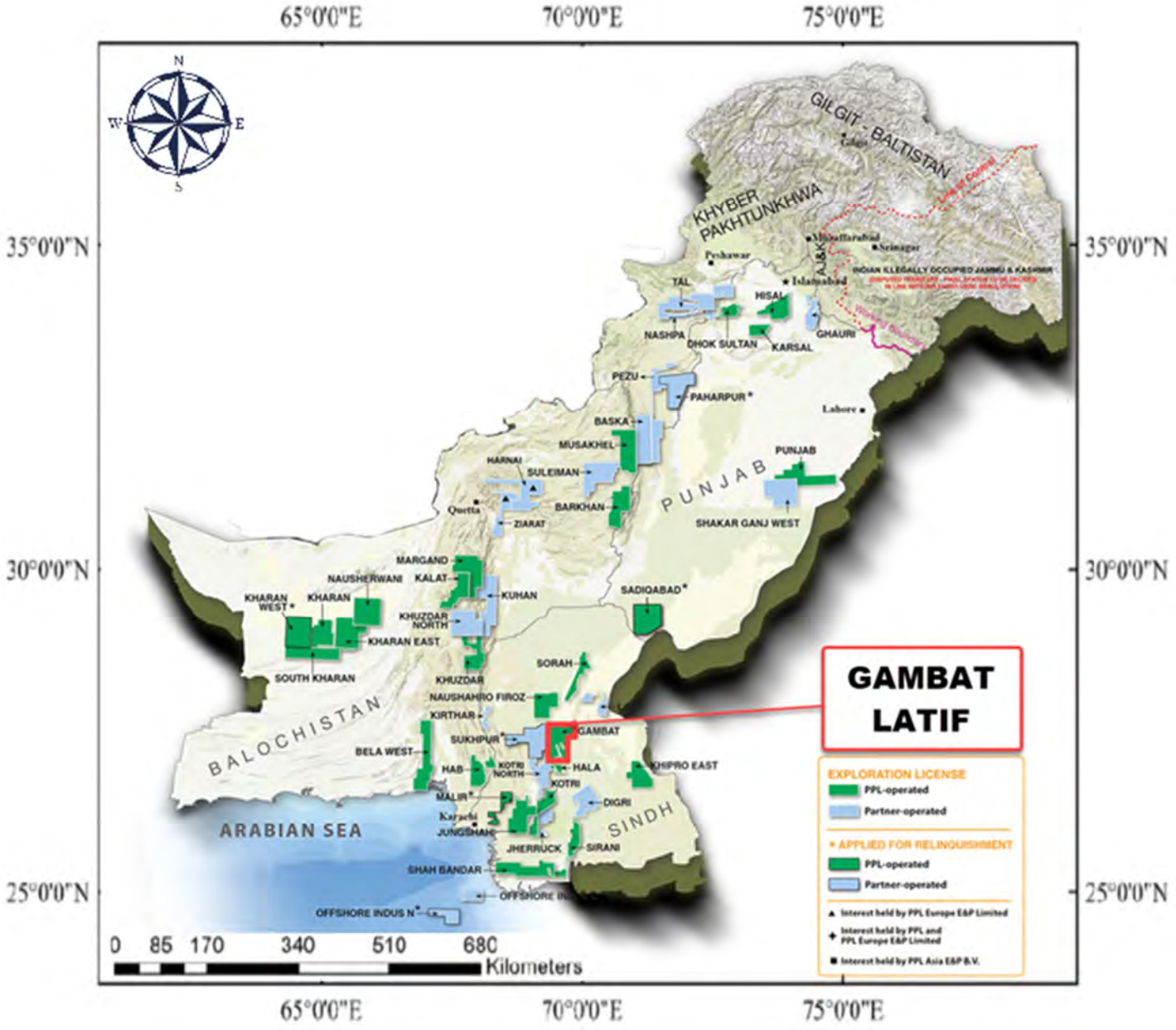

Figure 1. 1: Show the location map (www.ppl.com) of the study area

3D Seismic data of about 12 square km that consists of inlines and crossline. Three wells are provided which are Tajjal-001(gas), Tajjal -002(suspended) and Tajjal -003(abundent). Details of seismic and well data are given in the Table 1.1 & 1.2.

Lines	Minimum	Maximum
In-line	1298	1494
Cross-line	330	552

Table 1. 1: Details for Seismic 3D In-lines and Cross Lines

Names of wells/Status	Total Depth(m)	Starting well Depth(m)	LONG (Deg)	LAT (Deg)
Tajjal-03(Abandoned)	3800	54	69.367361	26.842821
Tajjal-02(Suspended)	3836	53	69.351603	26.822600
Tajjal-01(Gas)	4506	55	69.330525	26.856183

Table 1.2: Detail of Well Log Data

1.2 Aims and Objectives:

The main objectives of the study are;

- 3D seismic interpretation for identification of subsurface structure and probable zones favorable for accumulation of hydrocarbon.
- Petrophysical analysis of the major reservoir to identify the prospect hydrocarbon zone.
- Petro elastic of the shales present within the reservoir to delineate their mechanical properties.
- Seismic inversion of the reservoir to find the reservoir characterization.
- Static modelling of reservoir.
- Seismic based TOC estimation within conventional and unconventional reservoir.

1.3 Methodology:

This study was carried out in the way

- Review the existing literature to completely understand the geology, stratigraphic and tectonic set-up of the study area.
- 3D Seismic interpretation is performed using commercial software, mainly named as Kingdom, Techlog and Petrel software.
- To compute petrophysical properties of reservoir, well logs data are used.
- To perform the seismic inversion, the well logs and the seismic data are used.
- Static modeling for showing reservoir properties in 3D. Seismic based TOC content within the reservoir shale is estimated by using seismic and well logs data.
- For the future prospects, possible recommendations on the basis of final results.

1.4 Significance of the study:

This research work will be helpful for identification of subsurface structures Gambat-Latif area that shows the favorable stratigraphic trap for hydrocarbon accumulation and trapping. Petrophysical analysis for hydrocarbon estimations using well log data at reservoir level helps to find potential quantitatively at the reservoir level. By integrating all these geophysical techniques possible hydrocarbons zones can be identified and new potential zones can be marked. The potential of the shale rock within the Lower Goru Formation can be estimated. Total organic content (TOC) is calculated with the help of the well log data and this will apply to the seismic to find out the high and low seismic based TOC zones.

CHAPTER-02

GEOLOGY AND STRATIGRAPHY

2.1 Introduction:

In geological point of view the Gambat-Latif lies in lower Indus basin of Pakistan. The dominant fault Normal faulting which is observed due to the extensional regime. These extensional tectonic regimes of southern Indus basin have structure which have ability to reserves along with stratigraphic traps. The environment of the area is dry and hot due to the Thar and Cholistan deserts. There is no outcrop exposed in the study area but rocks from recent age to Triassic age are encountered in well data and can be interpreted on seismic section. Historically the basin formed because of rifting of Indian plate from Gondwanaland in Jurassic period. In this area different exploration companies take interest to explore the hydrocarbon. In 2007 OMV Pakistan explored first well in Gambat latif block. In this area natural resources are present especially oil and gas which is explore from lower cretaceous rocks.

2.2 Geological and tectonic background

Indus basin occurs between India and Pakistan. The most of the part lies in Pakistan while Indian covering western part of an area 873,000 Kilometer square (Km^2).Pakistan composed of two onshore sedimentary basins which formed through different geological setting but joined together in cretaceous age along the chaman transform fault. One is Indus-basin and another minor remnant basin is pishin basin or Kakar Khorasan Basin. The upper part and lower part of the Indus basin is dividing by sargodha highs. Further The Division of Sukkar-rift within lower Indus basin into southern and central Indus basin (Wandrey et.al.,2004). The Indus basin remains categorized into the Upper- and lower-part Indus-basin whereas upper part of indus basin is further divide into Potwar and Kohat basin while the lower Indus Basin is divide into middle and Southern basin. (Kadri, 1995)

The north of the lower indus basin is covered by Sukkar rift, in east is covered by Indian shield, its west is surrounded by Kirther and Suleiman fold belt while in south is Arabian sea/Indus offshore basin (Ahmed,2012). The tectonic map of Pakistan stands below:

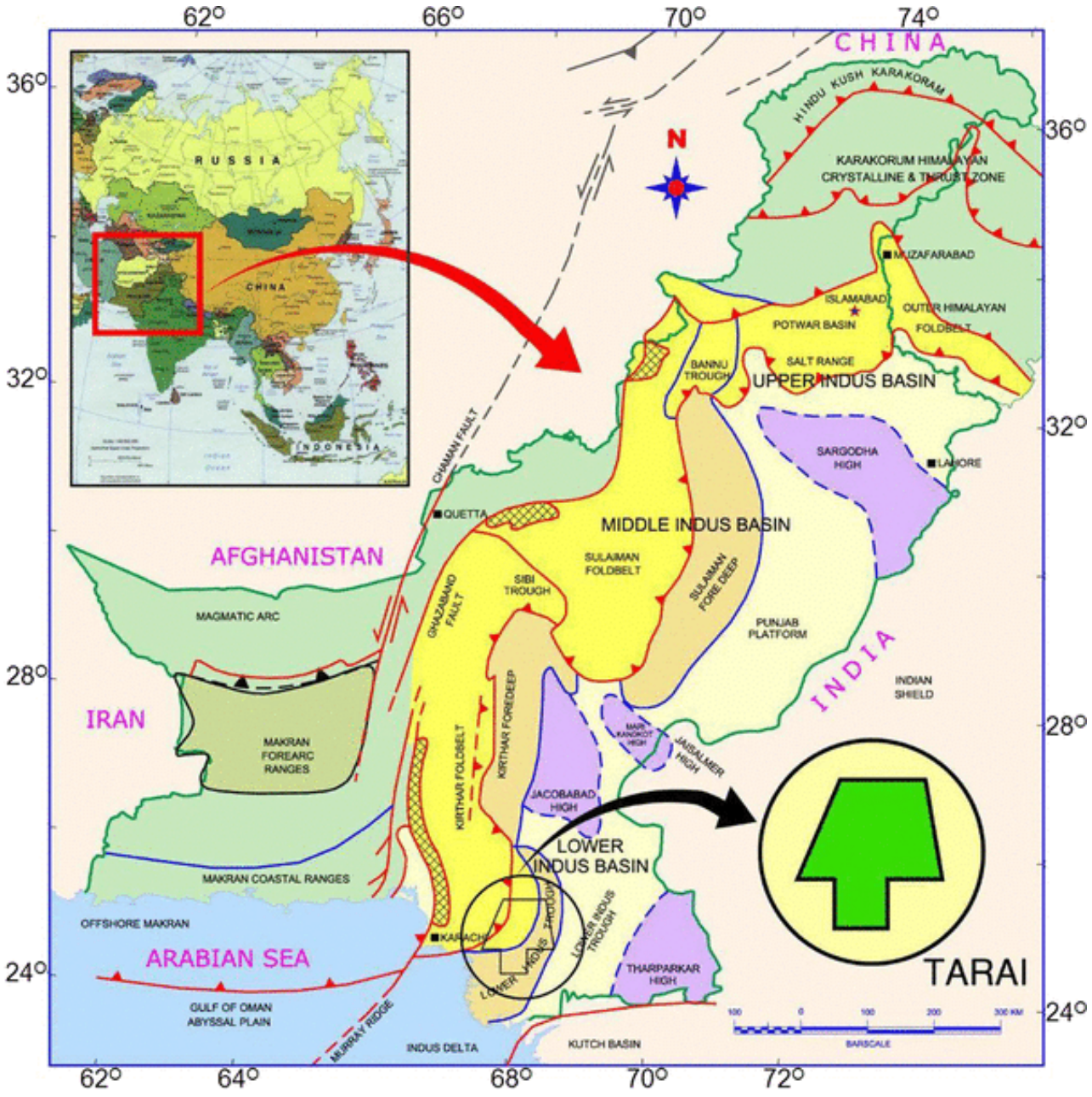

Figure 2. 1: Tectonic and location Map of Research (Touqeer et al., 2020)

In Pakistan the different structured and stratigraphic features are formed due to the three major plates.

- Indian plate
- Eurasian plate
- Arabian plate

During Permian age the Indian plates was lies in southern hemisphere joined with the southern part of Gondwanaland which lies between Antarctic,African and Australian plates. The deposits in the southern part of the Indian plate is permain age while same age deposit of Lower tobra formation in kohat potwar basin shows cold climate in Permian age (Shah, 1977). The environment of continental shelf and Shallow marine is image in the rock of Permain Nilawahan and Zaluch group rocks. In the early Jurrasic period horst and graban structure are formed and also divide the Indus basin in three sub basins by sagodha and MARI-Kandkot High. In late Jurassic rifting Australia and Antarctica are separated from India (Kemal et al., 1991; Zaigham and Mallicj., 2000).

In the earlier stage of the cretaceous age northward movement occur in Indian plate toward the warm latitude and during that time deposition of Sember and Goru formation occurred. These two formations are formed from shale and sands. That deposition occur at the west of the shelf margin in the area of Kohat and Sulaiman over a territorial erosional surface.Under the Chichali formation is Samana suk formation. On Indian plate during the start of creteaous age flysch deposits are formed by the Bengal seafloor. When indian plate begin rotation in the direction of counter clockwise its Seychelles split into parts (Waples and Hegarty, 1999). Volcanic activities established during late Cretaceous age. Due to volcanism in the western india developed during explosion the Deccan traps (Biwas and Desphande, 1983). The Indian speed of moving is about 15-20 cm/year. So, the plate is consciously moving but when it reaches to eastern part of Kreguelen hotspot. Islands are formed in a sequence at E 90^0 longitude. The Northern and north-west of the Tethyan Ocean is lock due to movement toward north and counter clockwise rotation of the Indian plate. In response of the Collision and that oblique rotation the formation of fold belt of Sulaiman and Kirthar (Jadoon et al., 1994). As a mountain ranges begin raising from northern and western side it can became the current source of sediment. That new source can replace the sediment direction from south to north. On the shelf between Eocene to the mid of Miocene on the Indian plate Carbonates platform spread up formed. Subductions of Indian plate beneath the Eurasian plate establish a trench. Geologically Kohat and potwar basin,are anticlines and trends overturned fold establish on detachment surface which establish during the converge of the plate and about 55 kilometer condensing(Kemal et al.,1991;jaswal et al.,1997).

2.3 Petroleum plays in the study area

Several nomenclatures used for Lower Goru Tops are shown in following figure 2.2. We used the nomenclature highlighted in yellow colour.

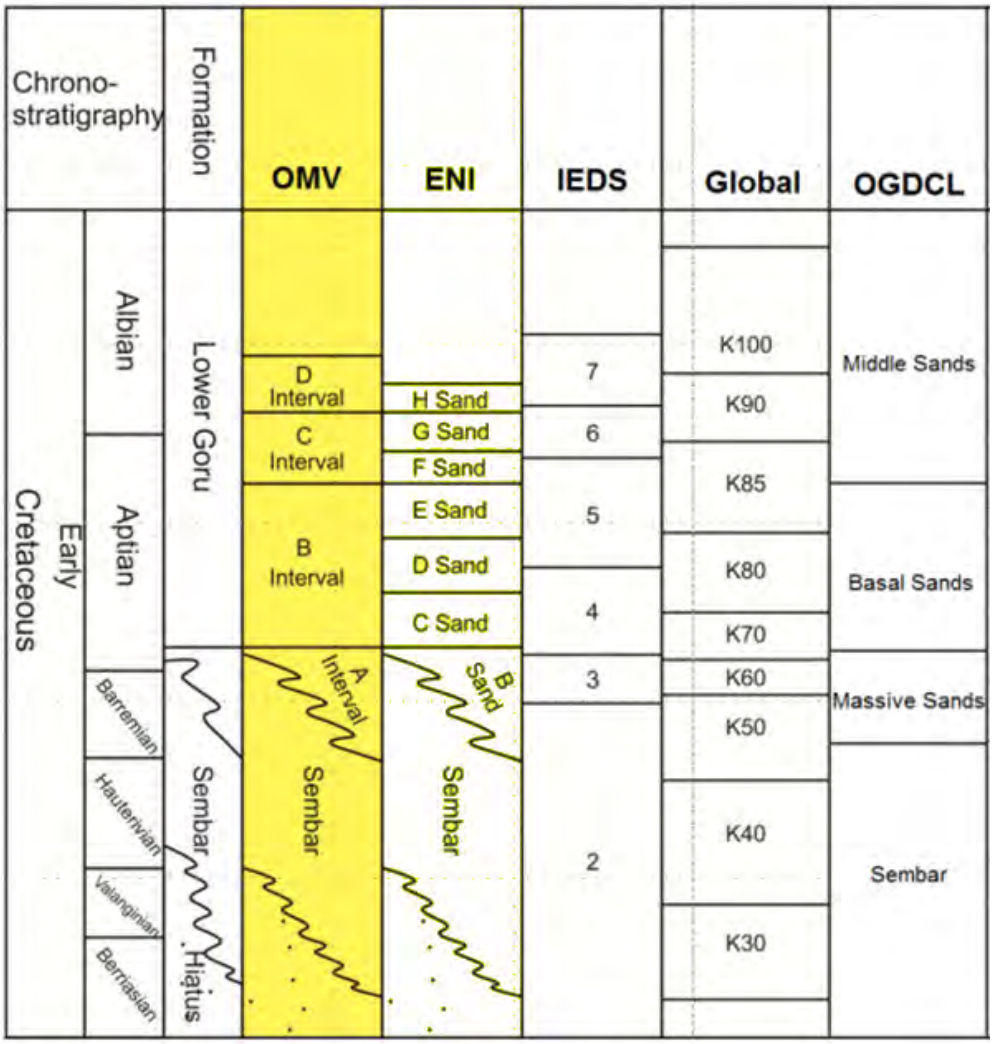

Figure 2. 2: All current Lower Goru sands terminology in the Pakistani oil sector, including Sembar (Kamran et al., 2014). In this analysis, we applied the operating company's name at the time of drilling.

2.3.1: Source Rock

Sember Formation is well known source within lower Indus basin. In Pakistan the lower Goru formation plays a very important role in exploration.it work as a seal, a Reservoir and also source rock. The sub division of lower Goru formation is like that Upper Goru work as a Seal, lower Goru a good reservoir and the middle one is source. The potential of unconventional shale gas is present in sizable amount in Talhar member of cretaceous age in lower Goru.

2.3.2: Reservoir Rock

In lower Goru secondary permeability occur in fractured of Chiltan Formation which act as a reservoir. It also called fractured reservoir.The lower Goru reservoir has a potential of hydrocarbon. The porosity

data and its permeability of reservoir shows an excellent potential. Its fundamentally compost of sands and mud stone.The two other formation is also have potiential of reservoir the Pab and Nari reservoir formation (Quadri and Shuaib., 1986).

2.3.3: Seal Rock

The Sember formation, Upper Goru, Ranikot and Ghazij formation react as a seal rock in the basin. For Chiltan limeston Sember formation act as a seal rock and upper Goru also play a role of seal rock for beneath Goru formation.

2.3.4: Trapping Mechanism:

On broadly scale the normal faults are simply noticed and interpreted in seismic data. For accumulation of hydrocarbon the most important structure are horst and graban which is presiding available in the area.Some local normal fault is also noticed in the area with the stratigraphic traps (Naeem et al.,2016).Figure 3.2 shows stratigraphic column of Tajjal Area.

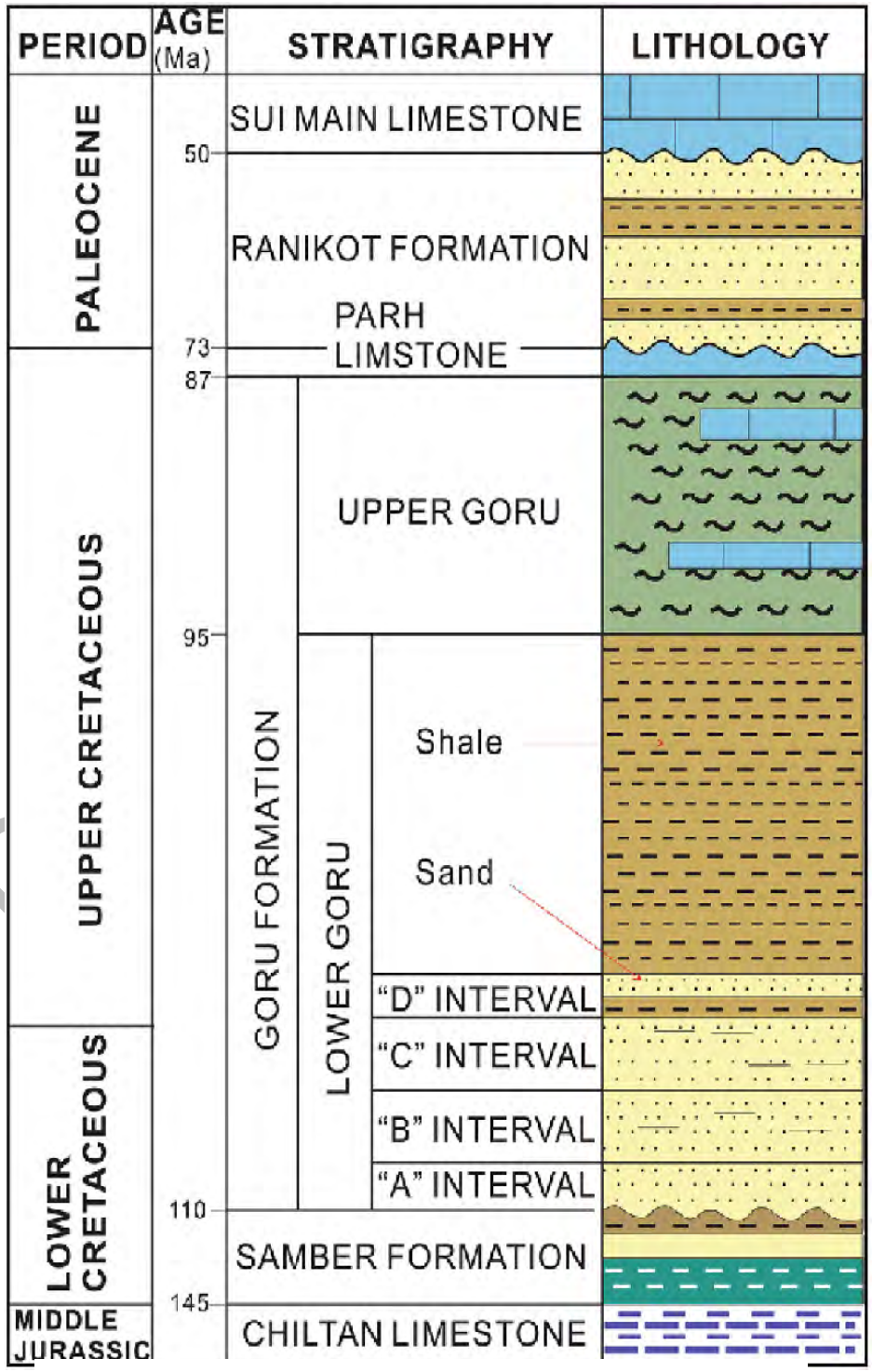

Figure 2. 3: *Stratigraphic column of Tajjal Area*

CHAPTER 03

SEISMIC STRUCTURAL INTERPRETATION

3.1: Seismic Interpretation

The seismic data interpreting is very important technique to collect the valuable information from sub-surface. This information includes stresses, structural, stratigraphic, velocity, alteration of reservoir fluids with time being and sub-surface rock properties. For a good interpretation needed feasible acquisition and also needed best possible processing carry out on the seismic data and also needed to understanding the local geology and early literature of well (Enwenode Onajite., 2014). The workflow shows s interpretation of 3D seismic data in figure 3.1.

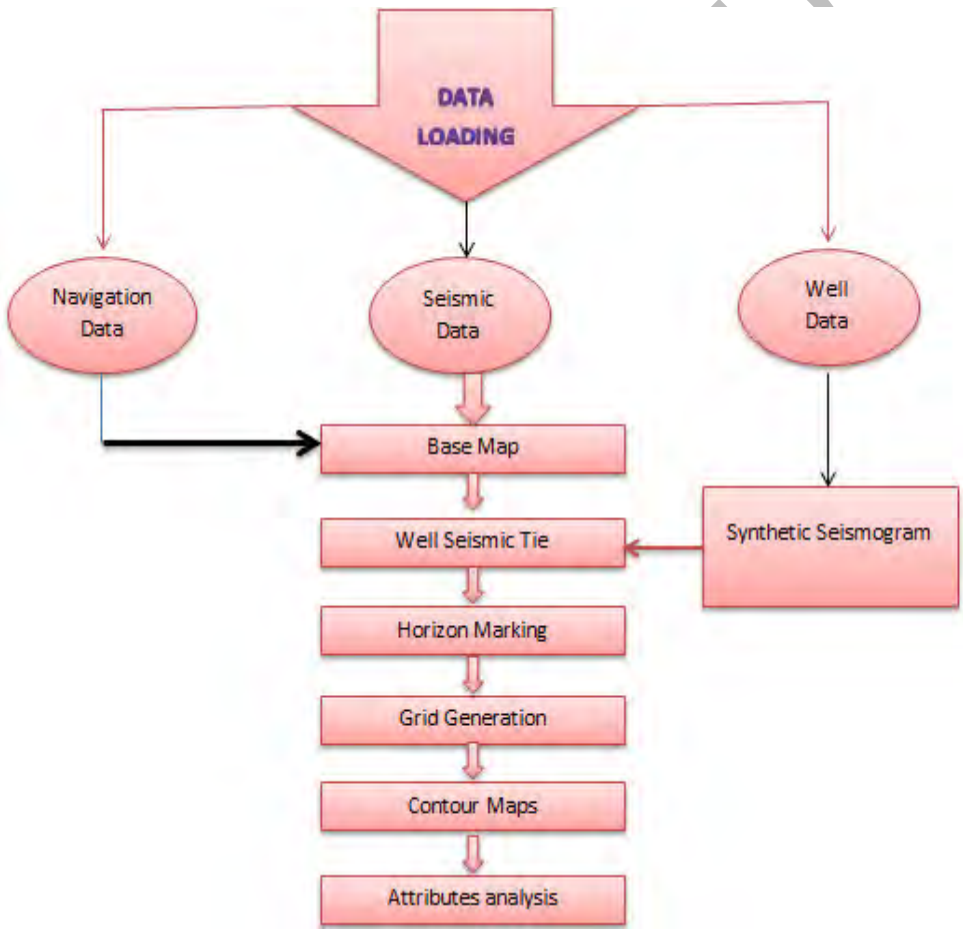

Figure 3.1: *Workflow of seismic interpretation*

For mapping geological structures beneath the surface Seismic reflection method (profiles) are highly used. Especially helpful when tied well data, surface outcrop with reflection section. The beneficial tool which expose the tectonic history is seismic profile (Robert., 1999).

3.2: Structural Interpretation

The seismic interpretation is divided into structural and stratigraphic interpretation. Stratigraphic interpretation is the analysis of seismic sequence as an expression of lithology and Structural interpretation analyze reflection geometries of two-way travel time. These both are recognized by seismic modeling. With the help modeling we make synthetic seismogram which is useful for the analysis of underneath layering of earth to interpret the important physical event. Structural analyses are mostly executed on two-way travel time rather than depth. Stacking velocities are obtain from seismic data i-e from bore hole sonic log or during acquisition through these velocities time contour maps is converted into depth contour maps. Therefore, the 3D seismic data is very important for productive growth of oilfields in composite geological structure (Kearey et al., 2002).

In our recent study area of interest, we have implemented structural interpretation in which we have picked out and marked different structures like normal faults on the seismic section. Generation of Synthetic seismogram is helpful for marking of the specific horizon. This synthetic seismogram is created with help of well log data. In beneath the surface, to investigate the comprehensive style of the horizon, time grid was created which interpose the values of time between time grid nodes. Now to gain the final result of seismic interpretation we multiply the time grid with the proper velocity function to turn it into depth map.

3.3: Base Map of the Area

Shot point maps have fixed seismic lines and spatial orientation. Their well location is along with latitude, longitude and fixed position of shot point through which seismic data obtain for interpretation purposes. That is why Geophysicist generally used shot point maps. Base map of area is shown in figure 3.2.

3.4: Synthetic Seismogram

In the depth domain two logs are used to create artificial reflection record which are sonic and density data logs. With the product of sonic log and density log we generate acoustic impedance. Later Convolution of the reflectivity functions in time with specific source pulse or Richer wavelet. The relation which is used for the calculation of the reflectivity function:

$$RC = \frac{\rho_2 V_2 - \rho_1 V_1}{\rho_1 V_1 + \rho_2 V_2} \quad (3.1)$$

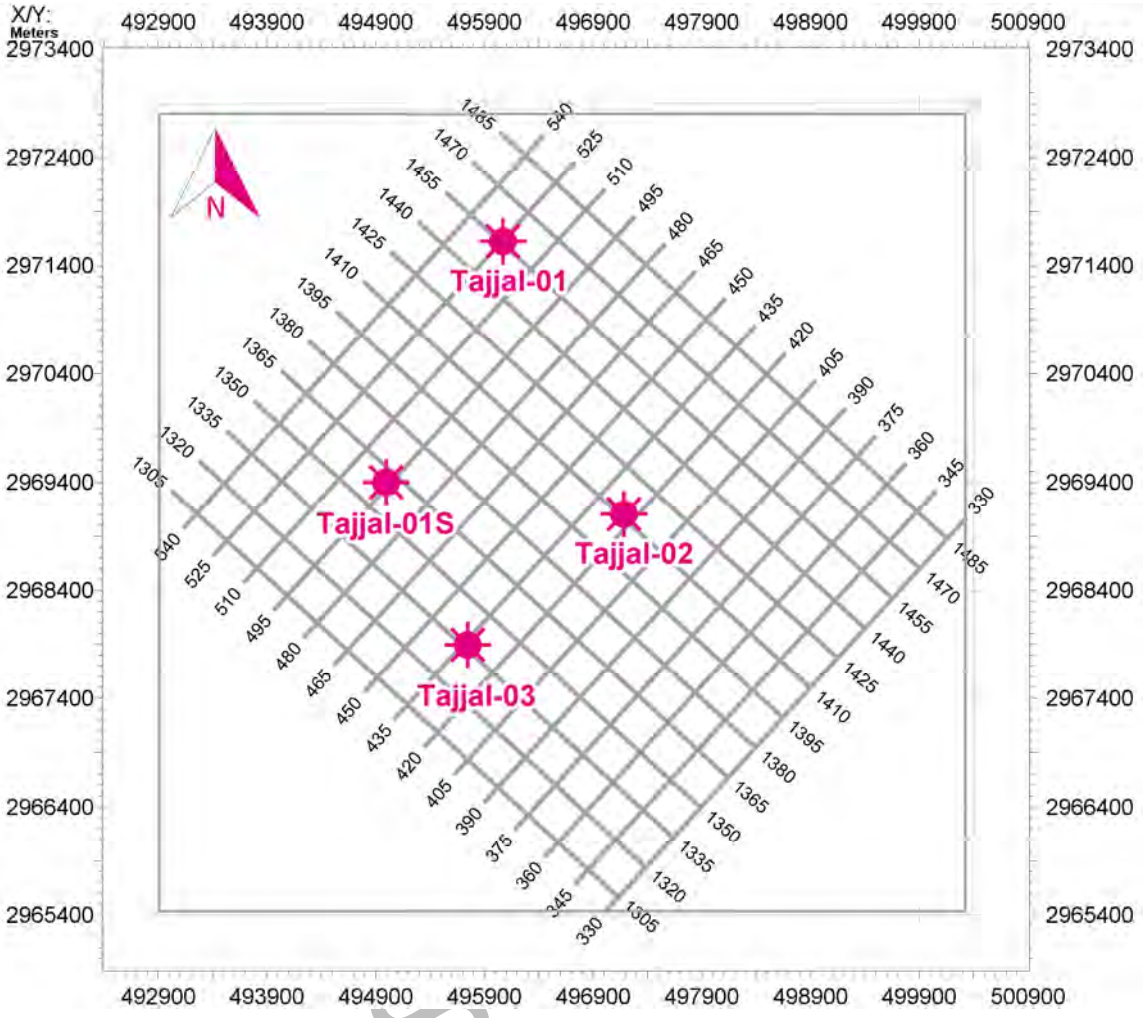

Figure 3.1: *Base map of the study area.*

where; ρ_1 and ρ_2 are the densities and V_1 and V_2 are velocities These are densities and velocities of under and upper layers respectively (Dobrin et al.1990). Synthetic seismogram x (t) is created by convolving source wavelet s(t) with earth reflectivity series r(t) represent the acoustic impedance contrast in the layered earth model (Keary et al.,2002).

$$x(t) = s(t) * r(t) \tag{3.2}$$

where x(t) is synthetic seismogram, s(t) is source wavelet and r (t) is reflectivity series. In synthetic model multiples incorporated or either not incorporated. Ray tracing method is used for creating furthermore complex model. In figure synthetic seismogram of well Tajjal_02 shown as under in figure 3.3.

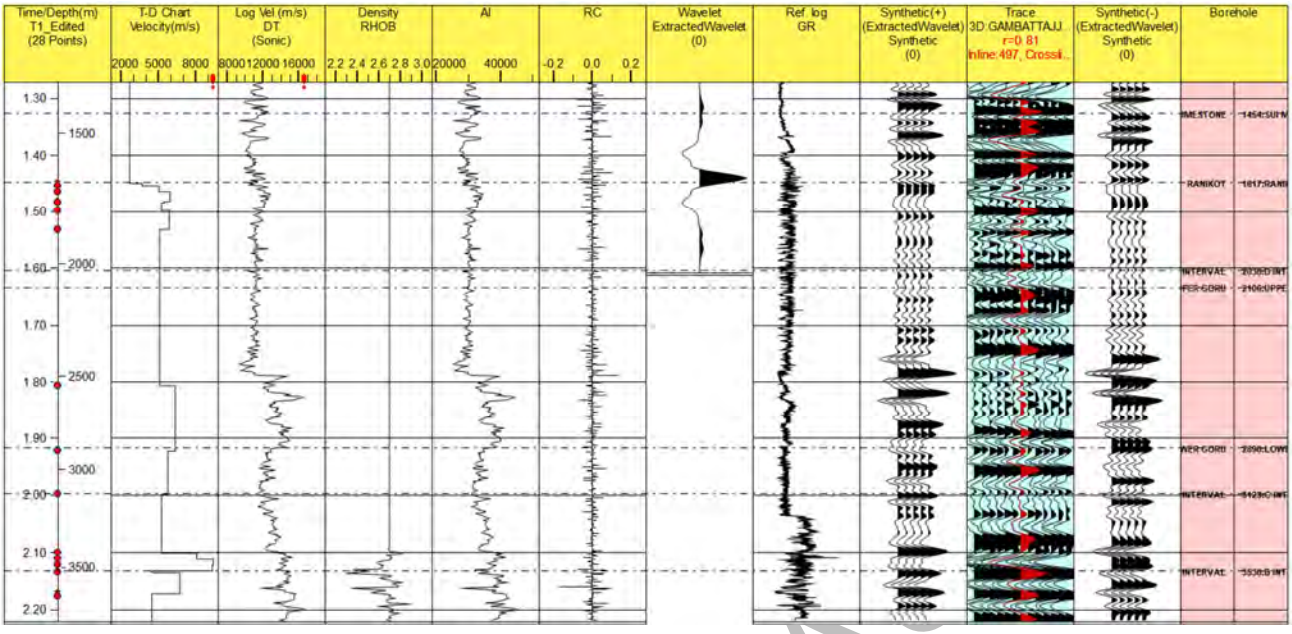

Figure 3.2: Synthetic Seismogram Tajjal-1 well.

3.5: Faults Marking and Horizon Picking

The seismic horizon interpreted and identified by applying available formation tops information. So, the interested formation is marked the upper and lower Goru. On seismic section these two formation are interpreted while shale line is marked at about 2.1 second in between these formations which separate upper and lower Goru formation using well data of Tajjal _01. On basis of lithology features lower Goru formation is further divided into different intervals. On the seismic section Normal faults are also interpreted in extensional tectonic. The direction of marked fault is NE-SW. Variance attribute was applied to seismic volume in order to locate the fault surfaces and attribute is displayed to show the structural variation and fault propagation in area which shown in figure.

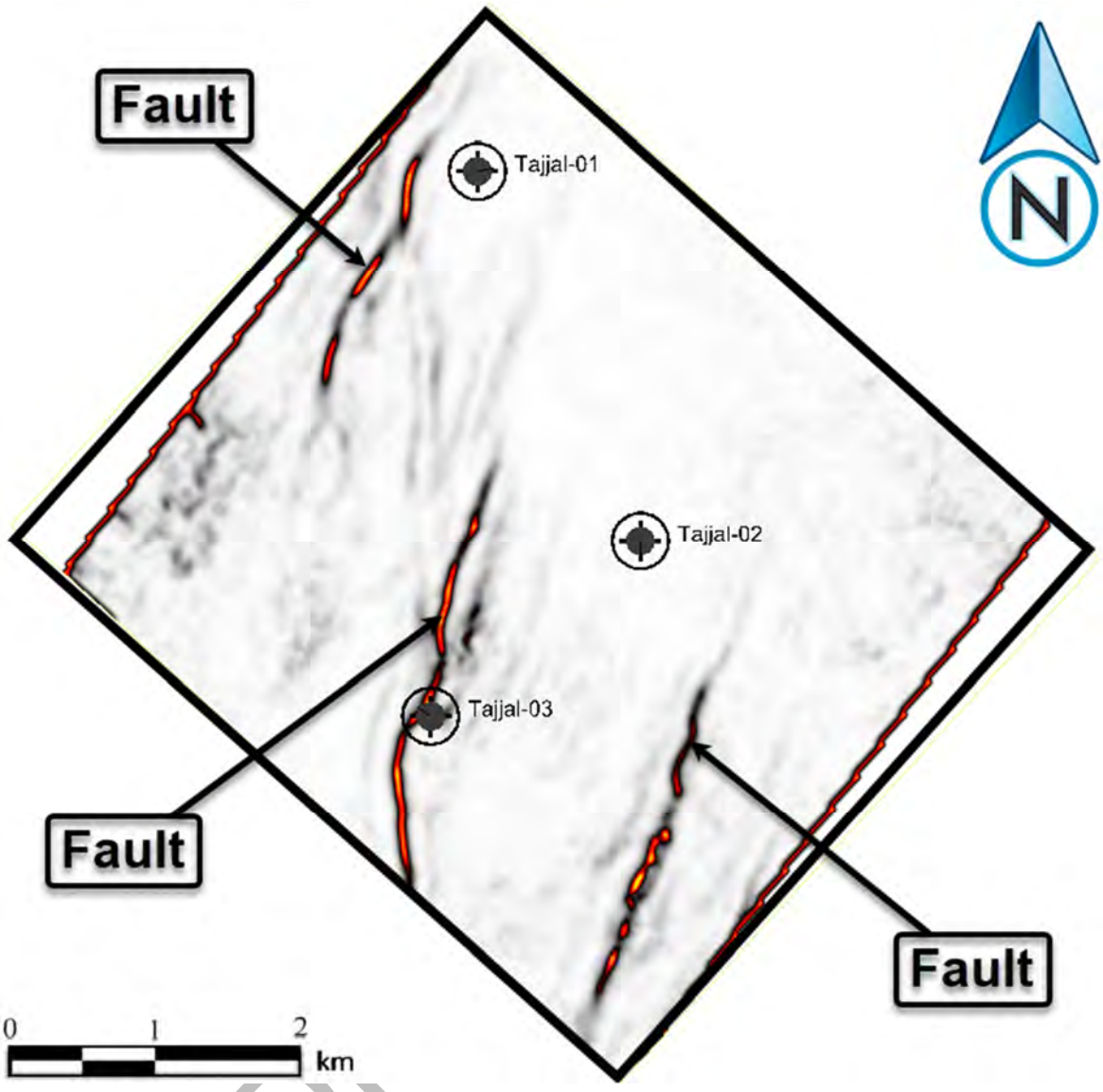

Figure 3.4: showing the variance attribute

3.5.1 Arbitrary Line Passing through all wells

An arbitrary line was marked on base map in order to correlate all wells in the cube. The well Tajjal-01 is present on inline 1454, while Tajjal 02 lies on inline 1455 and Tajjal 03 on inline 1444. Different Horizon in lower Goru like interval A, B and C are label with various colour are marked based on synthetic seismograms generated on each well. Furthermore, DT and GR logs are also run along the boreholes to confirm the tops with seismic horizons marked. The figure 3.4 shows the seismic amplitude change in decibel(db).

3.6: Fault polygon and Grid generation:

The polygon is used to present the horizontal extension of fault or regional trend of fault plane. All of the related faults on individual horizon. Fault polygon is generated at B-interval by digitizing all the marked fault traces on the base map at different inlines on which fault are marked in order to

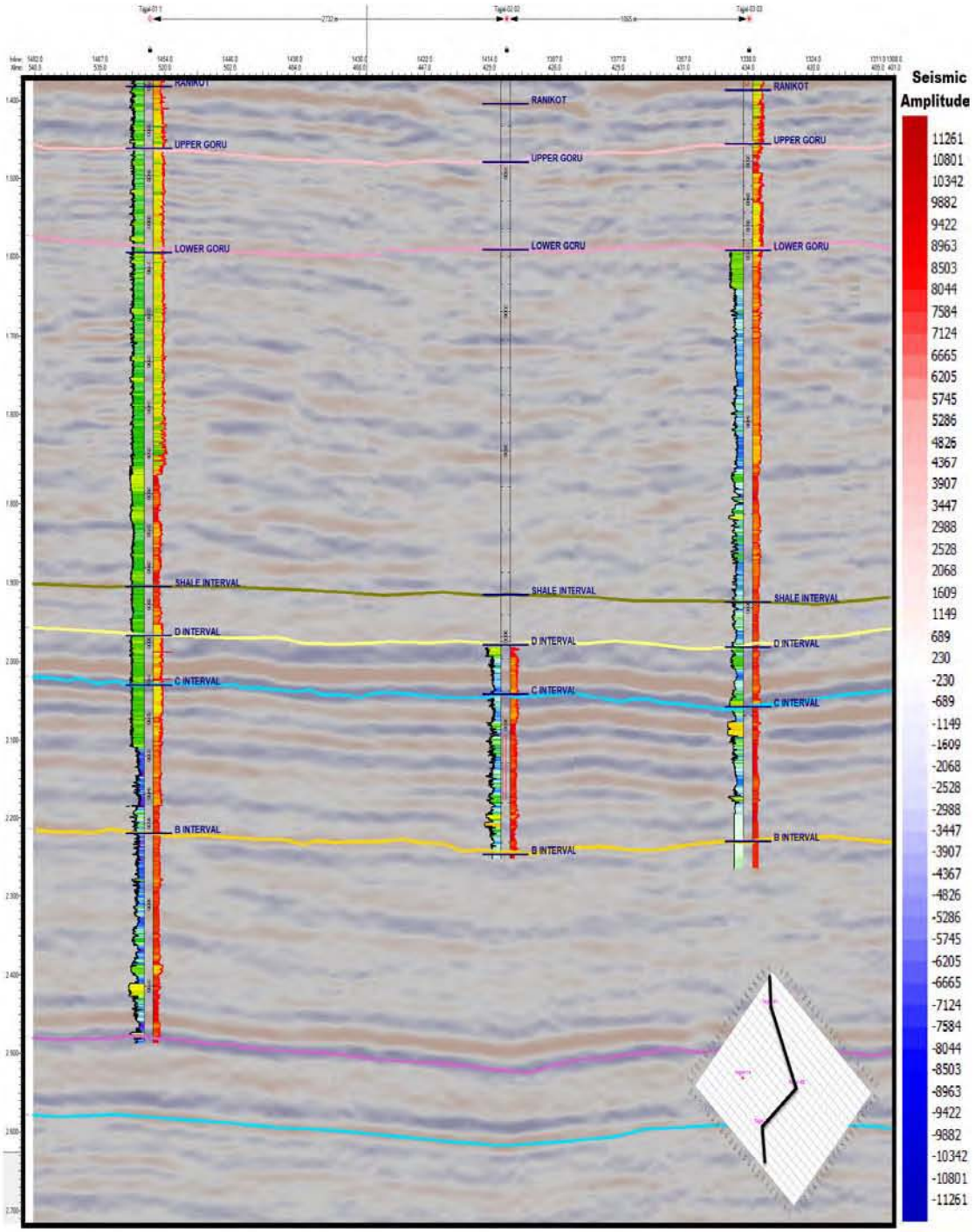

Figure 3.5: *Seismic to well tie on an arbitrary line passing through all wells shown on base map.*

encompass all the faults in contour maps. Faults polygon and time grid for B and C interval is shown in figure 3.4 and 3.5 respectively.

Before depth or time contouring, to interpolate the values for missing points grids are created. The change occur in any physical parameter the grids tells us about like change occur in depth, time is permanently or spatially. After digitizing the 3D cube the Grid are created at the interest ed horizon of all the interval. Time grids for B-interval and C interval are generated in which times varies from 2.29-2.401 seconds and 2.12-2.18 seconds respectively.

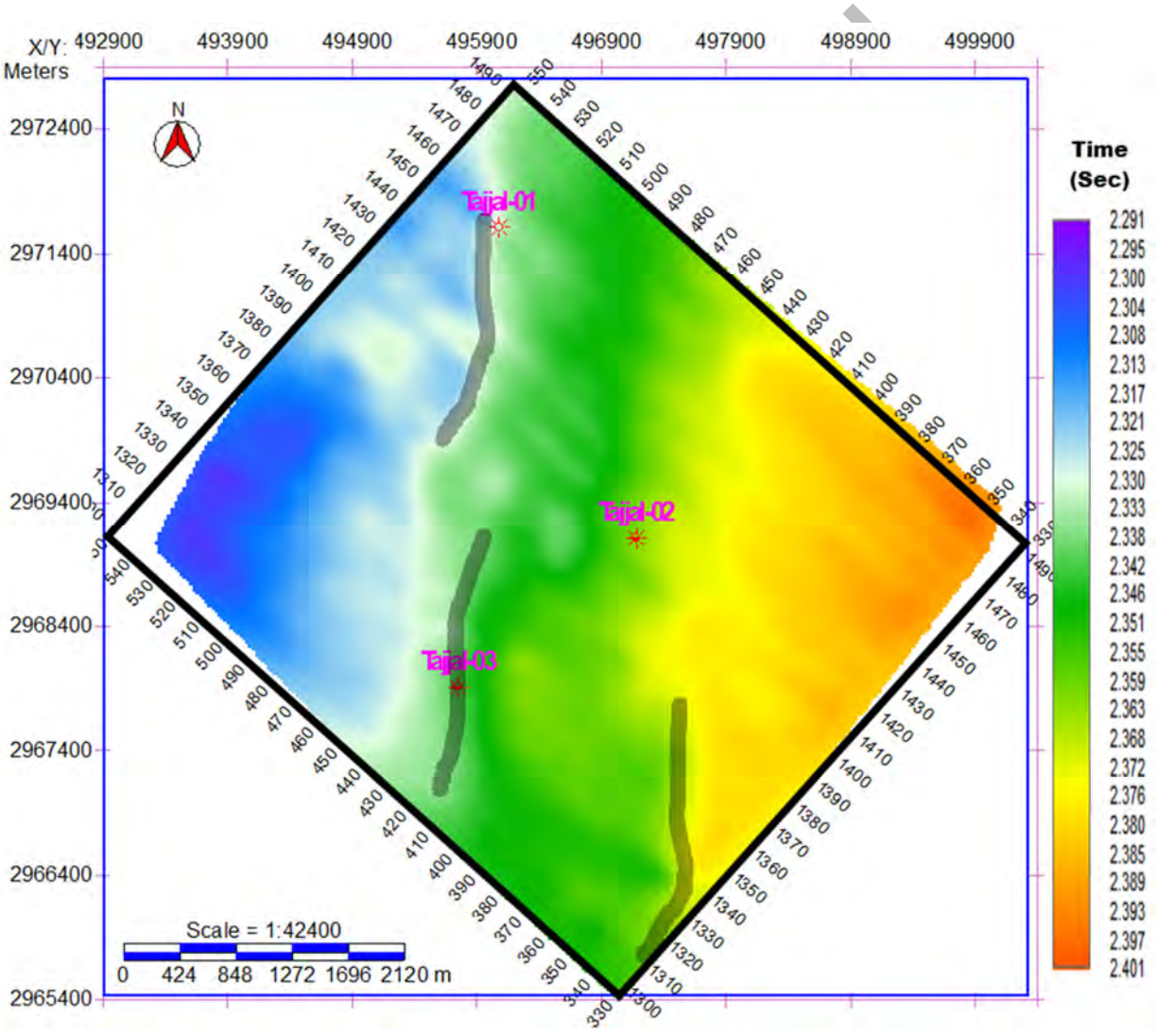

Figure 3.6: *Grid of time for B interval.*

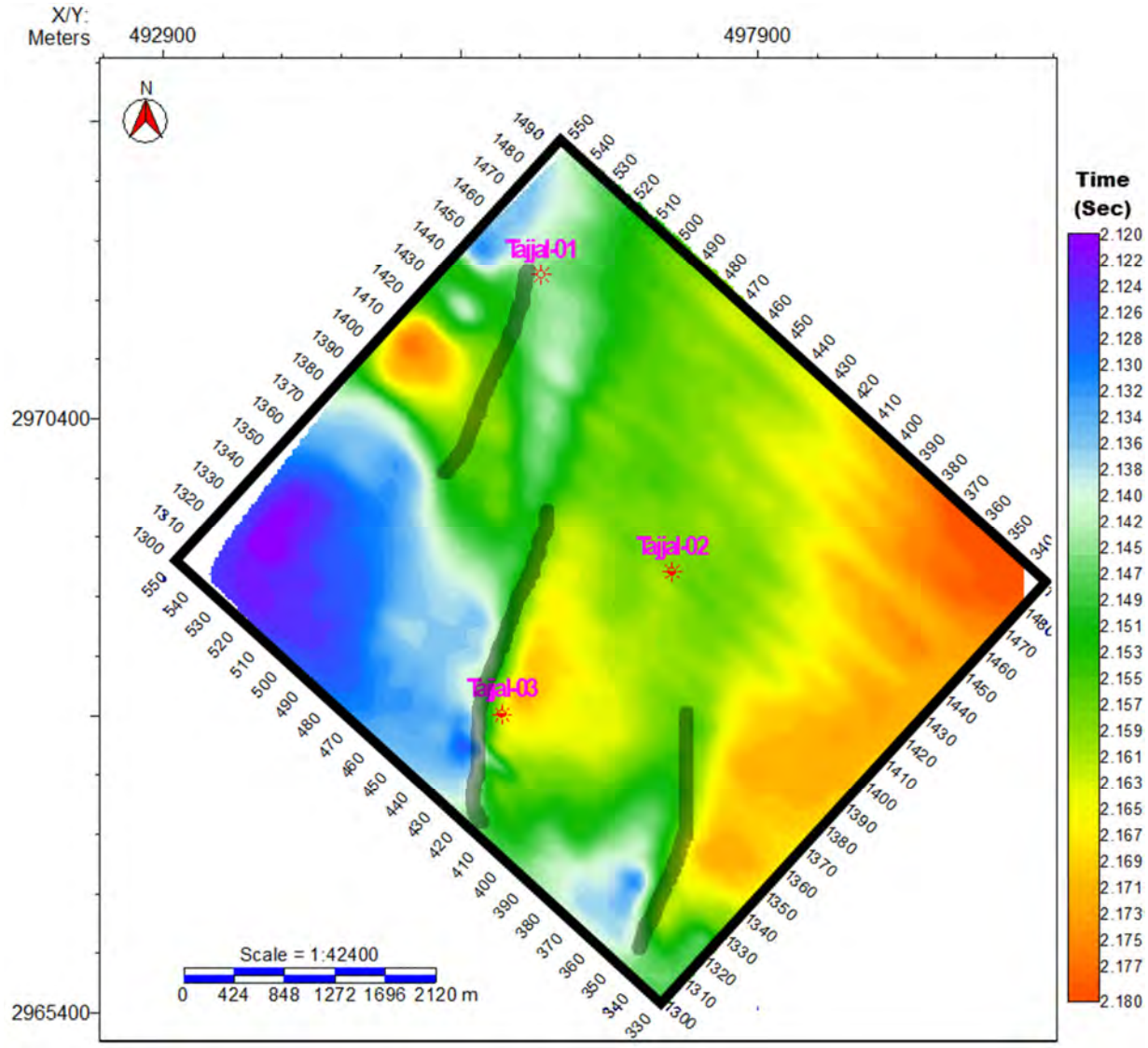

Figure 3.7: *Grids of time for C interval.*

3.7: Contour Mapping

The lines have point of same physical properties in space and time is called contours. Time-depth maps of B and C interval show the position of horizon and the type of structures formed at these horizons in time and depth domain respectively.

3.7.1: Time Contour map of B-interval

Time of lower Goru B-interval varies from 2.39 to 2.52 seconds and the depth varies from 3607 to 3804 meters as shown in figure 3.7 and 3.8 respectively, 0.002 seconds and 4.4 meters are the contour interval in time and depth contour maps, respectively.

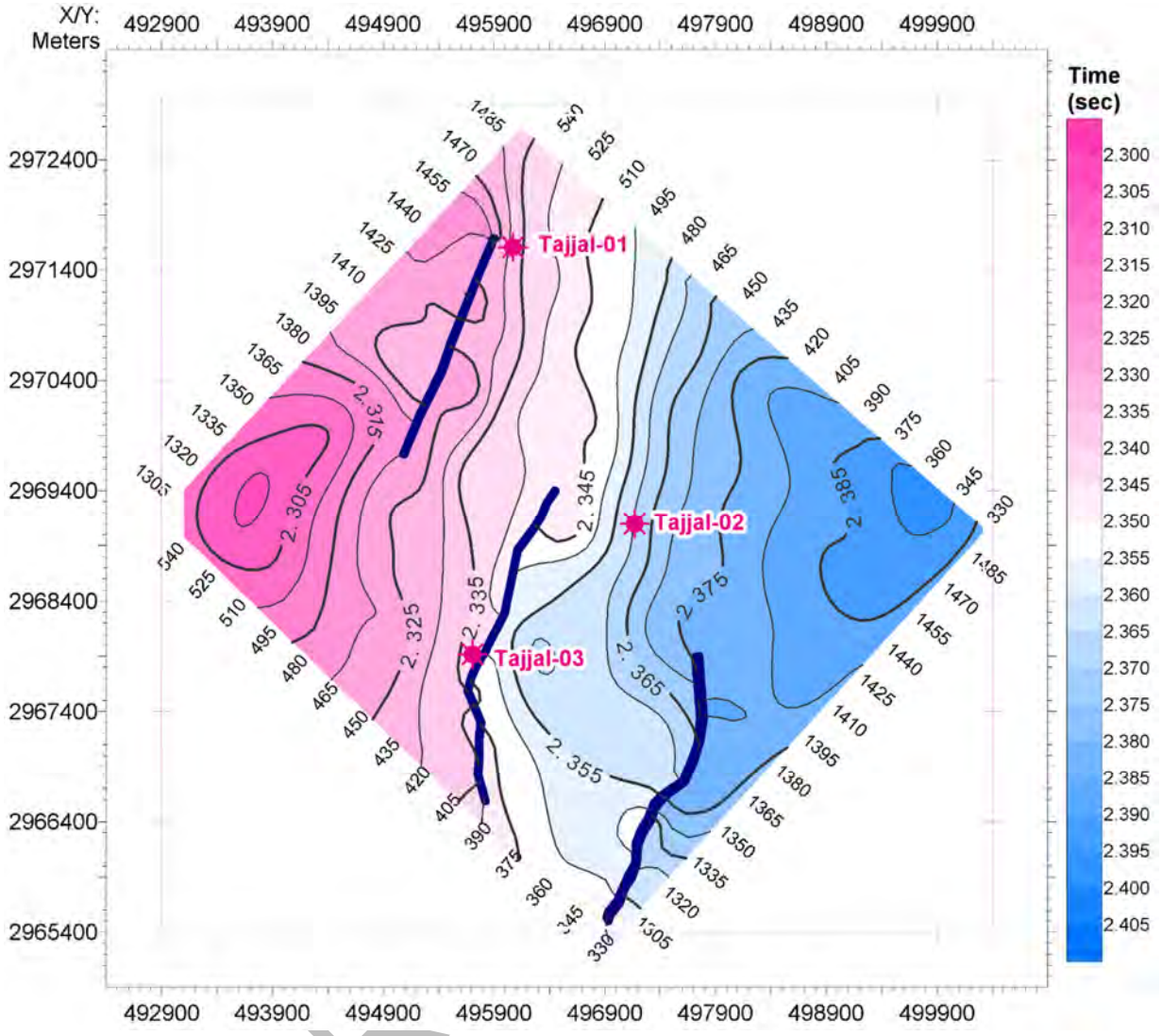

Figure 3.8: Time Contour Map of B-interval

3.7.2: Time Contour map of the C-Interval

Time of lower Goru C-interval varies from 2.39 to 2.52 seconds and the depth varies from 3607 to 3804 meters as shown in figure 3.8 and 0.002 seconds and 4.4 meters are the contour interval in the time and depth contour maps, respectively.

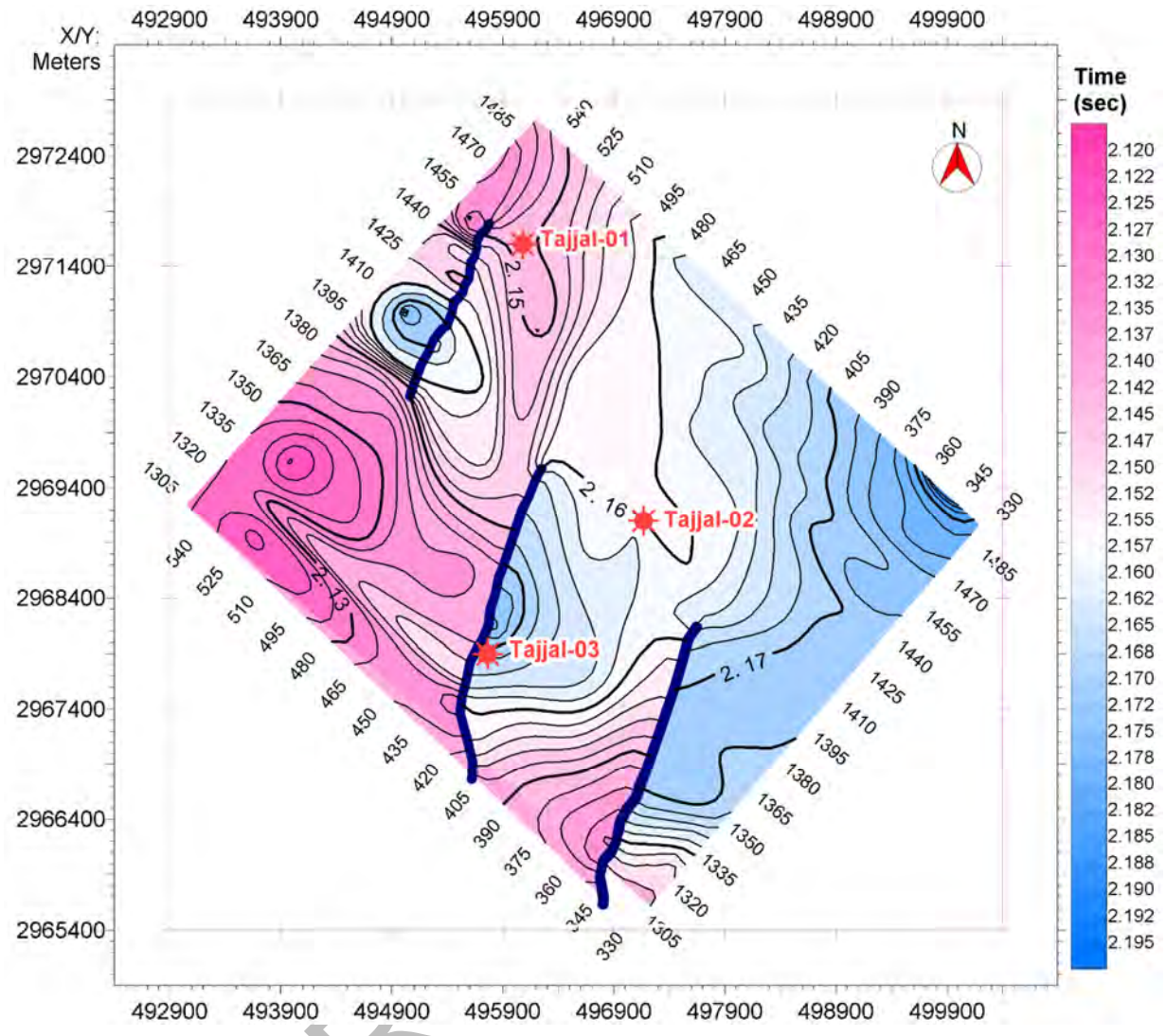

Figure 3.9: *Time Contour map of C-interval*

3.7.2: 3D Structural Trapping and Grids of Study area

3D view best explains the subsurface scenarios especially for finding prospect or drilling points. In the following 3D view of structural interpretation of the study is presented which depicts a clear half graben of faulted zones of Goru formation which shown in figure 3.9 and 3.10.

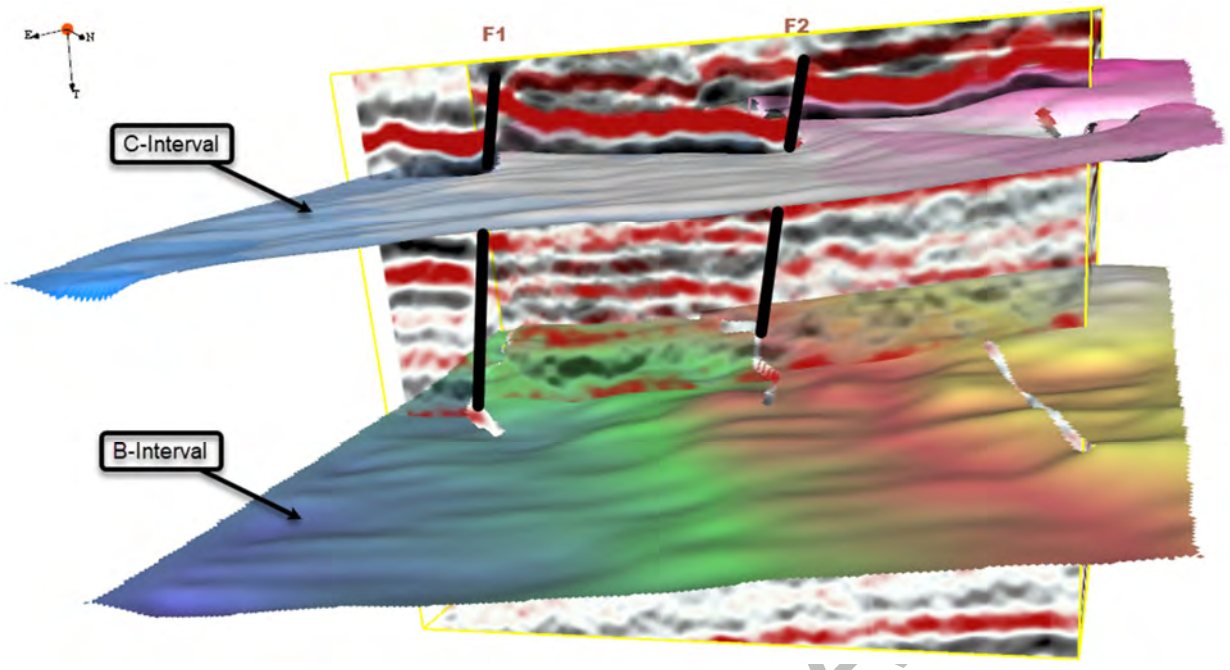

Figure 3.10: *3D Structural Trapping and Grids of Study area*

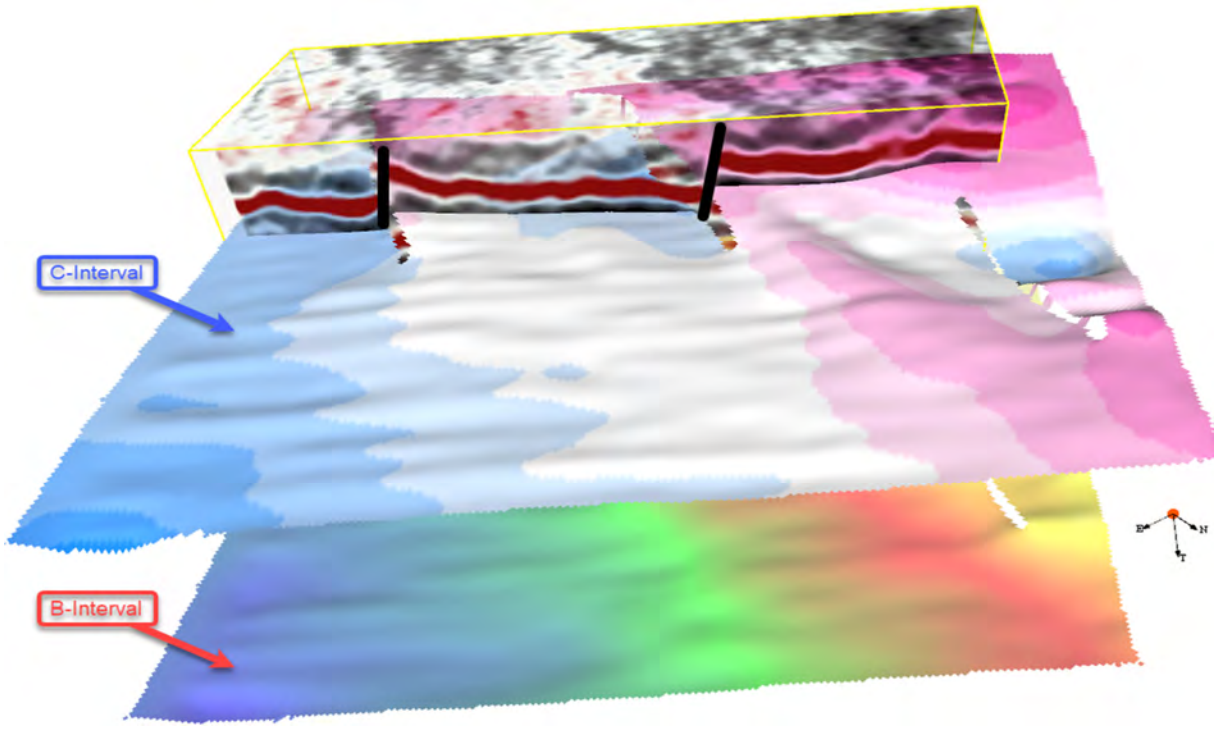

Figure 3.11: *3D Structural Trapping and Grids of Study area*

CHAPTER 04

PETROPHYSICAL ANALYSIS

4.1 Introduction to petrophysics

The relation of Petrophysical Interpretation to quantitative study of rock properties and their interaction with fluids inside them. In Petrophysical Interpretation measures resistivity, density and porosity for the estimation reservoir quality. Petrophysical Interpretation is also used for the hydrocarbon saturation (Sh), volume of shale (Vsh), calculation of total porosity (PHIT) and Water Saturation (Sw). Petrophysical Interpretation is interplay of fluids and rock properties of formation. Petrophysical Interpretation is used to find the network of pores in the rock skeleton, Saturation of hydrocarbon in the void spaces and the potential of rock to flow fluids through pores network. For the good characterization of reservoir formation require physical sample, magnetic, chemical, nuclear and electrical reading build through wire-line sondes, coring, and logging. Well logs data need the knowledge of geophysics, geology, electronic, drilling instrumentation, geochemistry and geo-mechanics. The hydrocarbon industry develops different technique used for the evaluation of formation is acquisition and interpretation techniques but these techniques are also used for environmental study, mining coal and hydro-geology. However, the measurements are influenced by borehole environment and condition (Cannon, 2015).

Logs are divided into three different general types.

- Resistivity logs
- Nuclear logs
- Sonic or Acoustic logs

The petrophysical logs are divided into following types:

4.1.1: Porosity Logs

Porosity logs are further divided into three different logs which commonly used for the measurement of formation acoustic response.

- Density Log (RHOB)
- Sonic Log (DT)
- Neutron Porosity Log (NPHI)

These logs are run in track 03.

4.1.2: Lithology Logs

Lithologies are determined by:

- Caliper Log
- SP-Spontaneous Potential Log
- GR-Gamma Ray log

These logs are run in track 01.

4.1.3: Resistivity or Electrical Logs

- MSFL-Micro Spherically Focused Log
- LLD-Deep Later log
- LLS-Later log Shallow

4.2 Log Derived properties Analysis:

Log derived properties analysis are explained one by one as under.

4.2.1 Gamma Ray Logs

The Gamma ray sonde measured the radioactive material like potassium, Uranium and Thorium etc. API (American Petroleum Institute) is the unit of GR log. For the estimating of Shale or clay volume the GR log is used. The GR Sonde is ability to measure the emitted radiation from bore hole with help of scintillation counter of sodium lodide. Shale are made up of 50-70 percent of clay mineral like kaolinite, smectite and illite etc .Gamma ray log measure the natural radioactivity of the formation while SP log is influence by formation water resistivity (Rw).GR log have higher value in shale formation as compared to other formation like sandstone and carbonates show low valve because shale have higher value of radioactive concentration. The calculation Gamma Ray index (GRI) is the early step in to evaluate volume of shale. There are two method to calculate the Volume of shale:

a. Linear Method

GRI can give us maximum volume of shale and we must find minimum volume of shale by non-linear method.

$$GRI = Vsh = \frac{GR_{LOG-GR_{min}}}{GR\_GRmin} \quad \text{(Senosy et al.,2020)}$$

Whereas,

GRI is the Gamma-Ray Index

GRlog is the Gamma-Ray reading of formation log

GR_{min} is the Minimum Gamma-Ray (Clean Sand and carbonates)

GR_{max} is the Maximum Gamma-Ray (Shale)

Non-linear relation changes with geographic areas or with age of the formations. The non-linear relation gives shale volume less than linear relations (Asquith and Gibson, 1982).

b. Non-Linear Method

In non-linear method we have various formula with help of which we can calculate minimum volume of shale.

Some non-linear relations are:

- Larionov (1969) for Tertiary rocks

$$V_{sh} = 0.083 * (2^{3.71GRI} - 1) \quad (4.2)$$

- Larionov (1969) for older rocks

$$V_{sh} = 0.33 * (2^{2GRI} - 1) \quad (4.3)$$

- Stieber (1970)

$$V_{sh} = 1.7 * [3.38 - (GRI - 0.7)2]1/2 \quad (4.4)$$

4.2.2 Spontaneous Potential

SP log work on the voltage of direct current. SP tool have fixed electrodes at the surface and these is also transferable in the well. Units for the measurement is milli-volts(mV).Due to the salinity of water in formation and filtration of mud within permeable beds the tool give response of the electro-chemical changes between borehole fluids. The SP log response is almost constant or straight line in case of

impermeable shale rocks .If the salinity is less than formation salinity of mud filtrate the deflection is negative to the left (Rmf>Rw) and if the Rmf <Rw the deflection is positive toward right of the shale which show permeable formation. These deflections of log magnitude are not related to permeability but response due to the differences in fluid resistivity.

SP log identified the permeable beds and also their respective boundaries, which also calculate clay or shale volume, and resistivity of formation water. The log action is caused by filtrate invasion, clay or shale presence, thickness of beds formation, hydrocarbon content, borehole diameter and formation resistivity (Doll, 1948). From SP log shale volume can be calculated by:

$$Vsh = \frac{PSP - SSP}{SP_{sh} - SSP} \quad (4.5)$$

OR

$$Vsh = 1 - \frac{PSP}{SSP} \quad (4.6)$$

Whereas,

V_{sh} is volume of shale.

SP_{sh} is Value of spontaneous potential (SP) in shale (usually assumed zero)

SSP is static spontaneous potential (clean sand or carbonates show maximum value)

PSP is Pseudostatic spontaneous potential (Shaly formation show Maximum value)

4.3 Calculation of porosities

Porosity can be calculated with the help of porosity logs, it can measure porosity indirectly, The log are used for the determination of porosity are:

- Density log
- Sonic log
- Neutron log
- Nuclear Magnetic Resonance (NMR measures porosity within cased borehole)

4.3.1. Density log

For measuring the bulk density the Density log is applied. Sum of fluid density and rock matrix is called bulk density. The measurement unit is used is gram per centimeter cube (g/cc).Its symbol is þ (Rho).The scale of density log is generally 1.95 to 2.95 g/cc. Gamma rays work as a source which produce by density logging tool within the formation.Cesium-137 or Cobalt-60 are sources for Gamma rays .Calculating the density porosity with help of formula is:

$$\emptyset D = \frac{\rho_{ma} - \rho_b}{\rho_{ma} - \rho_{ft}} \quad (4.7)$$

whereas,

$\emptyset D$: Density derived porosity

ρ_{ma} : Matrix density

ρ_b: Formation bulk density

ρ_{ft}: Fluid Density

4.3.2. Sonic log

Sonic device measure through 1 feet of formation by sound compressional waves traveling transit time. Sonic device is the composition of two or more receiver and one or more transmitters (Kobesh and Blezard, 1959).One of the modern Sonic logs tool are Borehole compensated (BHC) which reduces the spurious outcome of washouts and sonic tool tilting in the borehole ,also size changes as well(Schlumberger, 1989).

The transit travel time in microseconds per feet is the inverse of compressional wave velocity in feet per seconds. Both lithology and porosity effect interval travel time of the sonde. For calculating sonic porosity we will use formula for the formation matrix velocity:

$$\emptyset_{sonic} = \frac{\Delta t_{log} - \Delta t_{ma}}{\Delta t_f - \Delta t_{ma}} \quad \text{(Wyllie et al., 1950)} \quad (4.8)$$

Whereas,

$\emptyset_{sonic}$: Sonic derived porosity

Δt_{log} : Interval transit time of formation

Δt_{ma} : Interval transit time of the matrix

Δt_f : Interval transit time of fluid in the formation

This formula is used for inter granular porosity of carbonates (limestone Dolomite etc.) and consolidated sandstones. In case of carbonates rock to calculate the %age of fracture or vuggy porosities we can subtract sonic from total porosity.The formation delay time is increase due to hydrocarbon that is also called hydrocarbon effect. This type of outcome can affect the estimated porosities,so it should be removed. Sonic devices are design for the measuring inter granular and matrix porosity that is why the value in carbonates will be low. As we know that a fracture causes secondary porosities and the Secondary porosity Index (SPI) is effective in carbonates rocks. By adding compaction factor (Cp) in sonic logs is also useful for estimating porosities in un consolidated sandstones. The equation for estimating porosities in unconsolidated sandstones as:

$$\emptyset_{sonic} = \frac{\Delta t_{log} - \Delta t_{ma}}{\Delta t_f - \Delta t_{ma}} * 1/cp \quad \text{(Wyllie et al., 1950)} \qquad (4.9)$$

where,

Cp: Compaction factor = ($\Delta tsh * C$)/100

C is constant normally taken as 1.

4.3.3: Neutron Porosity

The neutron logs measured hydrogen index. The hydrogen index is the accumulation of hydrogen gas in a formation. The neutron logs estimate the the pores filled with fluids directly. The source of hydrogen is either hydrocarbon or water. Due to accumulation of hydrogen in gas filled pores can decrease value of porosity to low due to absorption of hydrogen in gas is fewer compare to oil and water. This is also called gas effect. When the neutron log value is decrease to low value a crossover is made with density (RHOB) log in the zone of gas bearing.

4.3.4: Effective Porosity

Effective porosity is always less than Total porosity. In Effective porosity the pores which are occupied by shale or clay are not included. The whole Porosity and effective porosity are same in clean sands. Mathematically the equation is:

$$\emptyset_e = \emptyset_{avg} * (1 - Volume\ of\ shale) \quad (4.10)$$

Whereas,

$\emptyset_e$ = used Effective Porosity

$\emptyset_{avg}$ = Total Porosity

VSH : Volume of Shale Rock

4.3.5: Total Porosity

Total or average porosity is the cumulative sum of various logs. From all the logs derived porosities calculate to reduce the error in estimation of porosity. The equation used for calculating average porosity:

$$\emptyset_{avg} = \frac{\emptyset_D + \emptyset_N + \emptyset_{sonic}}{3} \quad (4.11)$$

$\emptyset_D$: Density Porosity

$\emptyset_{sonic}$: Sonic Porosity

$\emptyset_N$: Neutron Porosity

4.4 Calculating Formation Water Resistivity

The different parameter is used in the header of Tajjal-01 well to calculate the water resistivity of formation are:

- Borehole Temperature (BHT)
- Total Depth (TD)
- Surface Temperature (ST)

- Resistivity of mud filtrate (Rmf)
- Formation depth (TD)

The equation for calculate Static Spontaneous Potential (SSP) is given below:

$$SSP = (SP_{clean} - SP_{shale})$$

Whereas,

SSP : Static Spontaneous Potential

SP_{shale} : Spontaneous Potential for shale

SP_{clean} : Spontaneous Potential for sands

4.4.1: Formation Temperature

Using formation depth equation to estimate the formation temperature.

$$FT = [\frac{BHT-ST}{TD} * FD + ST] \quad (4.12)$$

Whereas,

FT: Formation Temperature

BHT: Borehole Temperature

ST: Surface Temperature

FD: Formation Depth

TD: Total Depth

4.4.2: Rmf_2 Calculation

Now we can calculate the resistivity of mud filtrate.

$$Rmf_2 = \frac{ST + 6.77}{FT + 6.77} * Rmf_1$$

Whereas,

Rmf_2 = Resistivity of mud filtrate at formation temperature (FT).

Rmf_1 =Resistivity of mud filtrate at surface temperature (ST).

ST: Surface Temperature

FT: Formation Temperature

We use the relation for correction if Rmf_2 value is greater than 0.1 ohm meter.

The equation for correction as under:

$Rmf_{eq} = 0.85 * Rmf_2$

If the value below 0.1 ohm-meter, use Schlumberger chart (SP-02).

4.4.3: Calculation of Water Saturation (Sw)

Water saturation can be calculated by having resistivity of water (Rw) and the true resistivity of formation. The number of pores occupied by water in formation is called water saturation. Saturation of water can be calculated by SP static, water salinity (ppm), bottom hole temperature and surface temperature (Amigun et al., 2012).

4.4.4: Calculation of Hydrocarbon Saturation (S_h)

The hydrocarbon present in the pores spaces is known as hydrocarbon saturation. As we can determine the important value of S_w, in un-invaded zone it can leads to S_h.

$$S_h = (1- Sw) \quad (4.13)$$

Whereas,

S_h: Hydrocarbon saturation

Sw: water saturation

4.5 Petrophysical Analysis of Tajjal_01, 02 & 03

Petrophysics was carried out by examining the behavior of various log curve displayed in different scales and logs. Gamma Ray, Spontaneous Potential and Caliper log are first track logs.

A Gamma Ray (GR) log is useful for the determination between the formation of non-sandy and sandy. Caliper log is used to measure the shape and size of the borehole. Spontaneous Potential is the ability to detect the formation salinity, permeable beds and formation clay content which is based on salinity contrast between drilling mud and formation mud. For the formation water resistivity and oil water contact the Laterlog Deep and Laterlog Shallow logs Separation is used.The logs are used for the determination of porosity are Sonic log (DT), Neutron Porosity Log (Np HI), Density Log (RHOB).Considering the different logs response at reservoir level in well Tajjal_01,B and C interval of lower Goru formation properties are quantified.

4.5.1. Petrophysical Analysis of B & C-intervals of Tajjal 01, 02 and 03.

Depth of B interval ranges from 3659 m to 3838m.On the basis of different crossover formed in track-01 and track -02, probable zone of hydrocarbon is marked in figure 5.1 and calculated parameters is shown in table 5.1 and 5.2:

Petrophysical Results B & C Interval							
Well Name	Thickness (m)	Gross-Sand (m)	Net- Sand (m)	Av_SW (%)	Net Pay Zone (m)	PhiE (%)	Total H/C (%)
C-Interval							
Tajjal-01	3460-3659	199	120.626	26	7.125	9.1	74
Tajjal-02	3483-3671	188	42.250	81	5.375	7	19
B-Interval							
Tajjal-01	3659-3838	179	37.125	27	24.375	15-6	73
Tajjal-02	3671-3900	229	56.250	79	11.625	8.3-9.3	21

Table 4.1: Petrophysical Results Tajjal-01 and 02.

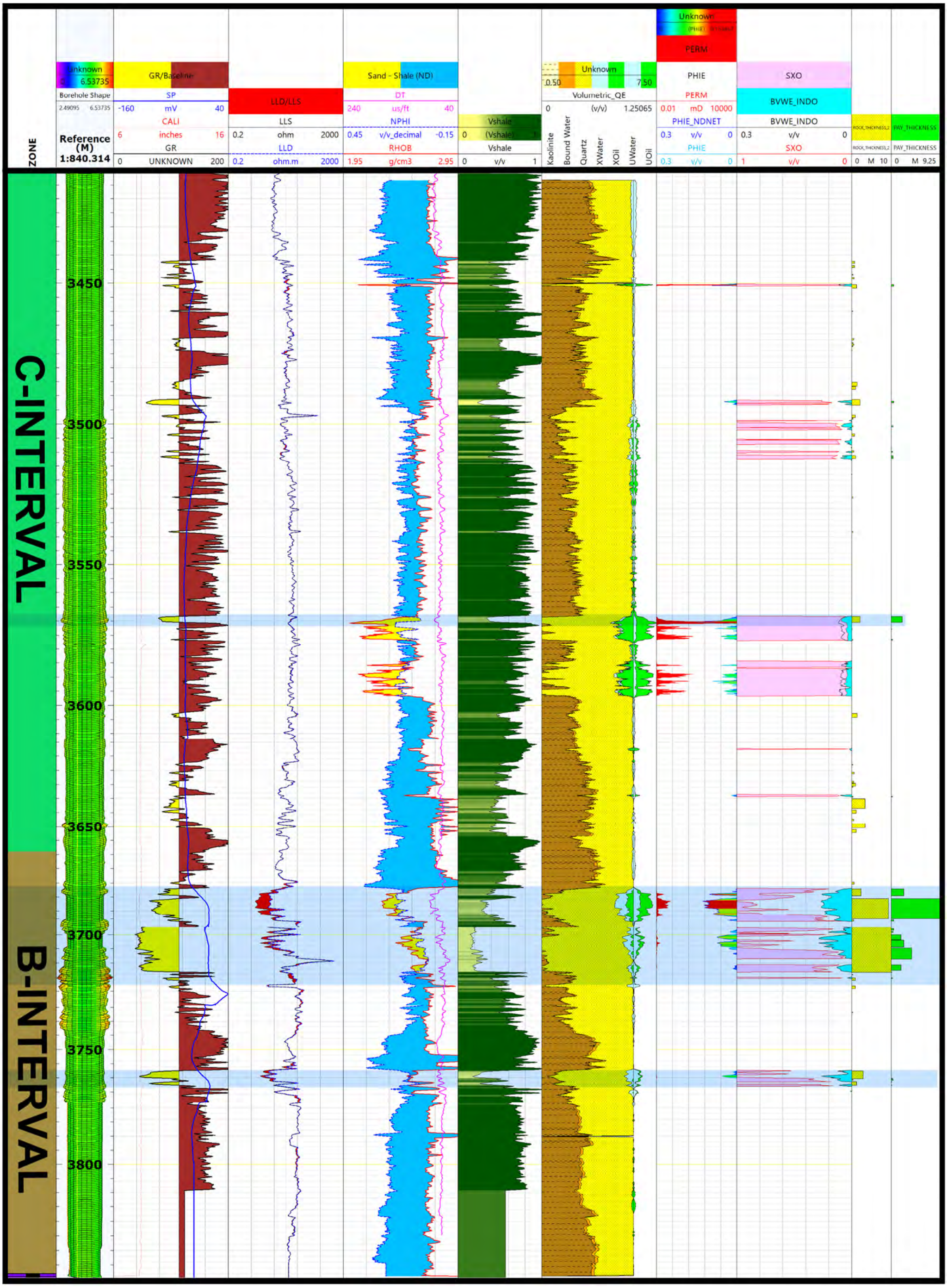

Figure 4.1: Petrophysical Results Tajjal-01

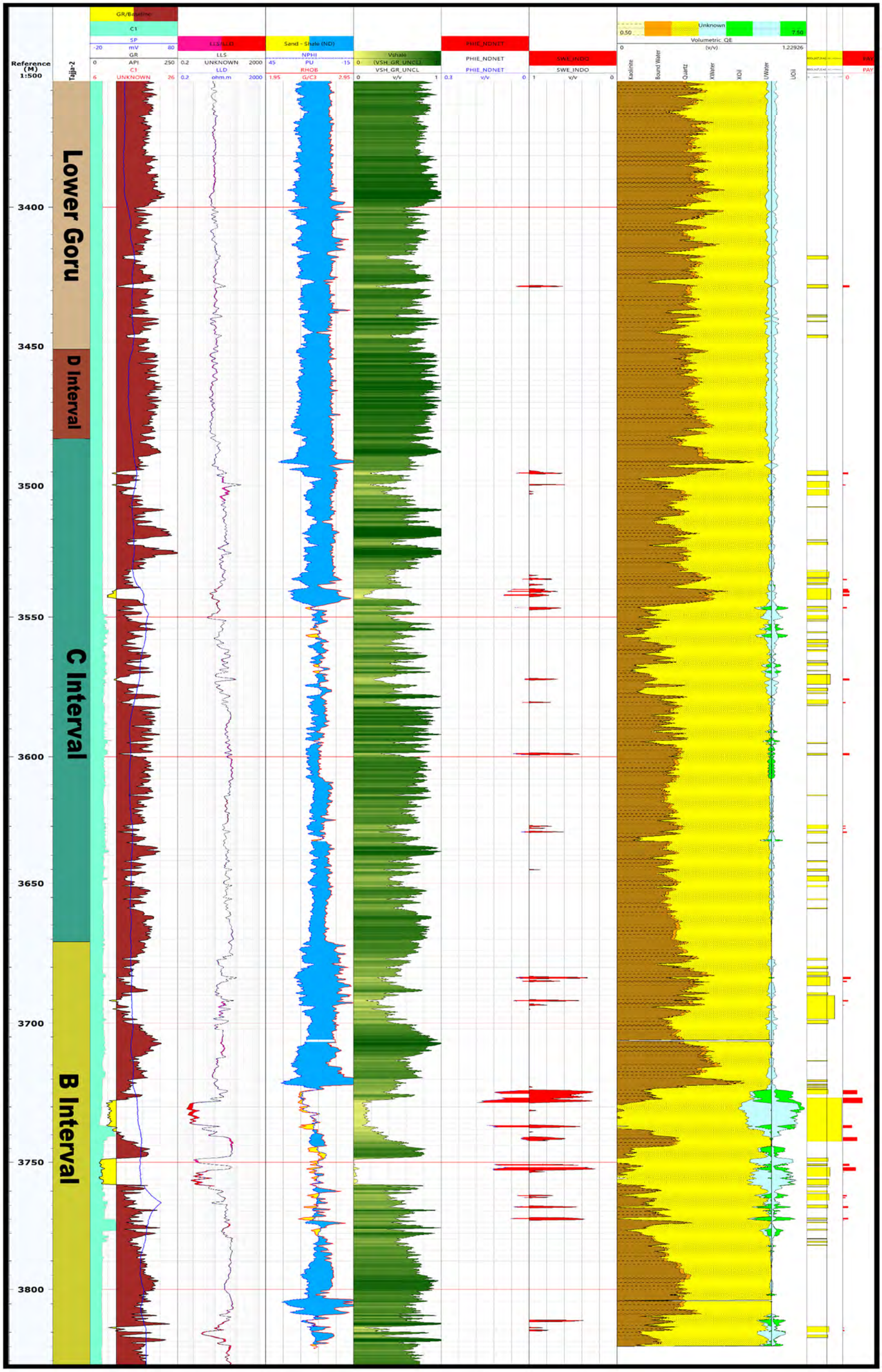

Figure 4.2: Petrophysical Results Tajjal-02

Chapter 05

INVERSION ANALYSIS

The converse process of forward modeling is called Seismic inversion. Inversion can result the Acoustic Impedance through the conversion of reflectivity data. The acoustic impedance is layer while the reflectivity is an interface property. Inversion is a mathematical way of evaluating a problem, checking it and improve it up to the problem is acceptable (Barclay et al., 2008).The earth reflectivity describe about boundaries whereas acoustic impedance can be converted into useful properties of earth such as fluid saturation and porosity. Before applying Inversion, we check the data quality because inversion depends on it for a proper wavelet extraction. Acoustic impedance is the type of inversion which gives best result as compare to interpretation of data. The important role for the creation of full band data is to obtain low frequency model which is not easy (Latimer, 2011).

For unconventional reservoir the seismic based TOC is important for the estimation. and also for the evaluation of shale/gas potential or the analysis of shaly rock, thermal maturity (Rickman et al., 2008). As we know that logs play an important role within source rock. The result of well logs of source rock which is totally different from reservoir rock (. Beers, 1945; Swanson, 1966; Passey et al., 2010).

5.1 Methodology:

It is used to make synthetic seismic at wells when models of velocity and density that change with depth are used to figure out how to make it. Acoustic Impedance of the subsurface is made by product of two models. The impedance model is made for a seismic trace that is almost vertical. This is how the density and velocity model figure out the reflection coefficient (RC) series. This Reflection Coefficient series is then convolved with a wavelet as shown in the figure (5.2). From the seismic, this wavelet is taken out. It looks like this in Figure: (5.2). In this example, we'll compare a synthetic trace with a seismic trace that shows where the geological layers are (Sheriff and Geldart, 1995; Dolberg et al.,2000; Veeken and Da Silva,2004).

The product of velocity with the density curve of all 3 wells (Tajjal-001, Tajjal-002 and Tajjal-003), are used for estimation of P-Impedance and also the Reflection Coefficient series are estimated from that P-Impedance. With the wavelet that RC (Reflection Coefficient series) is convolved then from seismic data that's extracted. The end result is the generation of synthetic seismogram. The comparing of the seismic data with synthetic seismogram shows good result with seismic data. The well logging data and seismic data is used to calculated seismic based TOC (Ali et al., 2018).

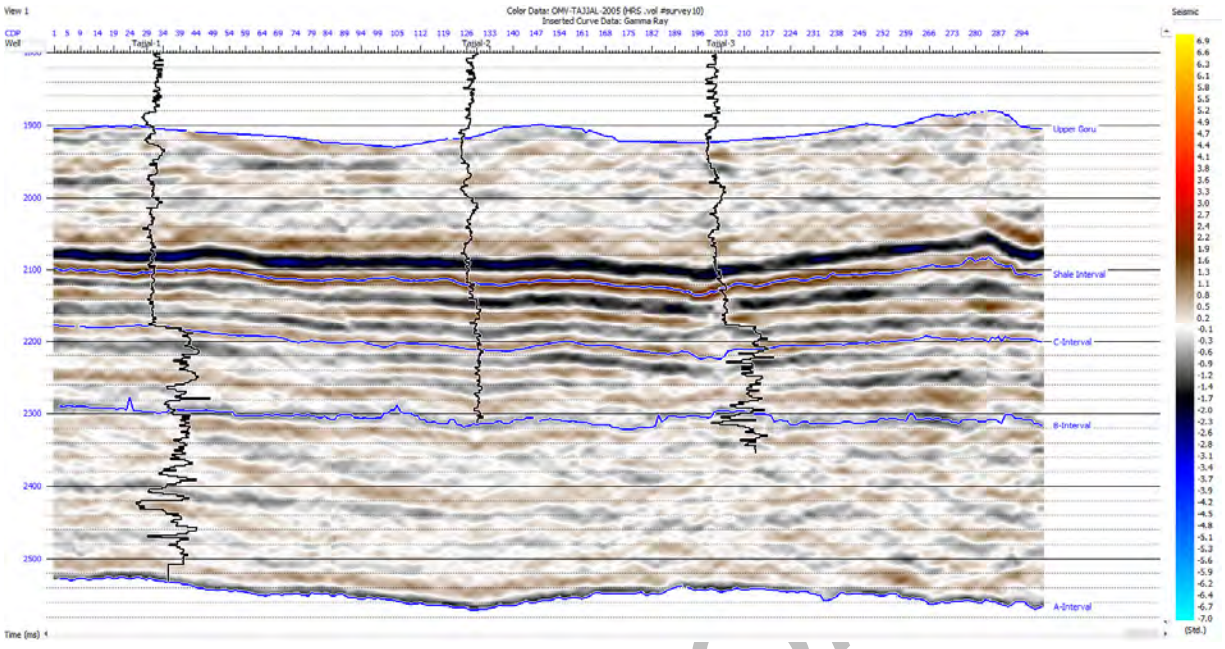

Figure 5.1: Cross-section of Seismic Data used for inversion analysis.

5.2 Post Stack Impedance Inversion*:*

The research work follows two types of inversion analysis by using p-wave impedance on inverted 3-dimensional data.

5.2.1 Building the Initial Model:

Initial model is generated from impedance log and the impedance log is from the well log data. The Initial model is vital role in final outcome of the seismic post stack inversion. The final results based on the primary model and have include the primary model to gain the lower frequency that is dissolute (Lindseth., 1979). Results of both these inversions are nearly similar but model-based inversion is performed at inline from which acoustic impedance is recovered.

5.3 Model-based Post Stack Inversion

In order to increase the resolution, the results in model-based post stack inversion. DT and Density logs are combined with seismic data. Model Based post stack Inversion is highly appropriate method for inverting the reservoir properties through seismic amplitudes data as it minimize the risk of recursive inversion by continuous changing the low frequency

model in order to avoid best least square fit (Russell.,1991).Acoustic Impedance of earth is gained by seismic inversion through which lithological properties can be calculated (Kneller et al.,2013).

5.3.1 Algorithm of Model Based Inversion

Model Based Inversion's basic assumption is to reduce and measure error (Misfit) between the synthetic and real seismic data. Approach used in MB inversion algorithm has a basic purpose to minimize the function which is shown in Equation 6.1 (Gavottiet *et al*., 2014).

$$J = Weight_1 x(S\text{-}W*R) + Weight_2 x\ (M\text{-}H*R) \quad (5.1)$$

Where;

J= Error between the real and Seismic trace which have to reduce upto acceptable level

S= Original seismic trace

R= Reflection coefficient series

W= Extracted seismic trace at well location.

M= Initial guess low frequency geological model or interpreted horizon.

H= Final integration operator which gives the resultant Impedance by convolution with reflectivity series R

5.3.2 Wavelet Extraction Process

In inversion process wavelet has fundamental importance, because it is used in correlation with seismic trace. Wavelet is mainly estimate of wave pulse for a seismic source which may contains many frequencies and is time limited (Cooke and Cant., 2010).

To perform the seismic inversion, a zero-phase wavelet is extracted through HRS software, which is then used in correlation of inverted and original extracted reflectivity series at well location of Balkassar-OXY-01. Such type of wavelet is also used in synthetic generation as discussed in chapter 3 to mark the horizon for seismic interpretation.

In 3D seismic data interpretation and Post stack inversion analysis, extracted wavelet should be zero or minimum phase to get the correct and appropriate results (Jain, 2013). For inversion analysis, phase shift amount of input extracted wavelet plays a key role. The larger phase shift leads to quite higher error in final impedance results (Kallweit et al., 1982).

As shown in figure 5.2,5.3 and 5.4 the total length of extracted wavelet is 100 ms and phase of extracted wavelet is set to be constant. The straight line that cross the frequency domain wavelet illustrates the phase of wavelet.

5.4 Band-limited Inversion (BLI)

Like other inversion algorithms Band-limited Inversion is also used for inverting impedance, P-wave velocity and density of the post stack data. Band-limited Inversion algorithms also constrain the upper frequency limit of the inverted model shown in figure 5.6. Before embarking the Band-limited Inversion, it is important to define the inter relationship between actual seismic trace and seismic impedance (Ferguson and Margrave.,1996). Using equation for zero offset reflection coefficient:

$$Z = V * \rho, \tag{5.2}$$

$$r_i = \frac{Z_{i+1} - Z_i}{Z_{i+1} + Z_i}, \tag{5.3}$$

$$AI_N = AI_1 exp(\sum_{i=1}^{n} r_i), \tag{5.4}$$

Where

Z == Acoustic Impedance

P ==P- Wave Velocity

P == density

r_j == reflection coefficient of i^{th} layer

AI_N =Acoustic impedance of N^{th} layer

AI_1 =Acoustic Impedance of 1^{th} top-layer

Now solving the above equation (6.2) for $(j+1)^{th}$ layer with the help of equation (6.3)

$$Z_{j+1} = Z_j\left(1 + \frac{2r_j}{1-r_j}\right) = Z_j\left(\frac{1+r_j}{1-r_j}\right) \tag{5.5}$$

If the impedance of first layer is known. Nth layer impedance can be calculated by equation (6.4)

$$Z_n = Z_1\left(\frac{1+r_1}{1-r_1}\right)\left(\frac{1+r_2}{1-r_2}\right)\ldots\ldots\left(\frac{1+r_{n-1}}{1-r_{n-1}}\right) \quad (5.6)$$

Acoustic impedance of the first layer should be calculated from a continous layer lyiong above the zone of interest (Sinhh and Maurya, 2015a).Now the acoustic impedance of jth layer can be found by equation (6.5)

$$Z_{n+1} = Z_1\prod_{k=1}^{j}\left(\frac{1+r_k}{1-r_k}\right) \quad (5.7)$$

Dividing equation 6.6 by Acoustic Impedance of fiest layed (j^{th})and taking logrithms of both side.

$$ln\left(\frac{Z_{j+1}}{Z_j}\right) = \sum_{k=1}^{j}\ln\left(\frac{1+r_k}{1-r_k}\right) \approx 2\sum_{k=1}^{j} r_k, \quad (5.8)$$

Solving for Zj+1 equation written above become

$$Z_{j+1} = Z_1\, exp\left(2\sum_{k=1}^{j} r_k\right) \quad (5.9)$$

Now above equation can be written as:

$$Z_{j+1} = Z_1\, exp\left(\gamma\sum_{k=1}^{j} s_k\right) \quad (5.10)$$

By solving the exponential of equation (6.10) gives the resultant impedance (Mauriya and Singh, 2015a and Waters, 1987a).

5.4 Sparse-Spike Inversion

There are 3 types of sparse spike inversion are used to invert the seismic data that are defined briefly in below

5.5.1. Linear Programming

The linear SSI computing technique first extracts the reflectivity estimation, then uses frequency domain restrictions to extract the seismic spectrum's minimum and maximum frequencies. The obtained reflectivity is then compared to the initial model. This will produce in a sparse reflectivity that will fit best among synthetic and obtained seismic data patterns, providing the number of function "s" is limited. The wavelet in the seismic data, which is the in-progress wavelet, is supposed to be known. The L1 norm is decreased, providing a layered subsurface media model. By minimizing the error %age, this technique produces an impedance model with sparse reflectivity's shown in figure 5.10.

5.5.2. Maximum Likelihood

For transforming the reflectivity model into such a series that can be altered out from seismic data, the Maximum Likelihood algorithm uses an iterative method. The waveform in seismic data is expected to be defined and the actual wavelet in the same way as it is in linear programming. Every trace in seismic data has a sparse reflectivity sequence that is projected by inserting RCs because once an optimal cure is found which is shown in figure 5.11. The broad-band reflectivity is before gradually changed so that the ensuing synthetic trace best matches the genuine trace with a certain level of tolerance. We have discretion over how distant the handing out can go from the beginning model to fit the real data in this approach.

5.5.3. Sparse Spike layer Reflectivity inversion

The origin detection of a dictionary of functions encoding thin-bed reflectivity patterns, and the formulation of the seismic trace as a superposition of these patterns, can be used to achieve sparse-layer inversion. To generate the seismic trace, this approach identifies a small number of patterns that are then added together. When suitable regularization parameters are applied for both approaches, synthetic studies show that sparse-layer inversion utilizing basis pursuit (BPI) can better resolve thin beds than a comparable sparse-spike inversion (SSI) and usually corresponds better to known reflectivity shown in figure 5.12.

5.5 Coloured Inversion

Seismic coloured inversion applied to stacked data shown in figure 5.8. Seismic coloured inversion technique started with the wavelet extracted from the seismic data followed by well-seismic log correlation in the surrounding of well. Synthetic seismogram is generated by using well logs data. After correlating well and seismic data Relative Acoustic Impedance (RAI) is calculated through fast-track Coloured Inversion (CI). In 2000 the whit comb and Lancaster generated a new method for the band limited seismic inversion is robust method. That is robust method is known is Coloured inversion which is published in 2000. Coloured inversion is the ability to clean the smearing effect and improve the characteristic of thin beds within seismic wavelet. The best inversion for stratigraphic and structural interpretation is Coloured inversion. In Coloured inversion shows the bands of frequencies in different colours that's why its name is Coloured inversion. Different colour shows different meaning the blue is for high while orange/red show low impedance. (www.wiki.seg.org).

5.6 Real data results

All currently available post-stack inversion techniques are applied to the 3D seismic volume of Gabmat-Latif in MIB (Figure 5.1). Model-based (MBI), Bandlimited (BLI), Colored Inversion (CI), Sparse-Spike (SSI), and Layer reflectivity inversions (SSLR) are among these techniques. Additionally, three wells located within the seismic block were used. By generating seismograms for each well, the seismic to well tie or simply the correlation coefficients in the research area were determined. These wells include Tajjal-01, Tajjal-02, and Tajjal-03, respectively, as illustrated in Figures 5.2, 5.3 and 5.4 As can be seen, the error is very little, as the correlation between the two impedances is high. Correlations of this magnitude are desirable for any high-resolution inversion method. On the correlation diagram for each well, an extracted wavelet from seismic (Figure 5.2-5.3) with zero phase, a bandwidth of 10-35Hz, and a dominant frequency of 15Hz is also shown. Two horizons on the seismic section, namely B, and C-intervals, were designated as the zone under research (Figure 5.4).

Comparative study of inversion methods produces more accurate and reliable understanding of subsurface. The Band-Limited Inversion (BLI), which omits the lowest and highest frequencies and retains only those included within the seismic band. Sparse-spike inversion (SSI) is a term that refers to a group of approaches in which it is assumed that the RC series are sparse. This entails selecting fewer notable or priority-based reflections and attempting to recover the reflectivity series from band-limited seismic data. Then, a convolutional model is constructed using any form of theoretical data. There are a few things that make the algorithms for SSI different from each other, like how sparsity is

calculated, how constraints are allocated, how the L1 and L2 (sparsity) norms are used, and how the local minima are avoided. This is because these algorithms are faster and more advanced than recursive inversion techniques like BLI, MBI, and SSI. However, we call these techniques "relative inversion techniques" because they show results in the relative acoustic impedance.

If you don't want to use recursive methods, you can use the Colored Inversion (CI) instead. It's known as band limited impedance inversion, and relative acoustic impedance is calculated using the seismic the operator that has been calculated is then mixed with all the seismic data traces. It's a good idea to use Colored Inversion (CI) for inversion not only because it's easy to use and quick to process, but also because it gives results in the Absolute Impedance domain. This is why absolute Impedance models are more realistic than the relative AI models. They include low frequencies in them, which makes them better than the relative AI models.

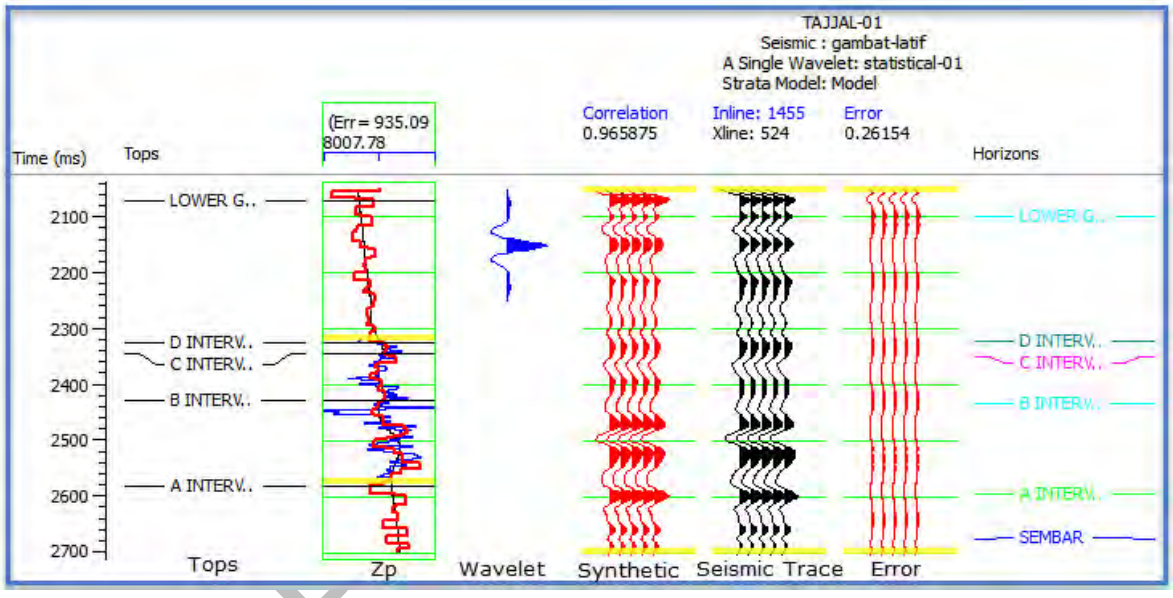

Figure 5.2: The Tajjal-001 Inversion Analysis (AI); Correlation b/w the Synthetic-Trace and Seismic-Trace remains 0.965875 whereas Error is 0.26154 b/w them.

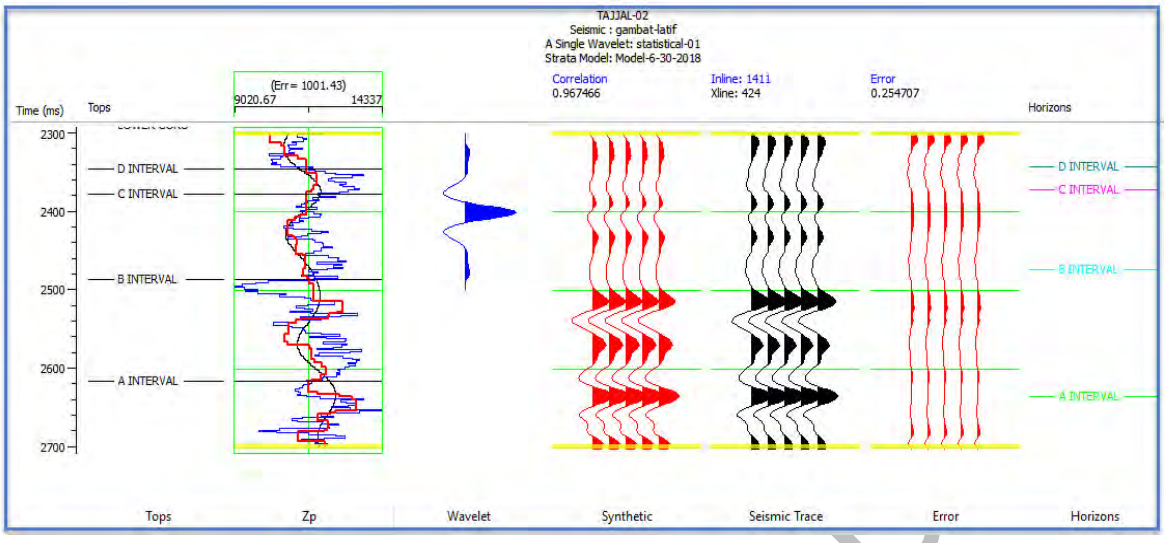

Figure 5.3: The Tajjal-002 Inversion Analysis (IA); Correlation b/w the Synthetic-Trace, and Seismic-Trace stays 0.976466 whereas Error remains 0.26107 b/w them.

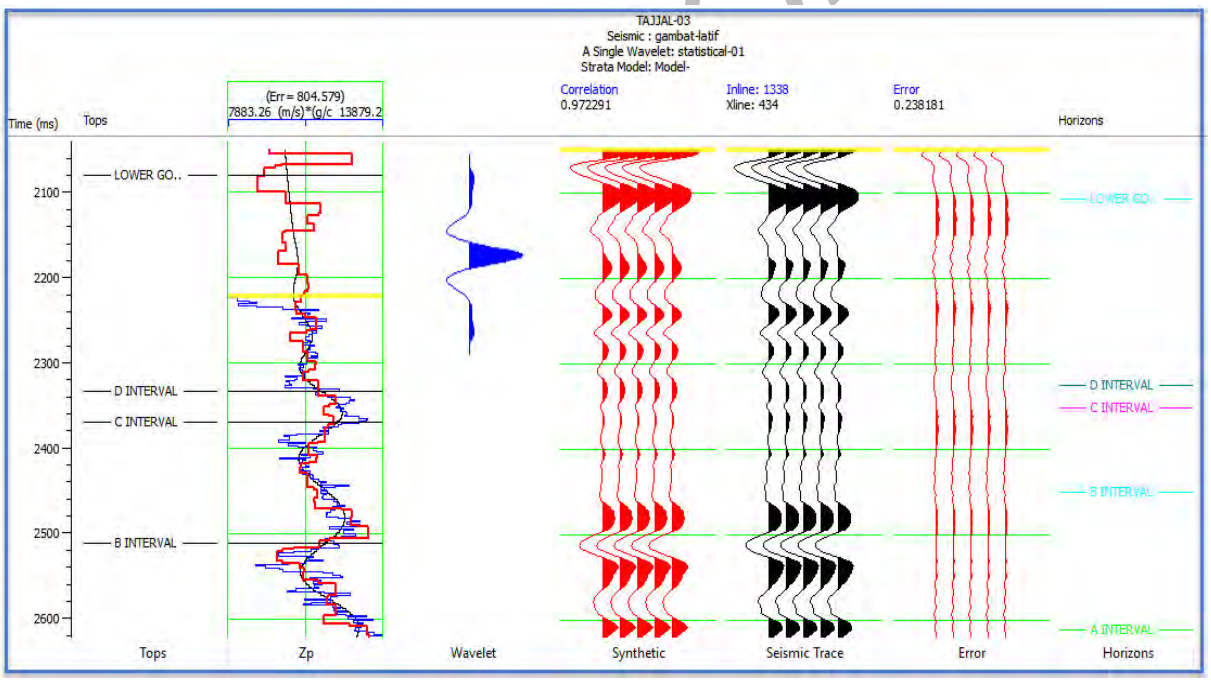

Figure 5.4: The Tajjal-003 Inversion Analysis (IA); Correlation b/w the Synthetic-Trace and Seismic-Trace is 0.978291 whereas Error remains 0.243381 b/w them.

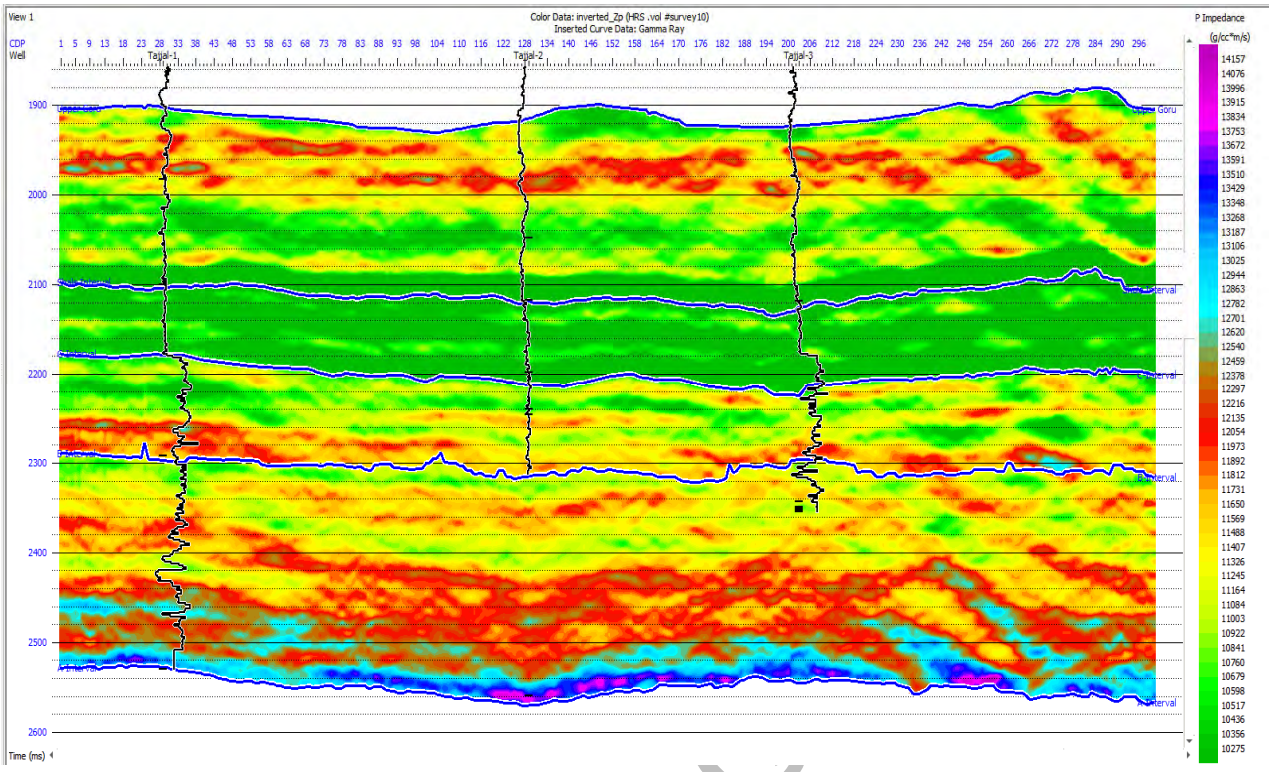

Figure 5.5: shows Gambat-Latif Model Based Inversion (MBI)

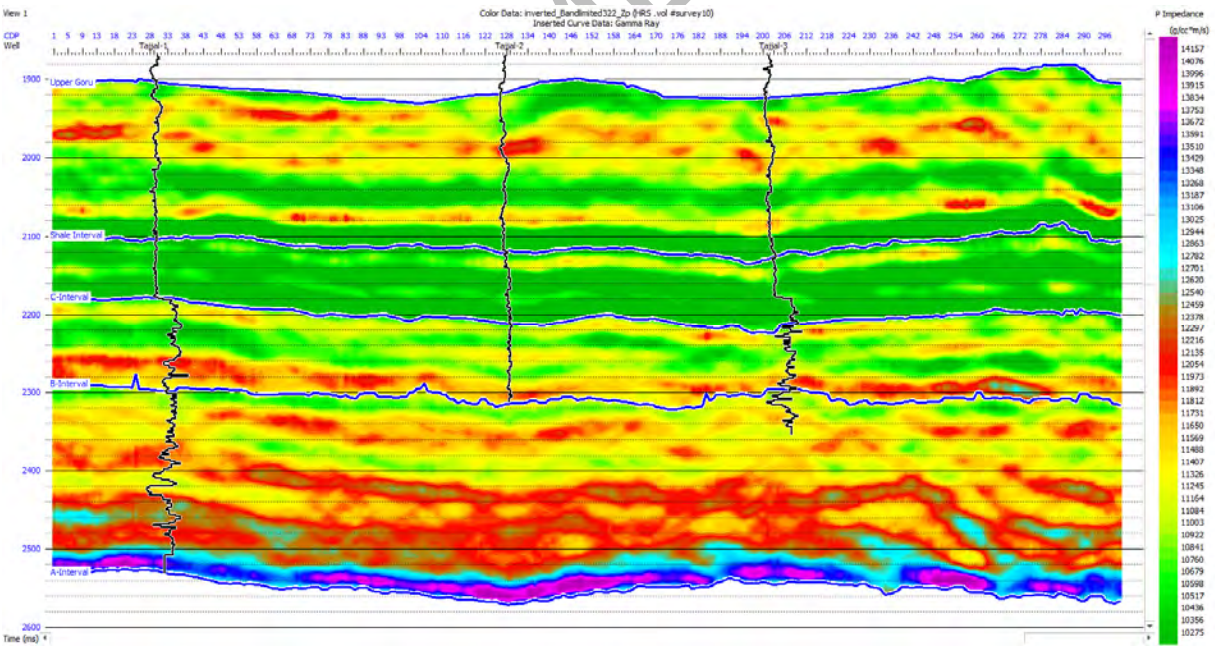

Figure 5.6: shows BL Inversion of Gambat-Latif Area.

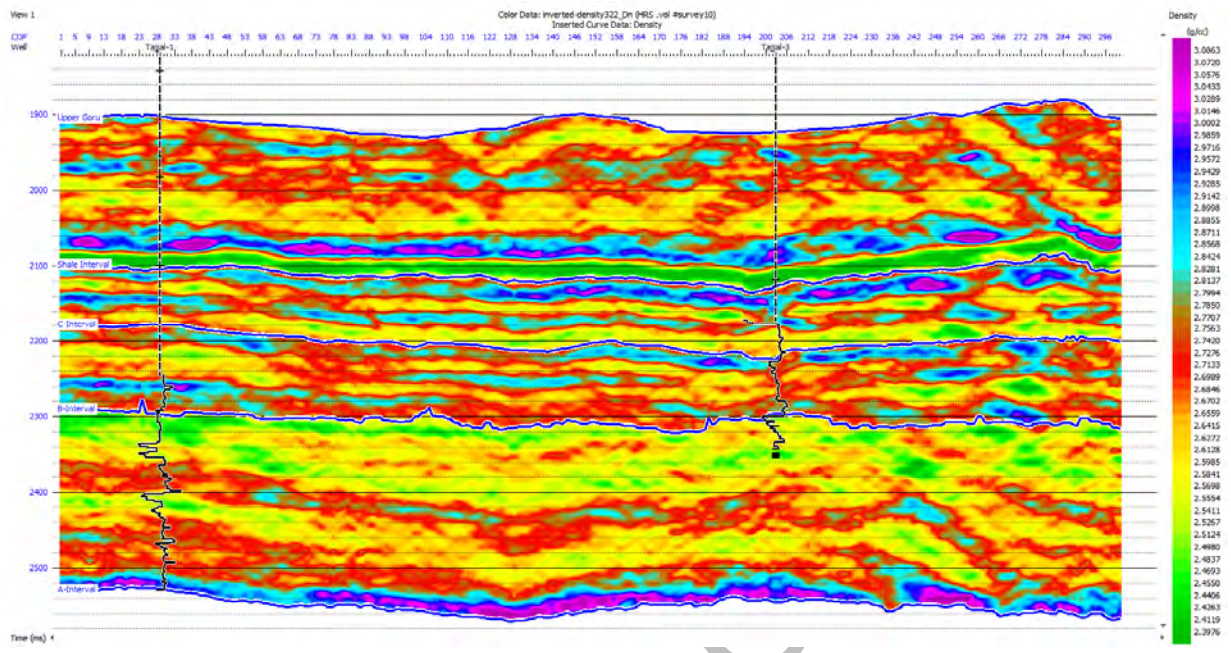

Figure 5.7: Inverted density section of arbitrary line

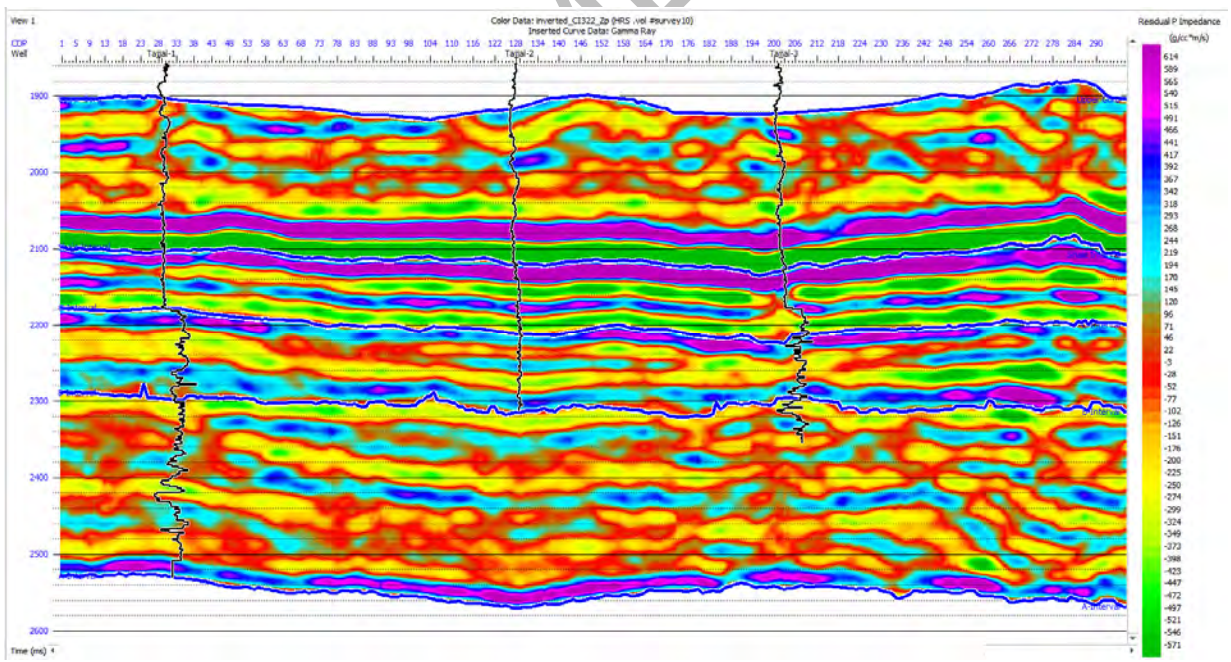

Figure 5.8: Colored inversion

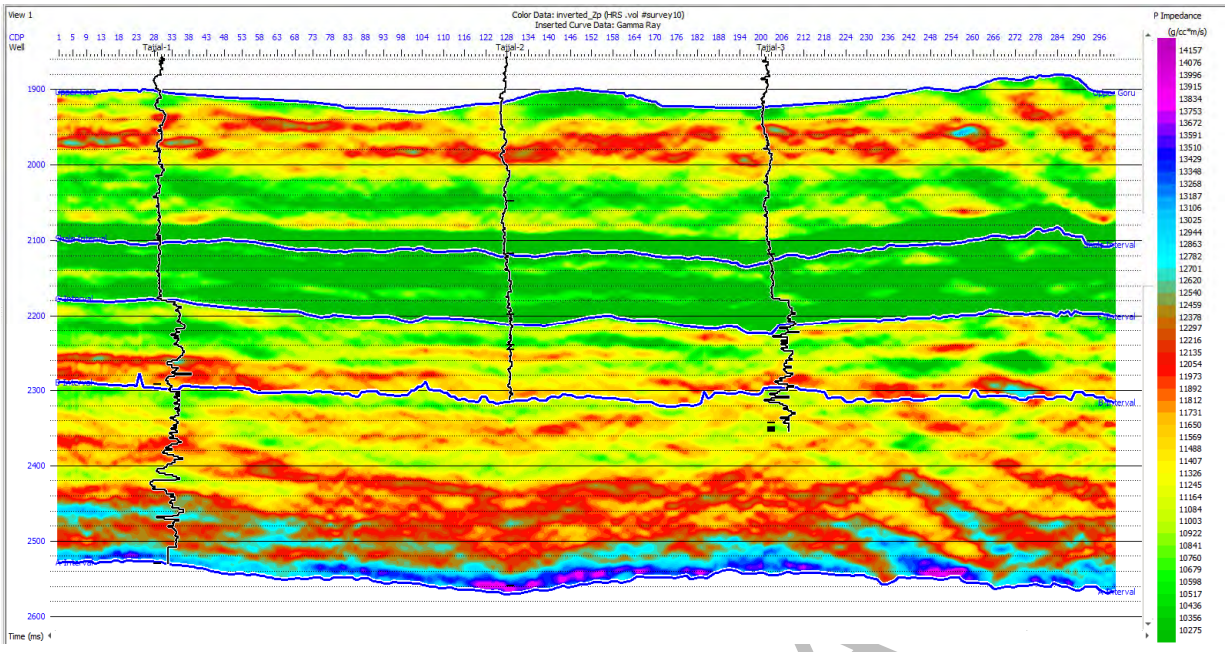

Figure 5.9: Model Based Inversion

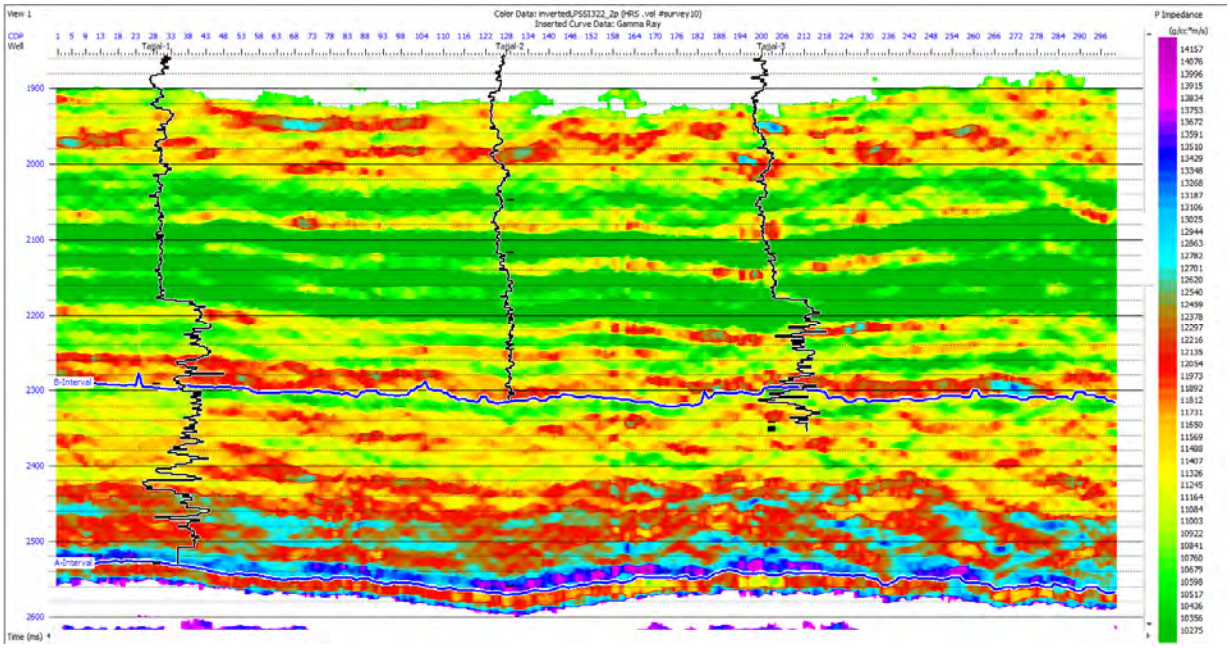

Figure 5.10: Sparse Spike Inversion (SSI) Linear Programming

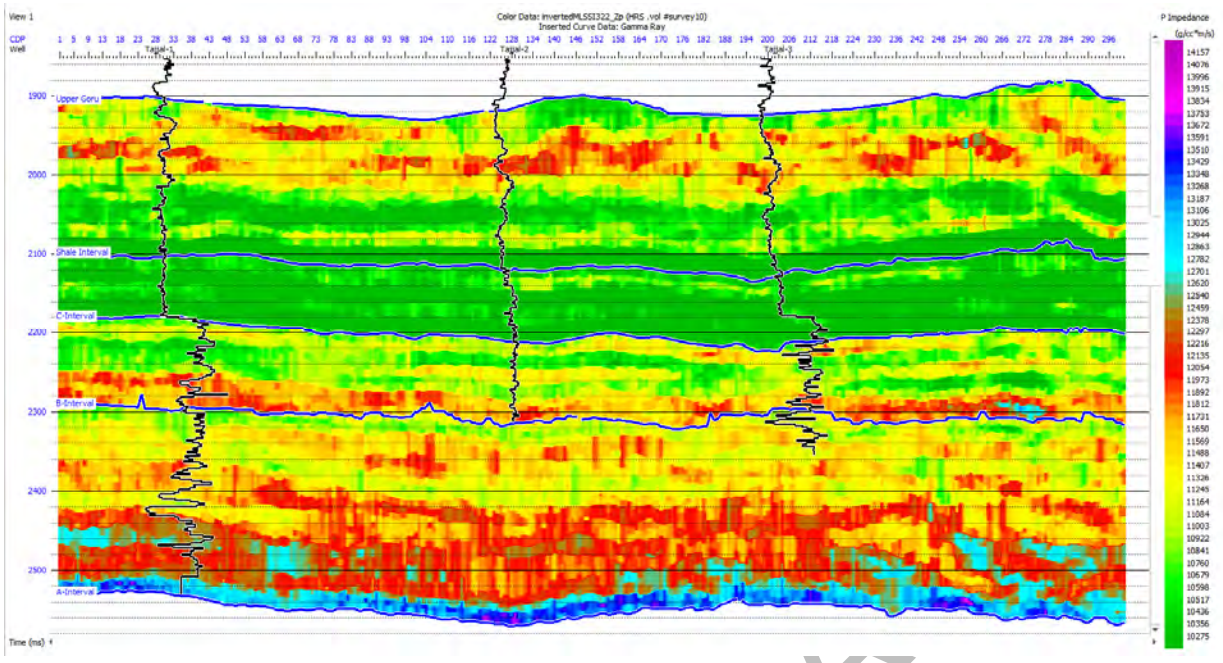

Figure 5.11: SSI Max likelihood

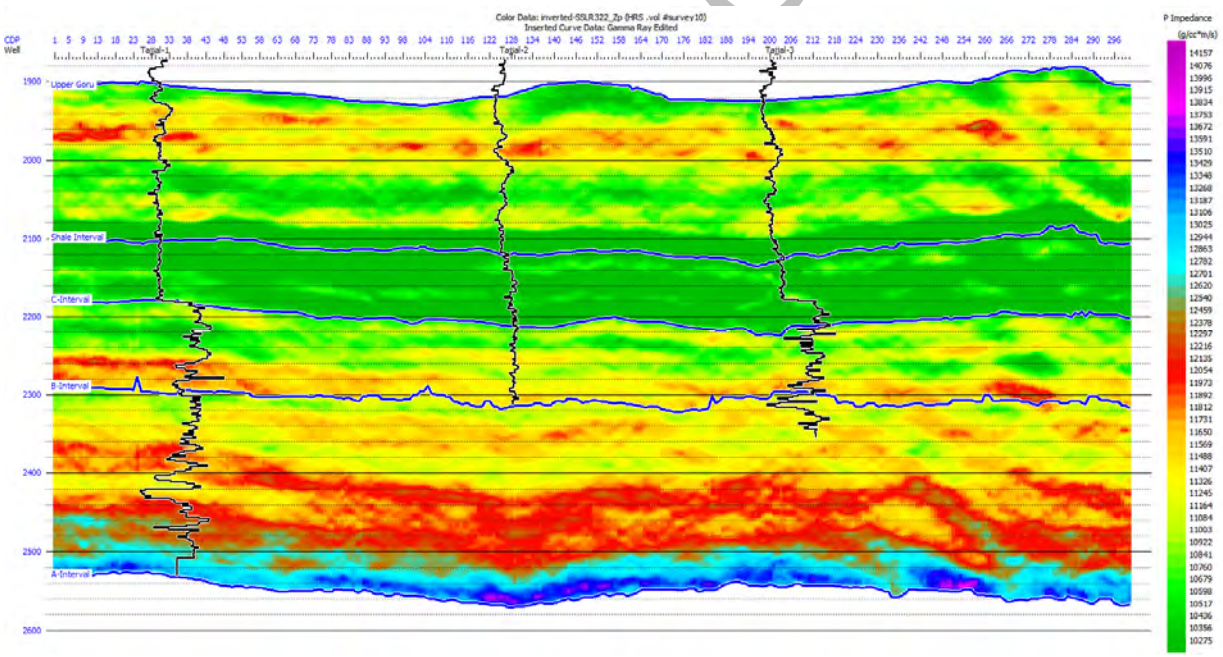

Figure 5.12: Sparse Spike Layer Reflectivity Inversion

CHAPTER 06

Static Reservoir Model

The static reservoir model, also known as the geological model or geo model, is a digital numerical model that describes the initial state of the reservoir prior to any hydrocarbon production. It depicts the spatial distribution of several rock types that contain hydrocarbons together with their various reservoir features. The primary goal of the static types model is to determine the amount of hydrocarbons that are contained in the subsurface. These hydrocarbon volume calculations can be performed for the entire reservoir or separately for a fault segment or any layer that was designated as a zone of interest during the model's building (Jan C. Rivenaes et al.).

The following are the inputs needed for a static reservoir model:

6.1 Geological data:

This data contains a wide range of qualitative and quantitative inputs needed to create a reservoir model. In order to establish and explain a reservoir's overall architecture, it is essential to comprehend the subsurface zone of interest's origin and depositional environment. The input data consists of reservoir zonation, sedimentological analyses, including core analyses, different stratigraphic models, including sequence stratigraphic and lithostratigraphic models, and reservoir characteristics impacted by the compaction and diagenesis processes.

6.2 Geophysical data:

Seismic data is the primary geophysical input used to create reservoir models. Other geophysical information, such as gravity or magnetic analyses, is not as significant. Seismic inversion data, which offers essential details about rock qualities, such as porosity and fluid distribution, as well as interpreted horizons and faults (often depth converted) are among the data from seismic surveys that are used.

6.3 Petrophysical data:

The wireline logs that are inserted into the borehole provide this data. Well log data is another name for petrophysical data. This information is a crucial component of reservoir modelling. It should be noted that the porosity and fluid saturation values are estimated indirectly using the log data from the density, neutron, acoustic, and resistivity logs rather than directly from the wireline logs.

The core data utilized for core analysis, which includes thin section investigations and laboratory analysis (XRD) to ascertain mineralogy and pore geometries, is also included in the category of petrophysical data.

6.4 3D Structural framework:

Using the techniques of fault modelling, horizon modelling, zonation, and layering of the reservoir, the 3D structural framework has been developed.

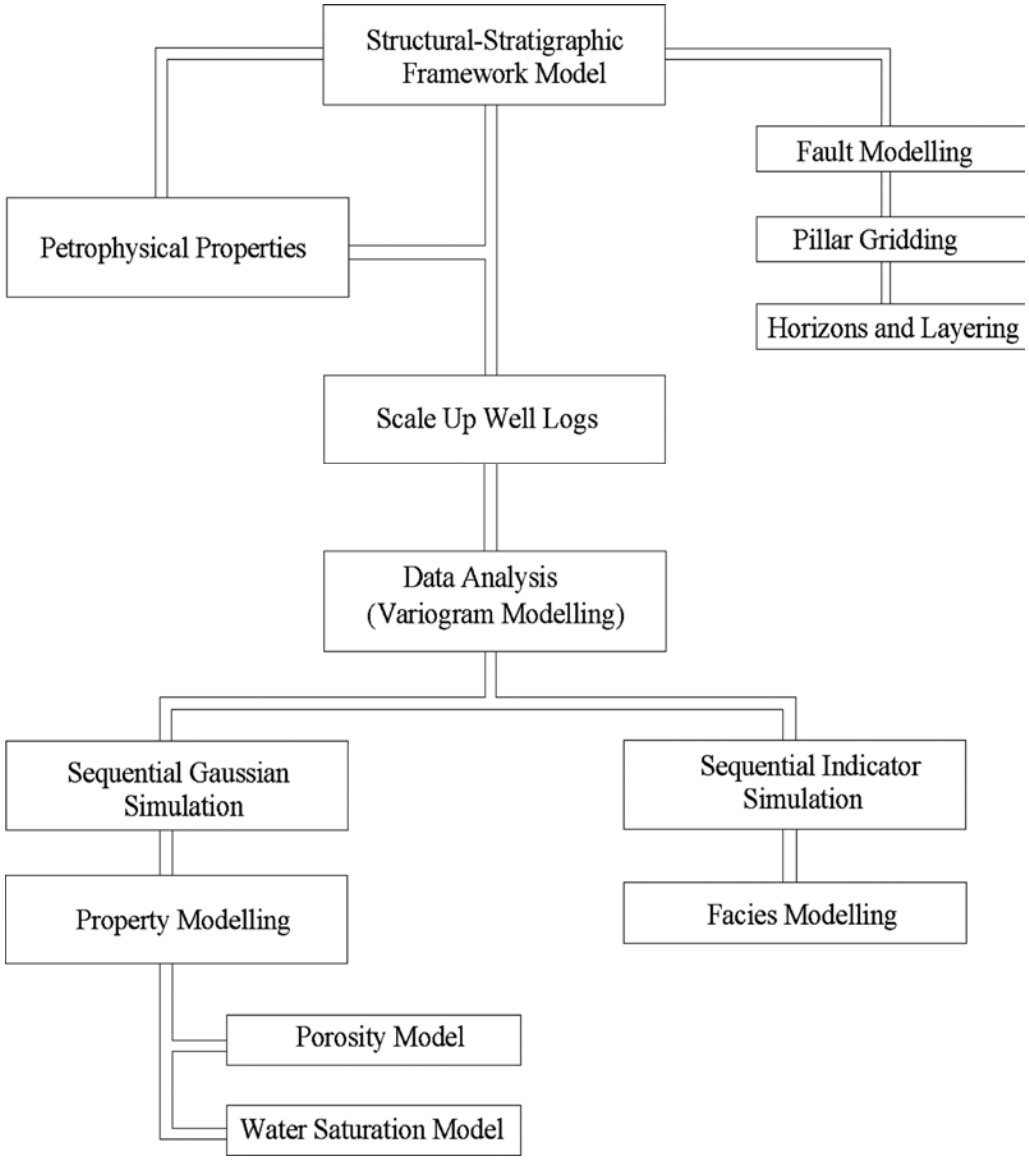

Figure 6.1: Flow chart diagram of the static modeling procedure in the current study.(Ali et al 2021)

6.5 Fault Modeling

It is a three-dimensional (3D) representation of the faults that were the subject of seismic data prior to the development of fault models. The fault is identified by the discontinuity in the seismic reflector, and this structure has NORMAL faults that have been identified. TWO faults in have been marked, as can be seen fault model with pillar gridding in figures 7.3.

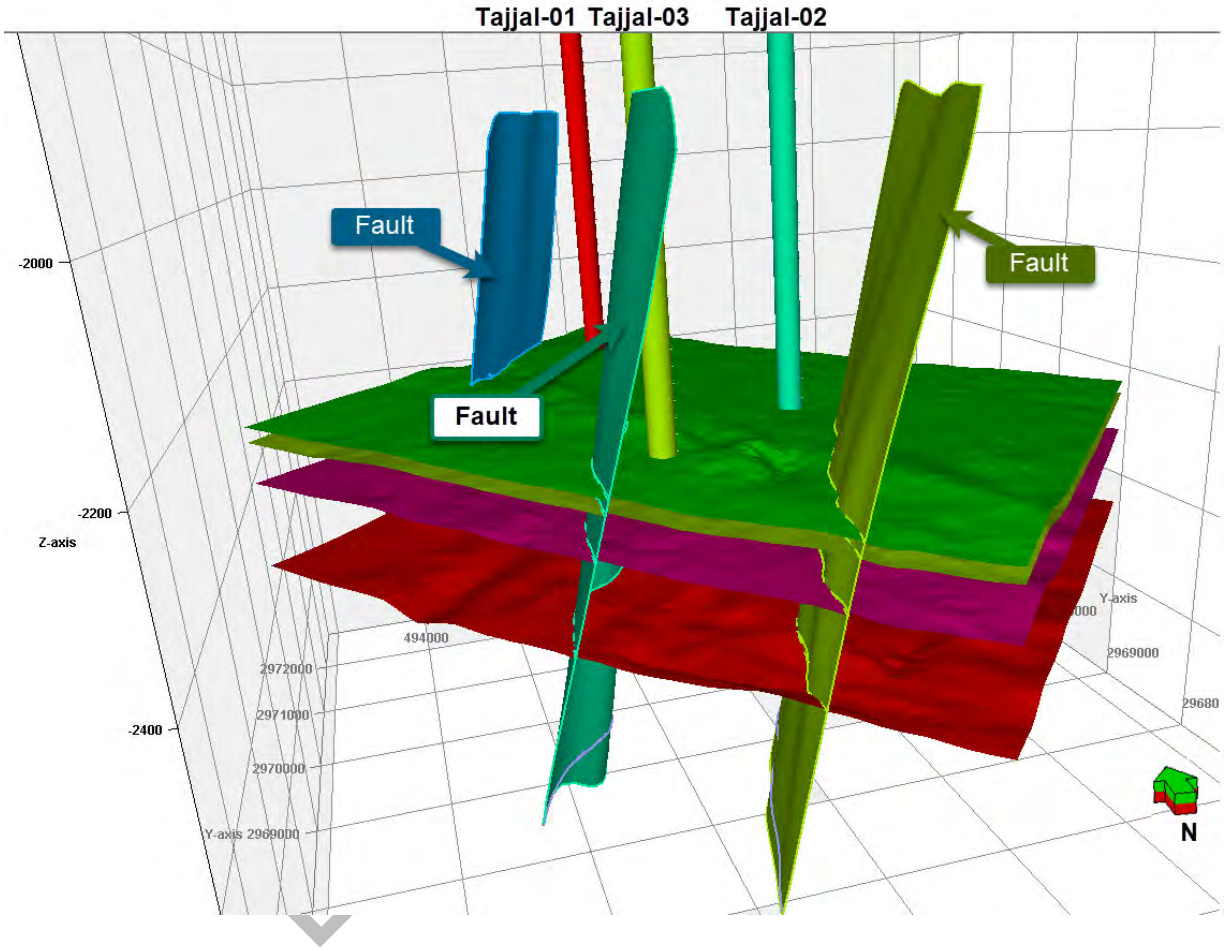

Figure 6.2: shows the 3D model of faults.

6.6 Horizon Modelling:

The horizon's top and bottom are seen in 3D. In this case, the A, B, and C Interval is a horizon that was initially indicated on a seismic section in time domain and afterwards changed to depth domain. After generation, a Depth Contour Map is displayed. The 3D perspective of A, B, C INTERVAL SURFACE, which has been acting as a Reservoir in this study effort, is shown in figures 6.3 below.

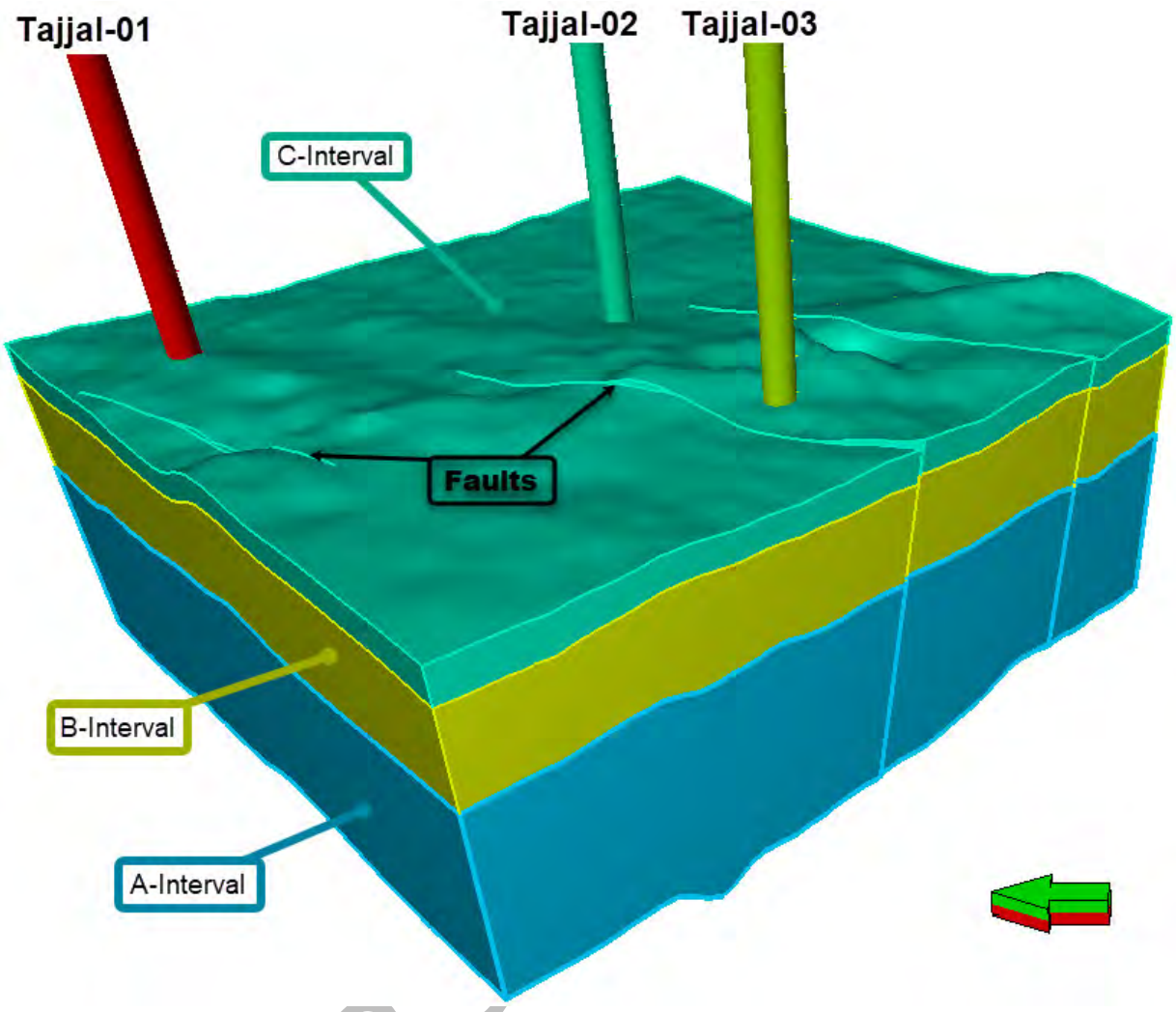

Figure 6.3: shows the horizon's top and bottom in 3D.

6.7 Facies model:

The main purpose of facies model is to integrate the reservoir heterogeneity shown by the sedimentary geology into the designing of Geocellular grid. Using a random process to colonize facies model, the modeler is permitted to test the expected proportion and dispersal of any facies.

In this research a facies model has been formed by doing electro-facies analysis of three wells of Gambat area, which has been explained in the previous chapter. Electro facies data helps in the formation of facies model in such a way that it extrapolates reservoir facies into uncored segments in such a way that it honors the relationship between Sedimentology and Petrophysics. Multiple snapshots of facies model have been represented below in figure 6.4.

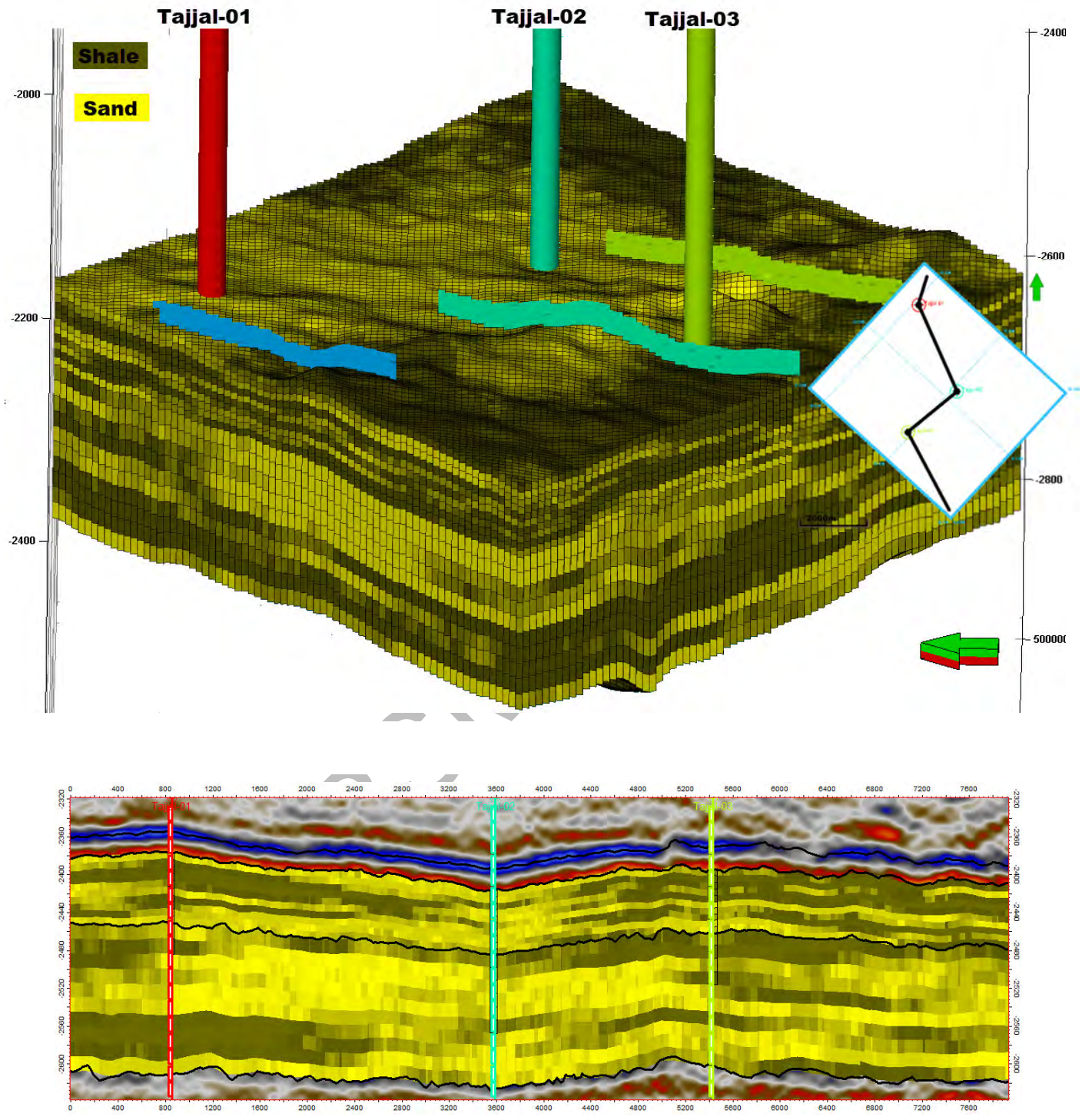

Figure 6.4: Shows the facies model of B and C Interval. In cross sectional view yellow colour shows sand.

During the process of modelling, variogram is also used that symbolizes the three-dimensional smoothness or coarseness of a data set (Deutsch & Journal 44-47). The main Objective of a variogram is to handle the smoothness of the data during interpolation and random simulation. Generally, there are three forms of variograms such as Exponential, Spherical and Gaussian. In this research project, Spherical variogram has been used with other properties.

6.8 Petrophysical model:

This model utilizes the petrophysical properties that has been taken from Petrophysical logs. Petrophysical model displays the petrophysical properties in a 3D way over zones such as B-Interval and C-Interval have been selected for the modeling purpose. These zones have been selected on the basis of petrophysical data obtained from wireline logs. This data includes Gamma-ray log, Resistivity logs, Neutron-Density logs, Sonic Log and Full-bore Formation Micro imager (FMI) log. The criteria for the selection of these zones is explained in the Petrophysics chapter of this research project. Out of many petrophysical properties that were calculated from Tajjal wells, effective porosity has been utilized for the formation of an effective porosity model of the Tajjal field with the help of three wells i.e. Tajja-l, 2 and 3.

6.9 Well- Logs Upscaling:

The reservoirs parameters have been estimated through the analysis of well logs. The calculated parameters include the volume of shale (V_{sh}) effective porosity (ϕ_e) and water saturation (S_w). Initially, facies were identified at the well locations referencing borehole logs predominantly using GR logs calibrated into GR zones. GR > 80 API were used to identify 'Shale Facies', GR 50 to 80 API correspond to 'Shaly Sand Facies' and GR < 50 API identifies the 'Sand Facies'. The interpreted lithologies (facies) are presented in Fig. 6.5.

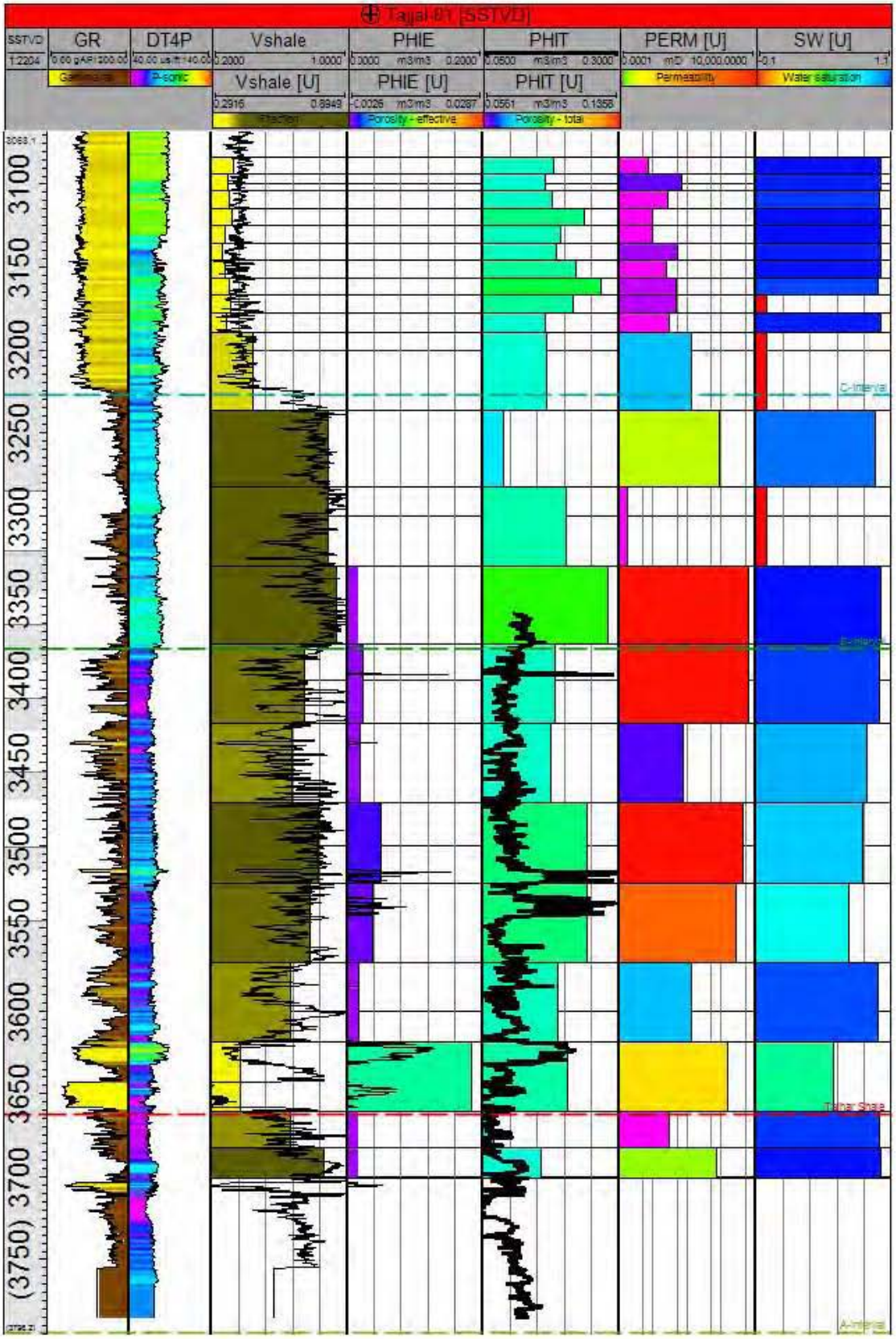

Figure 6.5: Shows Upscaled well log.

6.10 3D Porosity Model:

A 3D view of ϕ_e model of Gambat is shown in Fig. 6.6. The SGS method was used to estimate reservoir porosity beyond wells locations. The map shows good ϕe values at some region which ranges from 8 to 16% and indicate that the wells are located within good ϕe zones. For a detailed visualization of the ϕe distribution in subsurface, a cross section has been drawn as shown in Figure oriented from northeast to southwest direction. The 3D view depicts that B and C-Intervals are characterized by higher ϕ range (16%) towards the northeastern side, indicating that the reservoir holds economical quantities of hydrocarbons. This zone is correlated with clean shelfal and coastal sand deposits. However, the ϕ decreases towards southwest with range 0 to 5% which suggests that the chances of economical production to be pessimistic, as this zone is correlated with shelf and basinal settings where shale has accumulated.

6.11 3D Water Saturation (Sw) Model

A three-dimensional S_W model gives a direct indication about the percentage of hydrocarbons contained by the formation. For a prolific zone of interest, interpreter search out those locations where low S_W and high ϕe are present. Fig 6.7 shows a computed spatial distribution of S_W in the study area with low S_W around well locations. A cross section of S_W from northeast to southwest direction clearly reveals a sub-surface distribution of S_W ranging from 40 to 50% in the study area.

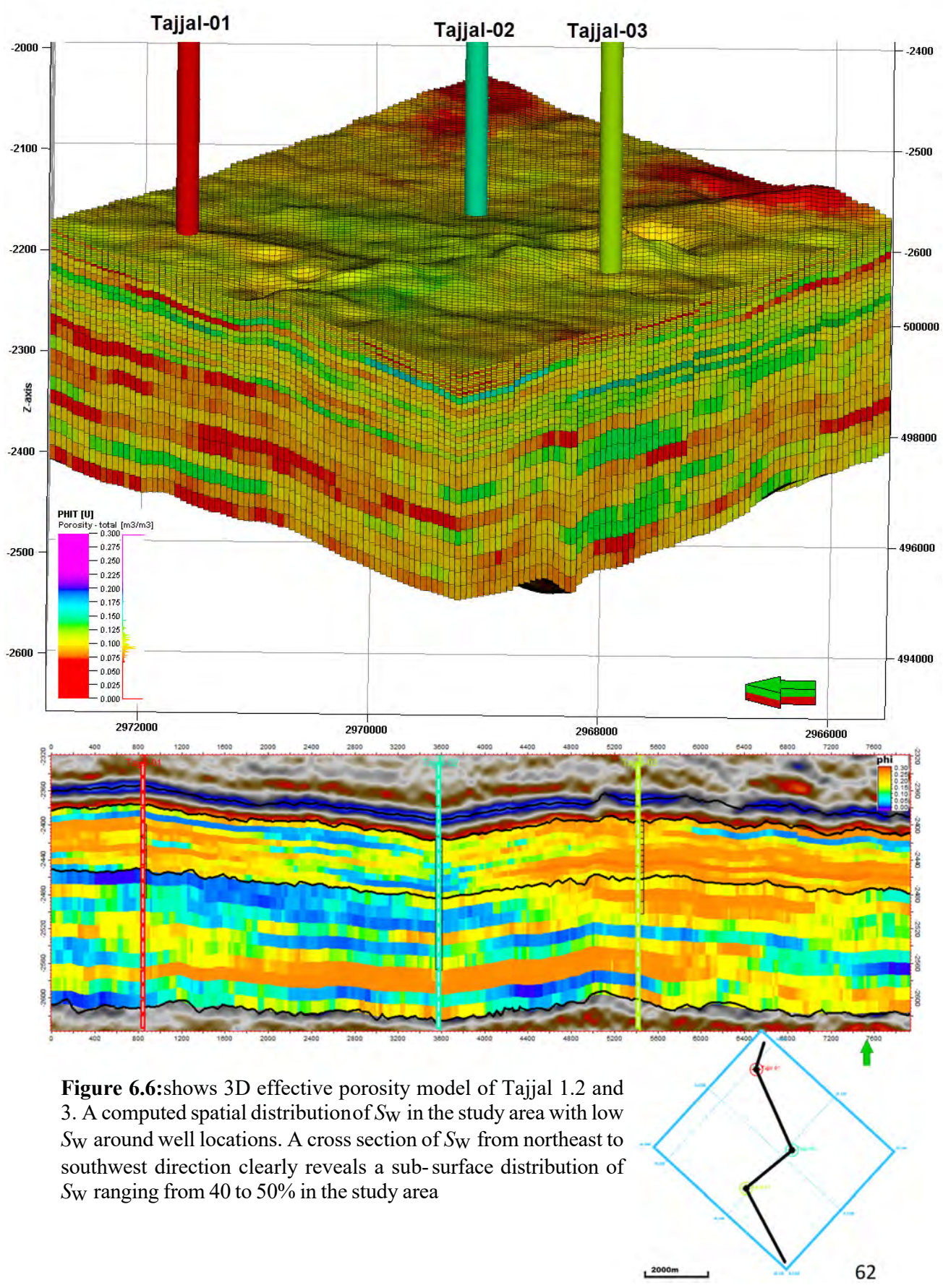

Figure 6.6: shows 3D effective porosity model of Tajjal 1.2 and 3. A computed spatial distribution of S_W in the study area with low S_W around well locations. A cross section of S_W from northeast to southwest direction clearly reveals a sub-surface distribution of S_W ranging from 40 to 50% in the study area

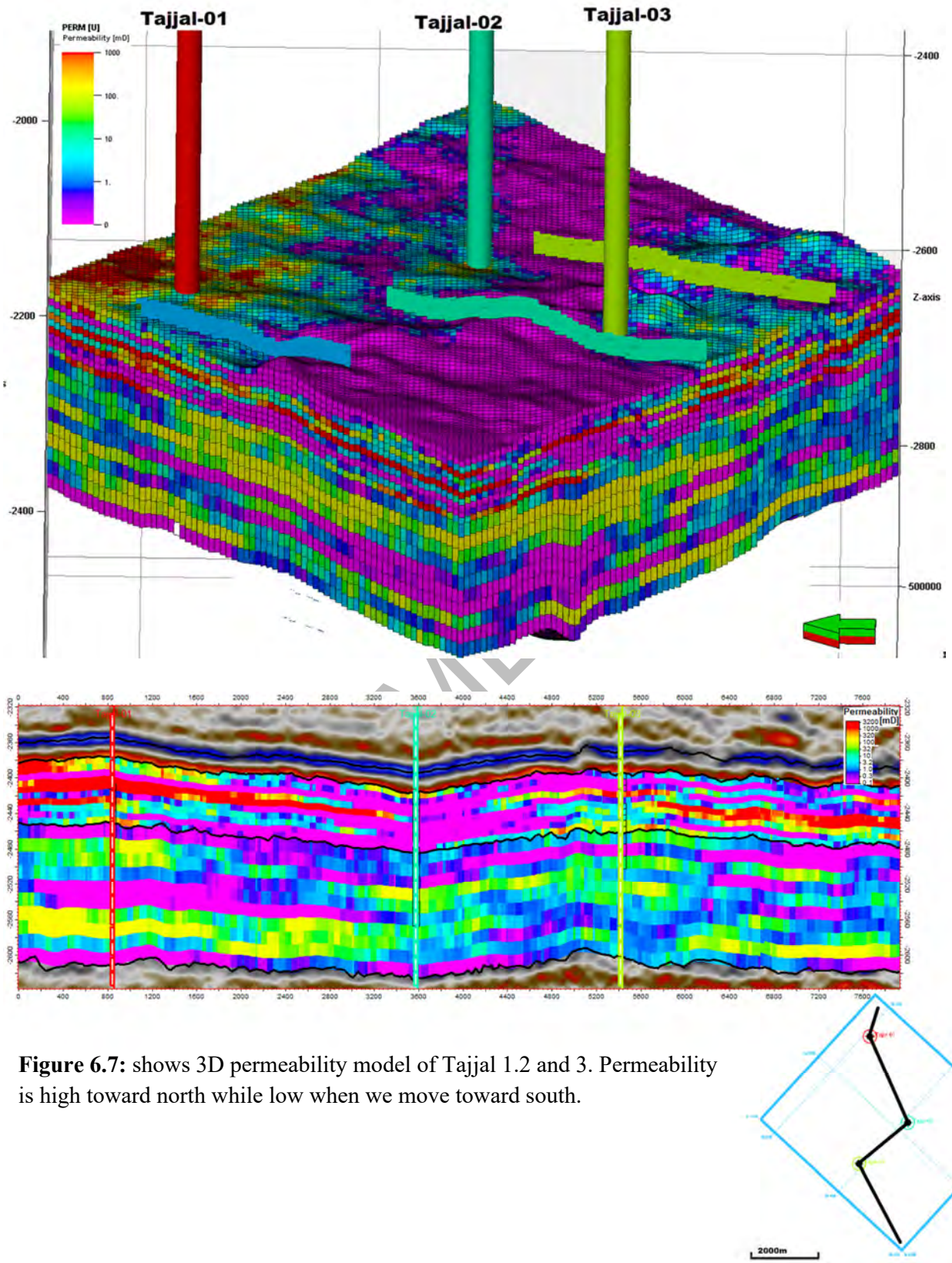

Figure 6.7: shows 3D permeability model of Tajjal 1.2 and 3. Permeability is high toward north while low when we move toward south.

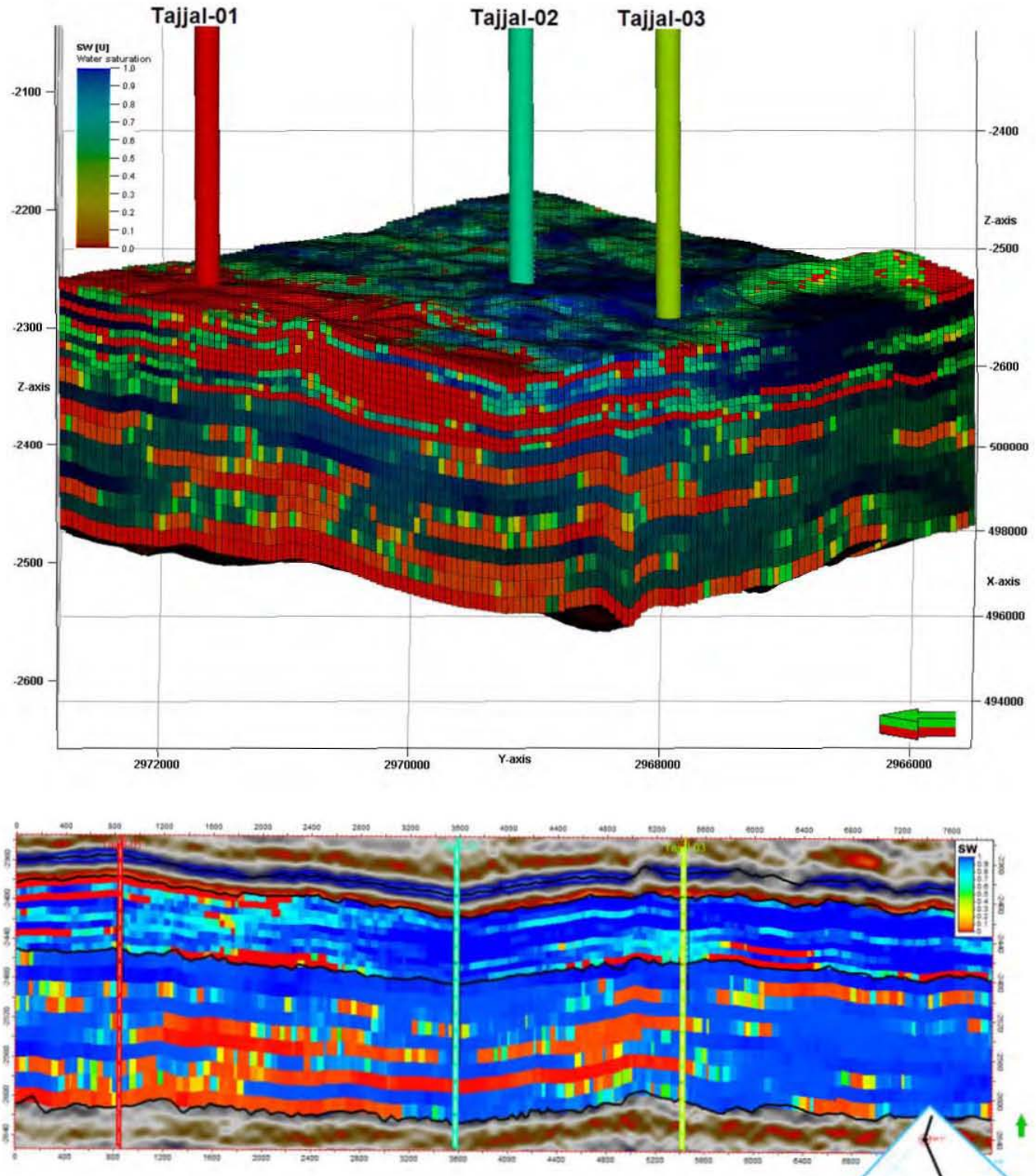

Figure 6.8: shows 3D Water Saturation (S_w) Model of Tajjal 1.2 and 3. A cross section of S_W from northeast to southwest direction clearly reveals a sub-surface distribution of S_W ranging from 40 to 50% in the study area.

CHAPTER 07

ESTIMATION OF 3D SEISMIC BASED TOC of B-INTERVAL SHALE

The TOC stand for Total Organic Content. It shows that how much organic carbon content present within geological formation. TOC is used to determine the source rock in petroleum play.Ranges nof TOC varies from 0 to 15%.For Good quality source rock TOC range from 1 to 2%. For very Good quality source rock TOC ranges from 2 to 4%. For Excellent quality source rock TOC is greater than 4%. while for poor and fair source quality ranges from 0 to 0.5% and 0.5 to 1.0% respectively (Peter,1986).

7.1 TOC estimation by Passey's (ΔlogR)

One of the method of TOC calculation is used in this research is ΔLogR method for the rock which is rich of clay using the relation given by Passey et al., (1990) as mention below:

$$\mathbf{TOC\ (wt\%) = \Delta logR * 10^{(2.297 - 0.1688 * LOM)}} \qquad \mathbf{7.1}$$

The calculation of LogR came to existence from the separation of resistivity curve with DT log. Higher the separation greater will be the rock maturity, the value of LOM value can be graphically calculated by Alyousaf et al., 2011.Schematic response of sonic-resistivity log at multiple reservoir conditions is depicted in figure 7.1.

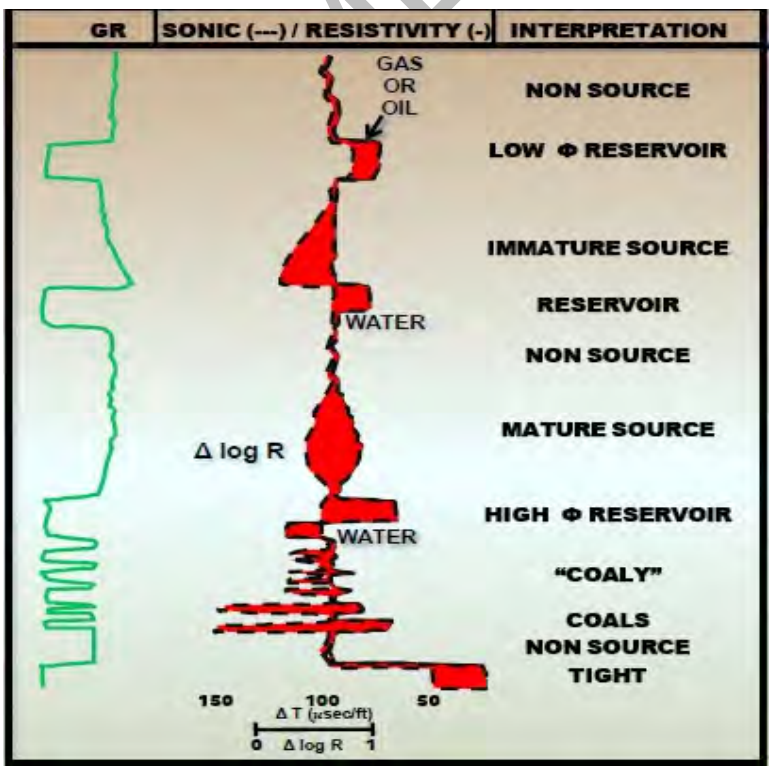

Figure 7.1: Schematic guide for interpretation of a wide variety of features observed on ΔlogR overlays

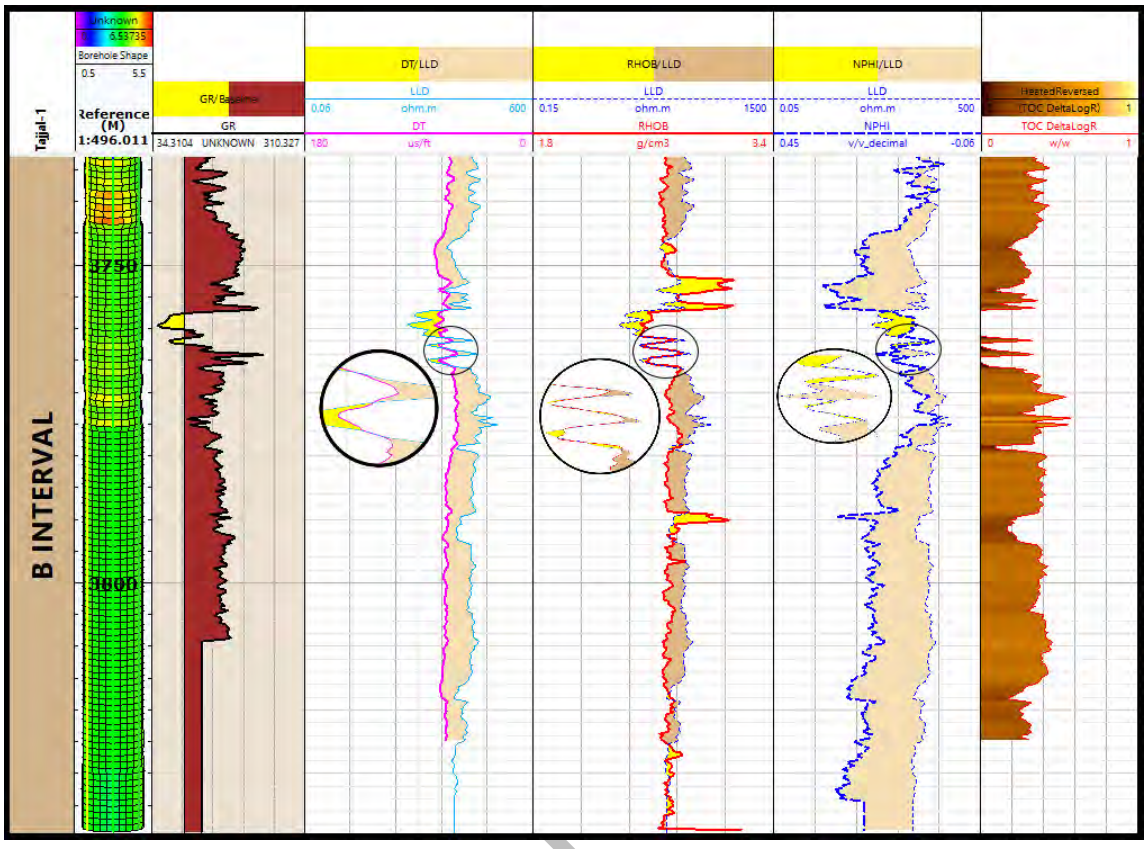

Figure 7.2: TOC estimated using well log data of Tajjal-01 by delta LogR method.

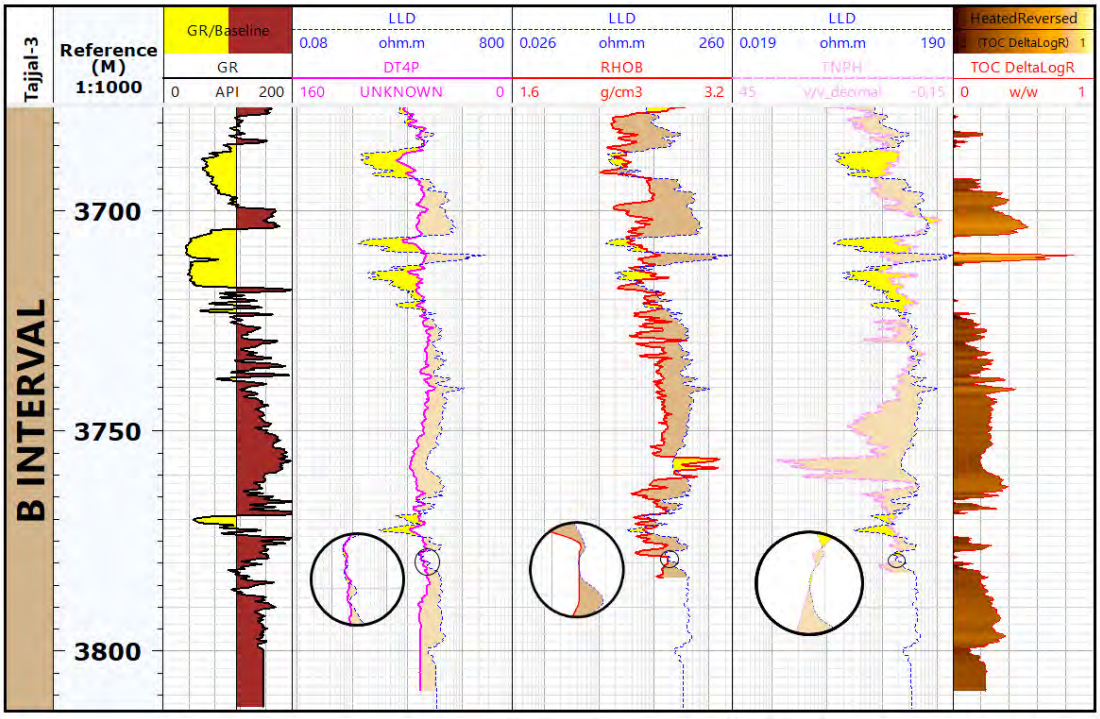

Figure 7.3: TOC estimated using well log data of Tajjal-02 by delta LogR method.

7.2 Seismic TOC map by Inversion Algorithms

The seismic data is turned into the impedance by Post Stack Seismic Inversion, which takes place after the seismic data has been collected. People in this study use BL Inversion to get information from the seismic waves. This method turns the seismic amplitude into impedances. When there is a TOC in the way, this impedance shows maximum and minimum values. The volume of shale log that is shown in Figure 7.1 and 7.2 helps to identify the shale rock in the seismic inverted section, which is where the rock is found. In this way, the high and low impedance zones in the shale rock of the Lower Goru formation can be seen. The shale rock in the B Interval has a high TOC level which is displayed in Figure 7.5. The maximum and minimum impedances in the shale rock of the B-Interval remain exposed in the figure. That resolve talk about the maximum and minimum seismic-based TOC values that will be talked about here. The seismic-based TOC has a range of 0 to 2.96 wt percent. Figure 7.5 indicates high seismic-based TOC values. The B Interval seismic-based TOC has a range of 4.42 to 6.07 wt percent. Total Organic content of TAJJAL-01 and TAJJAL-03 are shown in Figure 7.1 and 7.2. Impedance is a way to tell where the TOC is high and where it is low.

7.3 TOC distribution on 3D Static model:

As a first step in the development of 3D static models, the top and bottom of the reservoir should be positively identified on the seismic data. In the next step, the reservoir parameters obtained from well data analysis will be used as a constraint for the static models prepared from 3D seismic data. These well logs must be upscaled appropriately according to layering used in 3D model construction. Figure 8.4 show upscaling of TOC logs at each well along with their corelated well-tops. Time-depth relationship has been developed by generating a synthetic seismogram as shown in Fig. 5. The well tops were displayed on the seismic section to identify individual horizons for interpretation.

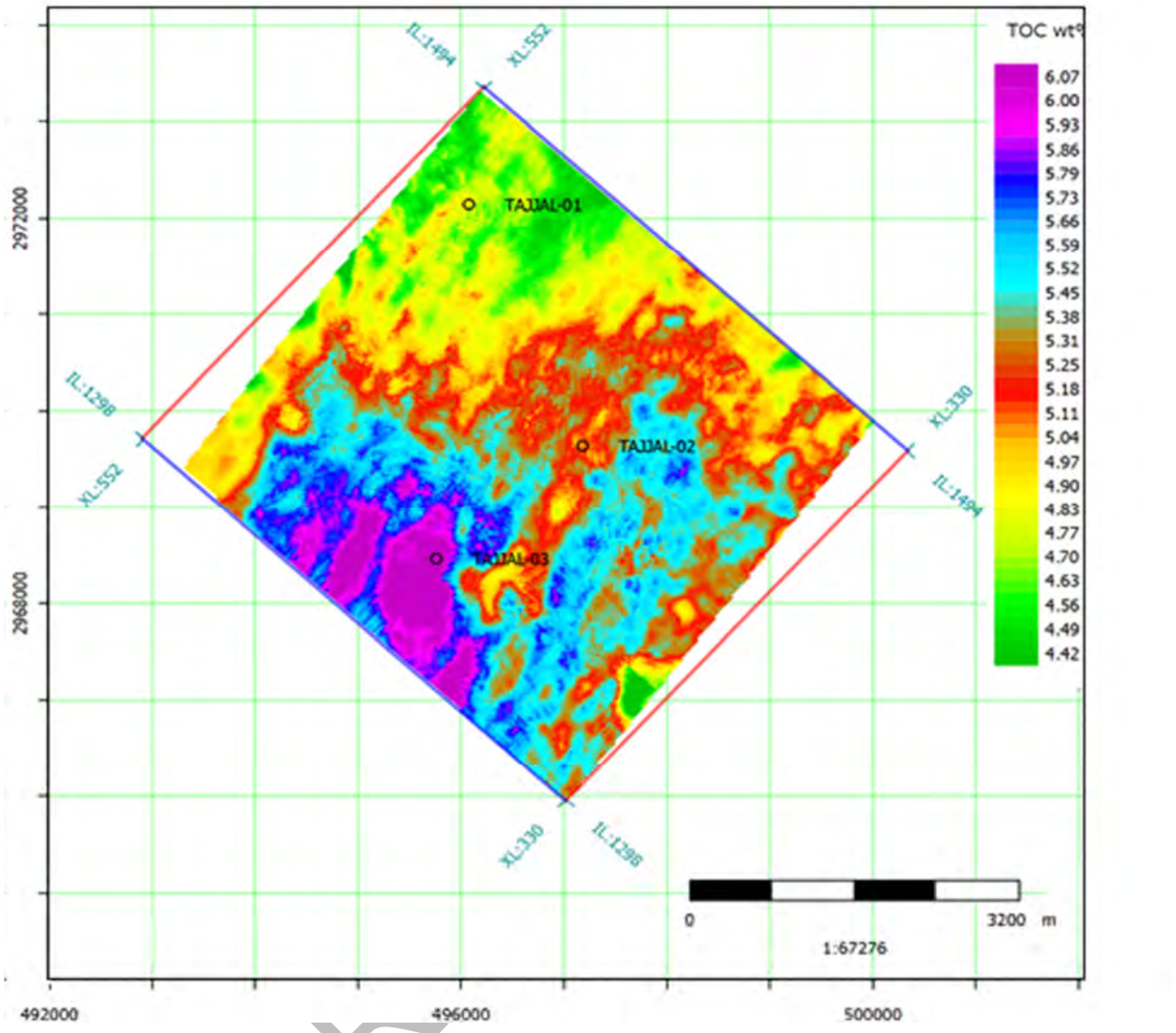

Figure 7.4: Distribution of TOC in the top of B-Interval. The map displays the Maximum and minimum TOC values in relevance to impedance values.

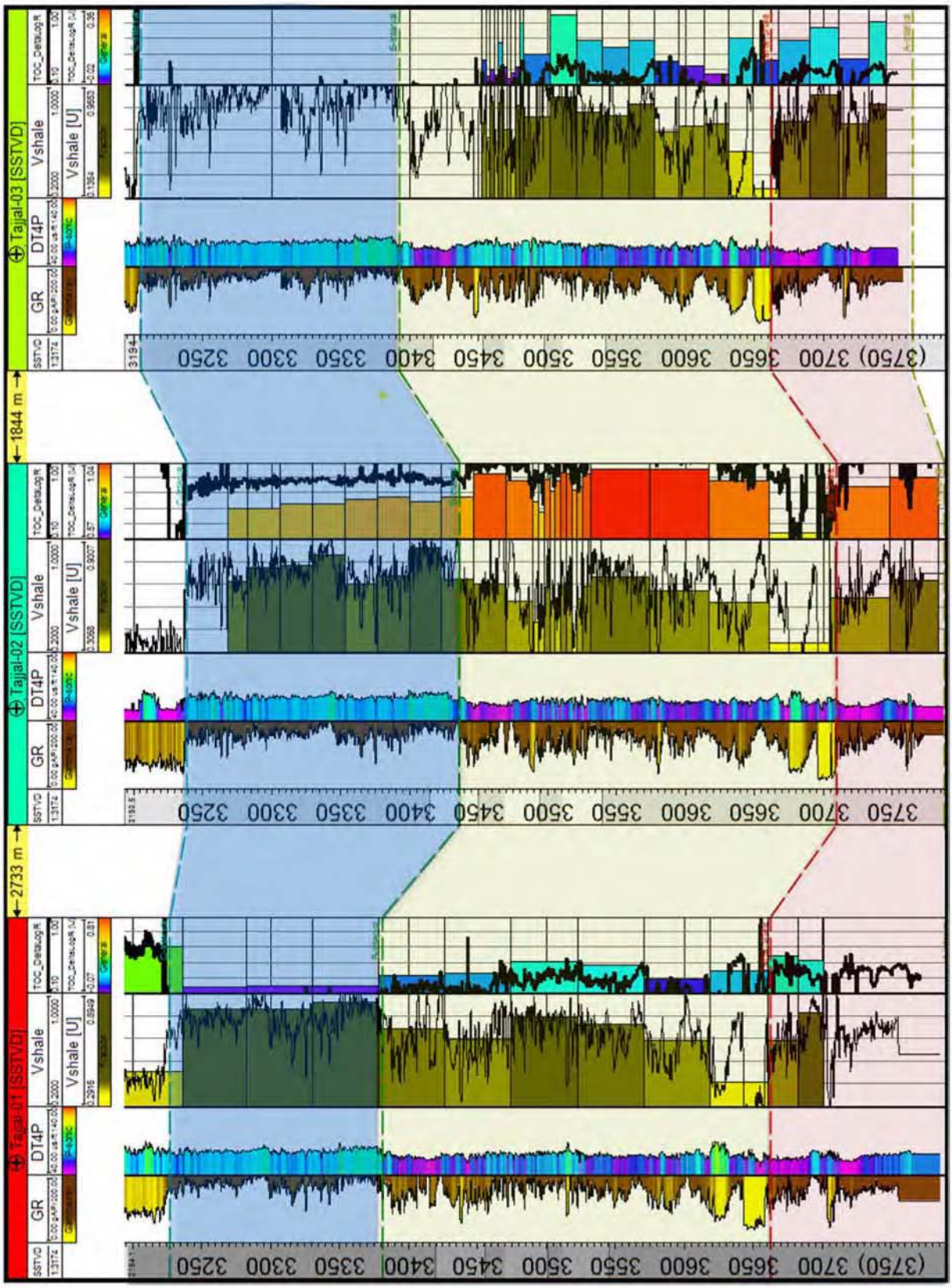

Figure 7.5: Upscaling of Well logs-based TOC estimation

In order to build 3D TOC model, the layering of the initial grid is required to make a grid skeleton. Then data from all available wells is calibrated using variogram analysis (Figure 7.5). These layers are inserted in the initial grid at regular depth intervals. The TOC log is then calibrated with known layers to define specific values at well locations. Modeling results indicate that TOC increases towards the southwest direction which is consistent with the more basin ward setting of the B interval shale (Talhaar shale).

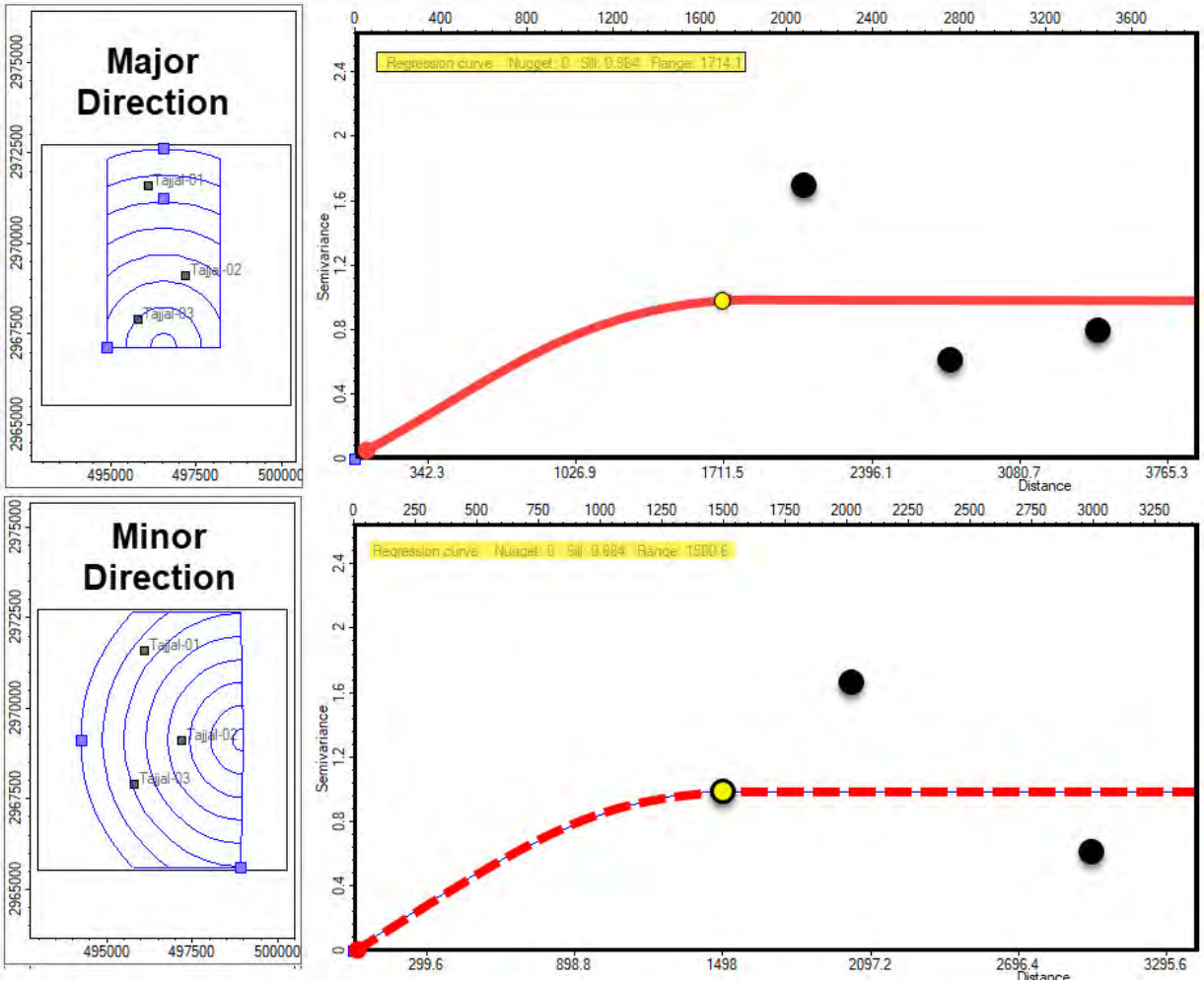

Figure 7.6: Variogram models in both major and minor directions for TOC.

7.4 Modulus of Compressibility

Modulus of Compressibility is the fractional change in volume per unit increase in pressure. For each atmosphere increase in pressure, the volume of water would decrease 46.4 parts per million. The compressibility k is the reciprocal of the Bulk modulus, B. The compression modulus measures the stiffness of the material or the ability of the material to withstand changes in length when subjected to compressive loads. The higher the compression modulus, the stiffer the material. The compression modulus is a crucial property in materials used to repair corroded piping. The spatial distribution of K is shown in figure 7.7.

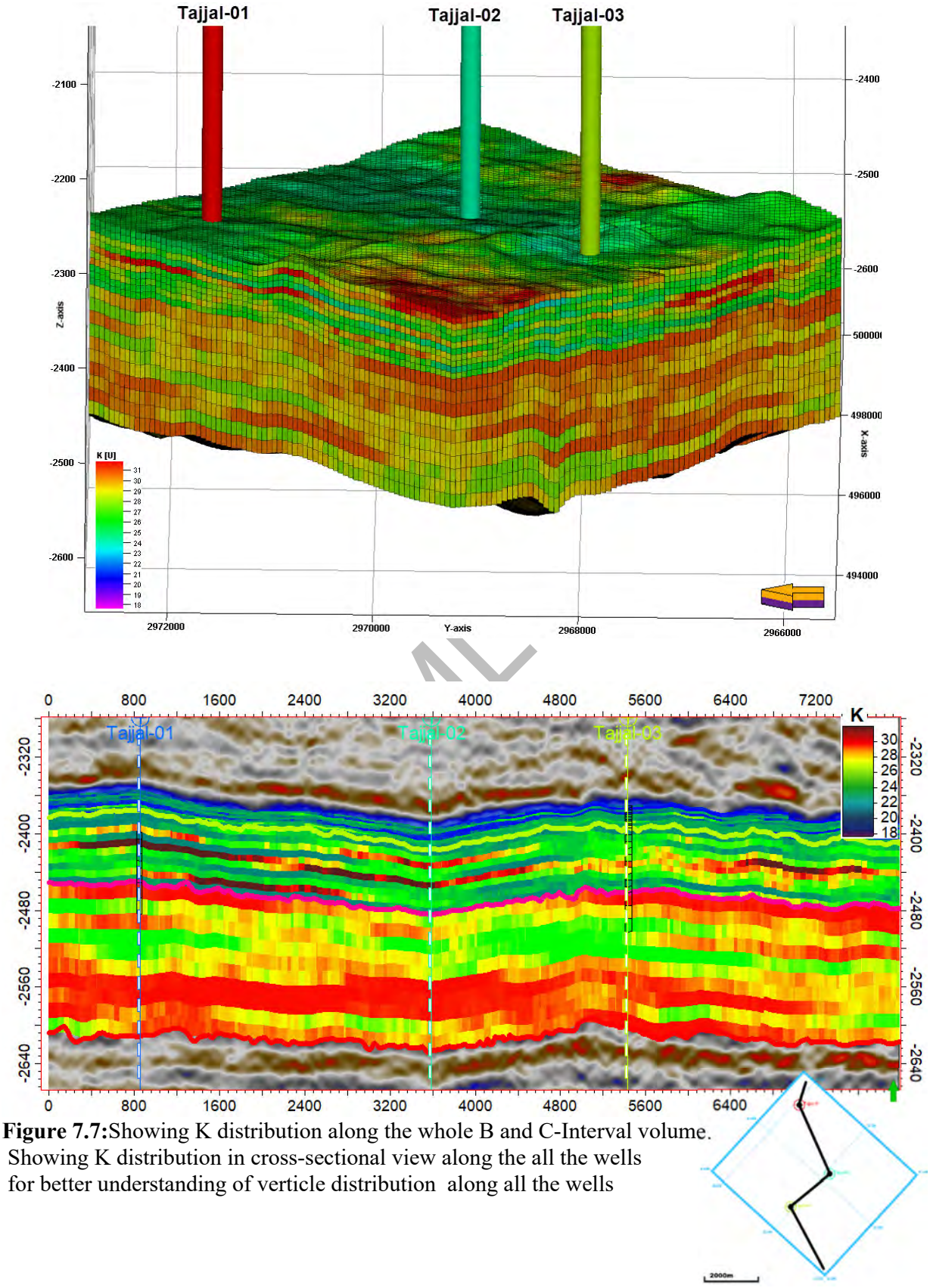

Figure 7.7: Showing K distribution along the whole B and C-Interval volume. Showing K distribution in cross-sectional view along the all the wells for better understanding of verticle distribution along all the wells

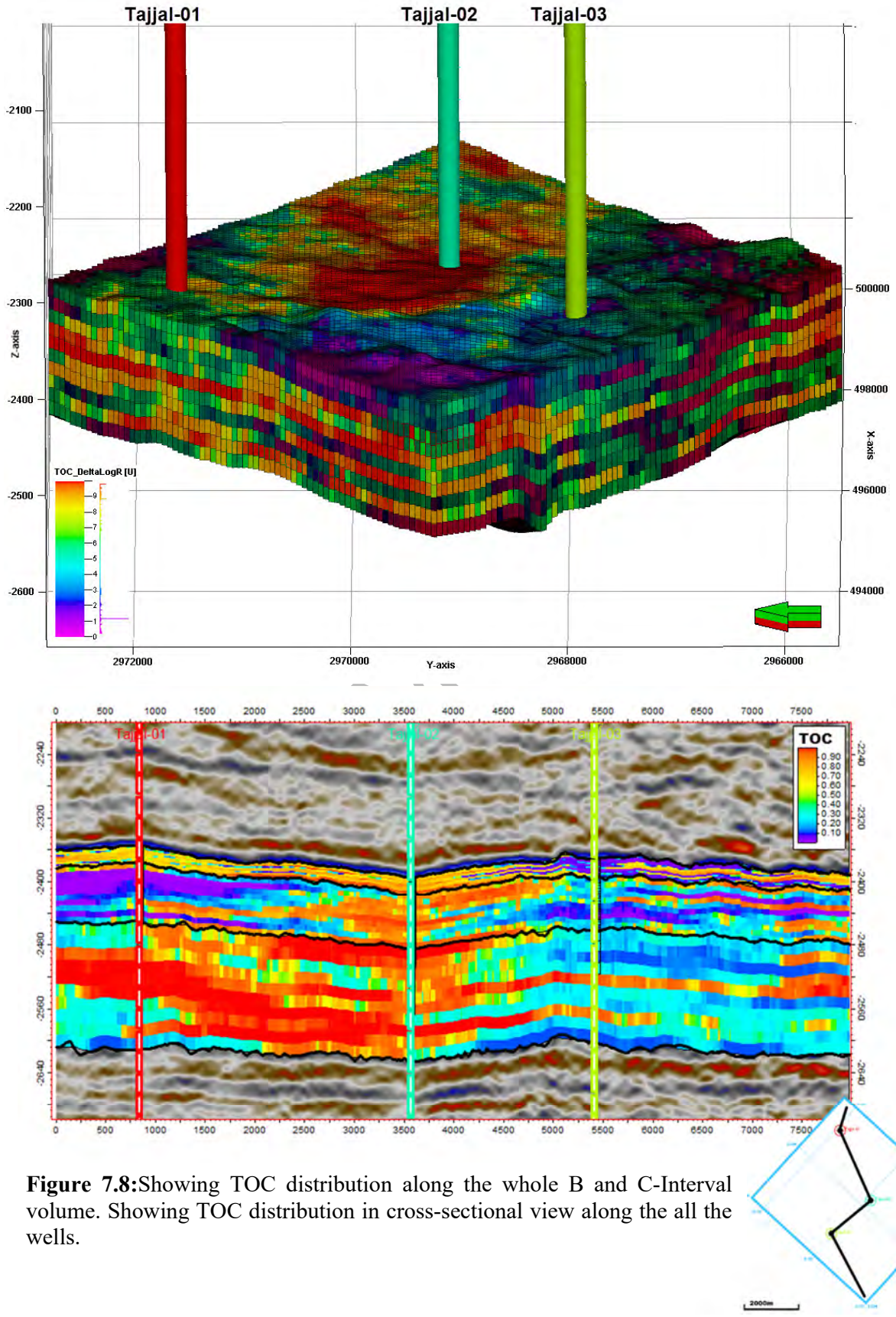

Figure 7.8: Showing TOC distribution along the whole B and C-Interval volume. Showing TOC distribution in cross-sectional view along the all the wells.

Conclusion

The Basic work of this research work is seismic interpretation, Petrophysics for conventional reservoir while seismic based TOC content estimation for the unconventional reservoir of the Gambat-Latif area of Lower Indus Basin.

- The 3D seismic data interpretation is performed by displaying the series of the inlines of the study area, mark major faults, and mark horizon's and utilizes this information to map the contour. The seismic interpretation of the study area gives information about the structure and dipping of the formation. The normal-faults are mark within seismic section. The 3 major faults are observed within extensional tectonic regime. Then Horizons are marked on the basis of the stratigraphic information and well tops information of the study area. C Interval, B Interval and A Interval horizon are interpreted on the seismic section. The strata are trending NW-SE for the study area. The time contour map of the lower Goru Formation (C and B interval) show that well location is in the shallow depth.
- Petrophysical interpretation shows that C interval and B interval of the lower Goru formation act as good reservoir. GR log of the TAJJAL-01 and TAJJAL-02 shows the interbedded sand, shale layers. There are good ranges of the effective porosities are estimated. For the case of TAJJAL-01, in B Interval, high average effective porosity (6%-13.95%), low average saturation of water (36-50%). In the C Interval of the Lower Goru Formation of TAJJAL-01, One Zone having thickness 3558-3596 m is marked in C-Interval that shows high average value of effective porosity (9.1%), low saturation of water (26%). In B Interval of TAJJAL-03, gives average effective porosity (9.30-8%), average saturation of water (46-53%). In C interval of TAJJAL-02, average effective porosity is estimated is 7% while the average saturation of water is estimated is 45%. This petrophysical results shows that B Interval is more important in exploration point of view as compare with the C Interval of Lower Goru Formation.
- In post stack seismic inversion, the seismic amplitude data is converted to the interface property to impedance property well known as rock property that itself is the multiplication of the density and sonic velocity. It gives information about the acoustic properties of earth layers. The Impedances values are low at reservoir. Bandlimited Inversion gives the best result as compare with the Model Based inversion (MBI) as MBI gives noise at the reservoir position. The results of the Bandlimited inversion and the model-based Inversion is comparing with the petrophysical results. The petrophysical results conforms the Bandlimited Inversion results are best match as compare to the Model Based inversion results. The Post stack seismic inversion conforms that the B Interval and C interval consist of low Impedance zones. Hence, B interval

and C interval of the Lower Goru formation act as a reservoir Within B interval and C interval of the Lower Goru formation, the high and low impedances are interpreted.

- Seismic based TOC is estimated by using Passey method. This extracted TOC map shows that the shale patches and B interval shale have good potential that they can act as a gas reservoir. The research work of the study area characterizes the conventional and unconventional reservoir. The bandlimited Inversion give best result as compare with the model-based inversion as the results are conformed by petrophysical analysis.
- In this research work, conventional and unconventional reservoir properties are estimated. Within the conventional reservoir, the petrophysical analysis shows that the B Interval sand is more preferable as compare with the C Interval sand. The results show that the B Interval shale is best for hydraulic fracturing as compare with C Interval shale rock as the B Interval shale rock is more brittle as compare with the C Interval shale rock. In short, the B interval of the Lower Goru formation is more important in both case i-e conventional and unconventional reservoir.
- This research work is helpful in identification and estimation of conventional and unconventional reservoir properties and seismic based TOC estimation. This work can be further proceeded to find out how much hydrocarbon is present within the Shale rock. And hence to identify the most promising zones for fracturing and hence the production.

REFERENCE:

- Barclay, F., Bruun, A., Rasmussen, K. B., Alfaro, J. C., Cooke, A., Cooke, D., ... & Özdemir, H. (2008). Seismic inversion: Reading between the lines. Oilfield Review, 20(1), 42-63.
- Karim, S. U., Islam, M. S., Hossain, M. M., & Islam, M. A. (2016). Seismic Reservoir Characterization Using Model Based Post-stack Seismic Inversion: In Case of Fenchuganj Gas Field, Bangladesh. Journal of the Japan Petroleum Institute, 59(6), 283-292.
- Cooke, D., & Cant, J. (2010). Model-based seismic inversion: Comparing deterministic and probabilistic approaches. CSEG Recorder, 35(4), 29-39.
- Latimer, R., 2011, 9. Inversion and Interpretation of Impedance Data, Interpretation of Three-Dimensional Seismic Data, 309-350.
- Alexander, T., Baihly, J., Boyer, C., Clark, B., Waters, G., Jochen, V., ... & Toelle, B. E. (2011). Shale gas revolution. *Oilfield review*, *23*(3), 40-55.
- Aliouane, L., & Ouadfeul, S. A. (2014). Sweet spots discrimination in shale gas reservoirs using seismic and well-logs data. A case study from the Worth Basin in the Barnett Shale. *Energy Procedia*, *59*, 22-27.
- Haider, B. A., Aizad, T., Ayaz, S. A., et al., 2012.A Comprehensive Shale Gas Exploitation Sequence for Pakistan and Other Emerging Shale Plays. SPE/PAPG Annual Technical Conference.
- Chen, F., Kissel, D. E., West, L. T., Adkins, W., Rickman, D., & Luvall, J. C. (2008). Mapping soil organic carbon concentration for multiple fields with image similarity analysis. *Soil Science Society of America Journal*, *72*(1), 186-193.
- Beers, R. F. (1945). Radioactivity and organic content of some Paleozoic shales. *AAPG Bulletin*, *29*(1), 1-22.
- Ullah, M., Asim, S., & Bashir, Y. (2020). Seismic Interpretation and Petrophysical Analysis of a Cretaceous Reservoir in Lower Indus Basin, Pakistan. *Petroleum & Coal*, *62*(4).
- Ali, A., Younas, M., Ullah, M., Hussain, M., Toqeer, M., Bhatti, A. S., & Khan, A. (2019). Characterization of secondary reservoir potential via seismic inversion and attribute analysis: A case study. *Journal of Petroleum Science and Engineering*, *178*, 272-293.
- Swanson, V. E. (1960). *Oil yield and uranium content of black shales* (No. TID-27491). Geological Survey, Washington, DC (USA).
- Passey, Q. R., Bohacs, K., Esch, W. L., et al., 2010. From Oilprone Source Rock to Gas-Producing Shale Reservoir– Geologic and PetrophysicalCharacterization of Unconventional Shale-Gas Reservoirs. Beijing, China,June, 8
- Sheriff, R.E., Geldart, L.P., 1995. Exploration Seismology, 2nd ed. Cambridge University Press, Cambridge, USA.
- Dolberg, D.M., Helgesen, J., Hanssen, T.H., Magnus, I., Saigal, G., Pedersen, B.K., 2000.Porosity Prediction From Seismic Inversion, Lavrans Field, Halten Terrace, Norway. vol. April. The Leading Edge, pp. 392–399.
- Veeken, P.C.H., Da Silva, M., 2004. Seismic inversion methods and some of their constraints. First Break 22, 47–70.

- Aziz, O., Hussain, T., Ullah, M., Bhatti, A. S., & Ali, A. (2018). Seismic based characterization of total organic content from the marine Sembar shale, Lower Indus Basin, Pakistan. *Marine Geophysical Research*, 1-18.
- Toqeer, M., Ali, A., Alves, T. M., Khan, A., & Hussain, M. (2021). Application of model based post-stack inversion in the characterization of reservoir sands containing porous, tight and mixed facies: A case study from the Central Indus Basin, Pakistan. *Journal of Earth System Science*, *130*(2), 1-21.
- Lindseth, R. O., 1979, Synthetic sonic logs – a process for stratigraphic interpretation:
- Geophysics, Vol. 44, No. 1, p. 3-26.
- Sams, M., & Saussus, D. (2013). Practical implications of low frequency model selection on quantitative interpretation results. In *SEG Technical Program Expanded Abstracts 2013*(pp. 3118-3122). Society of Exploration Geophysicists.
- Naseer, M. T., Asim, S., Shah, M. A., & Awais, M. (2021). Reservoir characterization for Lower-Cretaceous fluid system in Southwest Pakistan based on seismic spectrum decomposition and static wedge modelling. *Energy Reports*, *7*, 1306-1325.
- Cooke, D., & Cant, J. (2010). Model-based seismic inversion: Comparing deterministic and probabilistic approaches. CSEG Recorder, 35(4), 29-39.
- Kneller, E., Ferrer, A., & Langlois, J. (2013, August). Benefits of broadband seismic data for reservoir characterization. Santos Basin, Brasil. In 13th International Congress of the Brazilian Geophysical Society & EXPOGEF, Rio de Janeiro, Brazil, 26–29 August 2013 (pp. 966-970). Society of Exploration Geophysicists and Brazilian Geophysical Society.
- Gavotti, P. E. (2014). Model-based inversion of broadband seismic data (Doctoral dissertation, University of Calgary).
- Mahmood, N., Ali, A., & Hussain, M. (2021). The accuracy in pore pressure prediction via seismic and well log data: a case study. *Arabian Journal of Geosciences*, *14*(21), 1-10.
- Latimer, R. B. (2011). Chapter Nine: Inversion and Interpretation of Impedance Data.
- Robin, C.R., Smith, M.A., Royal, R.A., 1999. Organic facies in Cretaceous and Jurassic hydrocarbon source rocks, the Southern Indus Basin, Pakistan. Int. J. Coal Geol. 39, 205-225.
- Lindseth, R. O., 1979, Synthetic sonic logs – a process for stratigraphic interpretation:
- Geophysics, Vol. 44, No. 1, p. 3-26.
- Parvaiz, S., Ali, A., Javed, F., & Shah, M. A. (2022). Deformational pattern and seismogenic potential of the eastern Makran subduction zone. *Journal of Asian Earth Sciences*, 105298.
- Kadri, I. B. (1995). *Petroleum geology of Pakistan*. Pakistan Petroleum Limited.
- Asquith, G. B., Krygowski, D., & Gibson, C. R. (2004). *Basic well log analysis* (Vol. 16). Tulsa, OK: American association of petroleum geologists.
- Passey, Q., Creaney, S., Kulla, J., et al., 1990. A Practical Model for Organic Richness from Porosity and Resistivity Logs. *AAPG Bulletin*, 74(12): 1777-1794
- Schmoker, J. W., 1979. Determination of Organic Content of Appalachian Devonian Shales from Formation-Density Logs: GEOLOGIC NOTES. *AAPG Bulletin*, 63(9): 15041509
- Lecompte, B. ,Hursan, G., 2010. Quantifying Source Rock Maturity From Logs: How To Get More Than TOC From Delta Log R. In, Society of Petroleum Engineers

- Aziz, O., Hussain, T., Ullah, M., Bhatti, A. S., & Ali, A. (2018). Seismic based characterization of total organic content from the marine Sembar shale, Lower Indus Basin, Pakistan. Marine Geophysical Research, 1-18.
- Zhang, R., & Castagna, J. (2011). Seismic sparse-layer reflectivity inversion using basis pursuit decomposition. *Geophysics*, *76*(6), R147-R158.
- Hood, A., Gutjahr, C., Heacock, R., 1975. Organic Metamorphism and the Generation of Petroleum. *AAPG Bulletin*, 59: 986-996
- Sams, M., & Saussus, D. (2013). Practical implications of low frequency model selection on quantitative interpretation results. In SEG Technical Program Expanded Abstracts 2013(pp. 3118-3122). Society of Exploration Geophysicists.
- Cooke, D., & Cant, J. (2010). Model-based seismic inversion: Comparing deterministic and probabilistic approaches. CSEG Recorder, 35(4), 29-39.
- Latimer, R. B. (2011). Chapter Nine: Inversion and Interpretation of Impedance Data.
- Gavotti, P. E. (2014). Model-based inversion of broadband seismic data (Doctoral dissertation, University of Calgary).
- Reference:
- Chopra, S., & Marfurt, K. J. (2005). Seismic attributes— a historical perspective. Geophysics, 70(5), 3SO-28SO.
- Yilmaz. O. (2001) Seismic Data Analysis: Processing, Inversion and Interpretation of Seismic Data (Vol, 1 &2). Society of Exploration Geophysicists.
- Badley, M. E. (1985). Practical seismic interpretation Basin, Pakistan.
- Fischetti, A. I., and Andrade, A. (2002). Porosity images from well logs. Journal of Petroleum Science and Engineering, 36(3), 149-158.
- Fagin, S. W. (1991). Seismic Modeling of Geologic Structures: Applications to Exploration problems.
- Mellman, G., and Kunzinger, P. A. (2002). Forward Modeling of Seismic Data, Part 7. Geophysical Methods.
- Veeken, P. C. H., & Da Silva, A. M. (2004). Seismic inversion methods and some of their constraints. *First break*, *22*(6), 47-70.
- Veeken, P. C. H., & Da Silva, A. M. (2004). Seismic inversion methods and some of their constraints. *First break*, *22*(6), 47-70.
- Zou, C., Tao, S., Yang, Z., Hou, L., Yuan, X., Zhu, R., and Wang, L., 2013. Development of petroleum geology in China: discussion on continuous petroleum accumulation. *Journal of Earth Science*, 24(5): 796– 803.